https://doi.org/10.15388/vu.thesis.558
https://orcid.org/0000-0002-2239-291X

VILNIUS UNIVERSITY
CENTER FOR PHYSICAL SCIENCES AND TECHNOLOGY

Ahmed Mohamed Taha Abdelhamid Alfa

Effects of Pulsed Electric Field on the Structural and Techno-Functional Properties of Proteins

DOCTORAL DISSERTATION

Natural Sciences,
Chemistry (N 003)

VILNIUS 2023

This dissertation was carried out from 2020 to 2023 at the Center for Physical Sciences and Technology.

Academic supervisor:
Dr. Arūnas Stirkė (Center for Physical Science and Technology, Natural Sciences, Chemistry – (N 003)

Academic consultant:
Assoc. Prof. Dr. Federico Casanova (A National Food Institute, Technical University of Denmark, Chemistry – N 003)

This doctoral dissertation will be defended in a public meeting of the Dissertation Defense Panel:

Chairman – Prof. Dr. **Saulius Šatkauskas** (Vytautas Magnus University, Natural Sciences, Biophysics – N 011),

Members:
Prof. Dr. **Rasa Pauliukaitė** (Center for Physical Sciences and Technology, Natural Sciences, Chemistry – N 003),
Prof. Dr. **Guillaume Delaplace** (University of Lille, Natural Sciences, Chemistry – N 003),
Assoc. Prof. Dr. **Jelena Zagorska** (Latvia University of Life Sciences and Technologies, Natural Sciences, Chemistry – N 003)
Dr. **Monika Skruodienė** (Center for Physical Sciences and Technology, Natural Sciences, s, Chemistry – N 003),

The dissertation shall be defended at a public meeting of the Dissertation Defense Panel at 2 p.m. on 5th December 2023 in room A101 of the Center for Physical Sciences and Technology.
Address: Saulėtekio av., 3, Vilnius, Lithuania
Tel. +370 5 264 8884; e-mail: office@ftmc.lt

The text of this dissertation can be accessed at the libraries of the State research institute Center for Physical Sciences and Technology, Vilnius University, as well as on the website of Vilnius University: www.vu.lt/naujienos.ivykiu-kalendorius

https://doi.org/10.15388/vu.thesis.558
https://orcid.org/0000-0002-2239-291X

VILNIAUS UNIVERSITETAS
FIZINIŲ IR TECHNOLOGIJOS MOKSLŲ CENTRAS

Ahmed Mohamed Taha Abdelhamid Alfa

Impulsinio elektrinio lauko poveikis baltymų struktūrinėms ir technofunkcinėms savybėms

DAKTARO DISERTACIJA

Gamtos mokslai,
Chemija (N 003)

VILNIUS 2023

Disertacija rengta 2020 – 2023 metais Fizinių ir technologijos mokslų centre.

Mokslinis vadovas:
Dr. Arūnas Stirkė (Fizinių ir technologijos mokslų centras, gamtos mokslai, chemija –N 003).

Akademinis konsultantas:
Doc. Dr. Federico Casanova (Danijos technikos universitetas. Nacionalinio maisto institutas, Chemija – N 003).

Pirmininkas – prof. dr. **Saulius Šatkauskas** (Vytauto Didžiojo universitetas, gamtos mokslai, biofizika – N 011).

Nariai:
prof. dr. **Rasa Pauliukaitė** (Fizinių ir technologijos mokslų centras, gamtos mokslai, Chemija – N 003),
Prof. Dr. **Guillaume Delaplace** (Lillio universitetas, gamtos mokslai, chemija – N 003),
doc. Dr. **Jelena Zagorska** (Latvijos gyvybės mokslų ir technologijų universitetas, gamtos mokslai, chemija – N 003),
Dr. **Monika Skruodienė** (Fizinių ir technologijos mokslų centras, gamtos mokslai, chemija – N 003).

Disertacija ginama viešame Gynimo tarybos posėdyje 2023 m. gruodžio 5 d. 14 val. Fizinių mokslų ir technologijų centro A101 kab.
Adresas: Saulėtekio pr., 3, Vilnius, Lietuva
Tel. +370 5 264 8884; paštas: office@ftmc.lt

Disertaciją galima peržiūrėti i Fizinių ir technologijos mokslų centro bei VU bibliotekose ir VU interneto svetainėje adresu: https://www.vu.lt/naujienos/ivykiu-kalendorius

TABLE OF CONTENT

LIST OF ABBREVIATIONS

PEF	Pulsed electric field
nsPEF	Nanosecond pulsed electric field
MEF	PEF with Moderate electric field strength
EFS(s)	Electric field strength(s)
AC	Alternating current
DC	Direct current
PFN	Pulse-forming network
RC circuit	Resistance-Capacitance circuit
WPI	Whey protein isolate
SPI	Soy protein isolate
β-LG	β-lactoglobulin
α-LA	α-lactalbumin
BSA	Bovine serum albumin
kV	Kilovolt
ANS	8-Anilino-1-naphthalenesulfonic acid
Trp	Tryptophan
CSMs	Casein micelles
FTIR	Fourier-transform infrared spectroscopy
SEM	Scanning electron microscopy
EGCG	Epigallocatechin gallate
DLS	Dynamic light scattering

CHAPTER 1 INTRODUCTION

Climate change is becoming a crucial case for our planet due to its magnificent impacts on food security, human health, and biodiversity. Thus, green processing technologies are becoming essential for achieving sustainable development goals. Pulsed Electric Field (PEF), as a green processing technique, has become an emerging method used in many food applications in recent years. PEF uses brief, powerful electric pulses applied to food items, causing a variety of structural and physiochemical changes [1]. This technique has become more significant because of its capacity to increase the extraction yield of phytochemicals, improve food safety, maintain nutritional value, and prolong shelf life [2–4]. Additionally, PEF provides abilities for protein modification, which is vital for the stability and functional characteristics of food systems [5].

Milk proteins are particularly significant in the food industry due to their functional and nutritional values. Caseins and whey proteins, which make up milk proteins, have different structures and functions [6]. The structure of these proteins affects their interactions with other food components. Understanding the PEF-induced structural changes of proteins can help improve their techno-functional properties. Several studies were performed to investigate the effects of PEF on some plant and animal proteins [7–10]. However, the effects of high EFS on the structure of micellar caseins are yet to be fully studied. Due to their amphiphilic structure, proteins are utilized for stabilizing emulsion systems in many food products [11]. However, proteins are sensitive to changes in temperature, pH, and ionic strength. The proteins' interaction with polysaccharides is one of the methods to overcome the sensitivity of proteins to the surrounding environment. However, there is still a knowledge gap in research regarding the analysis of PEF-induced bovine serum albumin (BSA)/soluble starch interactions.

Moreover, the interaction between proteins and polyphenols, bioactive substances derived from plants, is getting much attention [12]. Anti-inflammatory and antioxidant activities are the main health-promoting qualities of polyphenols that have been acknowledged [13]. When these substances interact with proteins, the stability, bioavailability, and sensory qualities of food products could be altered [14–16]. Little is known about protein-polyphenol interactions when subjected to nanosecond PEF (nsPEF) treatment. Therefore, the main goal of this PhD thesis is to examine how PEF treatment affects the structure of micellar casein, interactions between BSA

and soluble starch, and between BSA and tea polyphenols (Epigallocatechin Gallate, EGCG).

In this thesis, we tried to investigate and clarify how PEF could influence the structure of CSMs and BSA and the interaction of BSA with large macromolecules (soluble starch) and small bioactive compounds (EGCG). In our research, we applied several chemical methods to investigate changes in protein's structural and functional properties. For example, Fourier transform infrared (FTIR) and circular dichroism spectroscopy were used to determine secondary structure alterations in proteins. Raman, Ultraviolet-visible (UV-vis), and fluorescence spectroscopic investigations were performed to study changes in the protein solubility, surface hydrophobicity, and protein structures. Moreover, physical-based methods were applied in this study to reflect the changes in the chemical structures. For instance, Differential scanning calorimetry (DSC) was used to investigate the thermal stability of emulsions stabilized by BSA/starch conjugates. Moreover, dynamic light scattering (DLS) was employed to study the changes in size of protein molecules as an indication for protein denaturation, aggregation, or unfolding after PEF treatment.

Aim of the thesis

To investigate the impacts of PEF on the structure of proteins and the interaction between protein/polysaccharides and protein with polyphenols.

Tasks of the thesis:

1. To investigate how PEF treatment can affect the interaction (Maillard reaction) between bovine serum albumin (BSA) and soluble starch.

2. To evaluate the physicochemical and stability of emulsions stabilized by PEF-treated and untreated BSA/starch conjugates.

3. To study how PEF can influence the structural properties of casein micelles.

4. To investigate how nsPEF could influence the interaction between BSA and Epigallocatechin gallate polyphenol (EGCG).

Statements for defense

1. PEF treatment facilitated the glycation between BSA and soluble starch and improved the stability of emulsions stabilized by BSA/ soluble starch conjugates.

2. The application of PEF treatment resulted in notable alterations in the secondary structure, particle dimensions, solubility, and disulfide bonding of micellar casein (CSMs).

3. nsPEF treatment changed the structure of BSA and facilitated the EGCG binding to the BSA.

The novelty of this PhD thesis

Micellar casein represents almost 80% of the total milk proteins. It is a crucial component to produce many dairy products, such as cheese and yogurt. Therefore, it is significant to investigate how PEF could affect the structure of casein micelles and its behavior in food processing and formulation. Moreover, PEF influences on CSMs were studied as it has not been fully investigated yet. Both BSA and CSMs can be utilized in biochemical investigations of protein structure and thermodynamics, such as spectroscopy and calorimetry. BSA is frequently employed as a model protein with a well-known structure in drug binding studies and drug administration systems. Thus, it was decided to study the effects of applying PEF technology on BSA structures and interaction and binding with polysaccharides and EGCG. The PhD thesis brings forth novel contributions in the following aspects:

1. By examining the effects of PEF on protein structures, protein-polysaccharide mixtures and their emulsifying capabilities, and protein-polyphenol interactions, this work reveals significant insights into the possible applications of PEF as an innovative food processing technique.

2. The thesis provides insight into the complicated changes that occur in the structures of BSA and CSMs when treated with PEF through thorough study. The effects of PEF on these proteins have not yet been studied. It investigates conformational, solubility, and surface hydrophobicity variations. This in-depth understanding of protein structural changes under PEF conditions provides a valuable viewpoint on protein functionality.

3. The thesis takes a pioneering approach to examining the intricate interplay between proteins and polysaccharides (BSA/Soluble starch) when exposed to PEF treatment. It investigates the binding mechanisms, particle size dynamics, and overall stability of protein-polysaccharide stabilized emulsions. These findings provide novel insights into the formation and potential utilization of these complexes in diverse food systems.

4. The thesis explores the novel domain of protein-polyphenol (BSA/EGCG) interactions under PEF conditions. This exploration opens new opportunities for applying the potential of these complexes in the development of functional food formulations.

CHAPTER 2 LITERATURE REVIEW

Pulsed Electric Field: Fundamentals and Effects on the Structural and Techno-functional Properties of Dairy and Plant Proteins

2.1 Introduction

Edible proteins are crucial macronutrients with industrial, functional, and nutritional applications. In particular, dairy proteins are a desirable raw material in various industrial applications because of their distinct functional characteristics and high nutritional value [17,18]. The dairy industry also significantly affects the European Union (EU) economy and global economic growth. Recent data from the European Commission (milk market observatory) indicates that the EU exported over 500,000 tons of whey powders in 2020 [19]. Due to their widespread use as an ingredient in food products, dairy proteins must possess exceptional functionalities, such as greater solubility and enhanced gelling, foaming, and emulsifying capacities [20]. To improve their functional qualities, it is necessary to modify the conformational and structural states of dairy proteins. The percentages of hydrophilic to hydrophobic residues on a protein's surface and the quantity of hydrogen bonds are the main determinants of a protein's solubility. Although variations in the quantities of sulfhydryl (-SH) groups and disulfide linkages can also affect a protein's ability to gel, a protein's surface activity directly correlates with its capacity to act as an emulsifier [21].

There is a noticeable rise in the use of plant proteins as an alternative to animal proteins in developing sustainable food systems [22,23]. In addition, their amphiphilic structures and affordable prices make them suitable for numerous applications in the food industry, such as emulsifiers and foam stabilizers [24,25]. However, the use of proteins can be limited by factors such as high molecular weight, low solubility, and weak electrostatic repulsion [26]. Thus, it is essential to develop emerging green technologies that can modify the techno-functional and structural properties of both plant and dairy proteins without compromising their flavor and nutritional value.

In the food industry, PEF technology has demonstrated promising outcomes for the inactivation of microorganisms and enzymes in an eco-friendly manner [27–31]. In PEF processing, high-voltage electric pulses with durations ranging from milliseconds (ms) to nanoseconds (ns) are directed to the food samples positioned between the two electrodes [10,32]. PEF technology has various advantages compared to long-established pasteurization methods, such as longer shelf-life, better retention of micronutrients and quality, and cost-effectiveness [33,34]. Consequently, PEF utilization in the food industry, particularly in the plant and dairy processing sectors, is rapidly increasing [28,35]. Additionally, studies suggest that PEF can alter the techno-functional and structural properties of food proteins and promote protein/polysaccharides glycation [7–9,21,36–45].

Although the precise mechanism by which PEF affects proteins is not entirely comprehended, some investigations indicate that during PEF processing, polar groups absorb energy, producing free radicals. These generated free radicals can alter the intramolecular interactions within protein molecules, i.e., Van der Waals forces, salt bridges, disulfide bridges, hydrogen bonds, and hydrophobic and electrostatic interactions [21]. Moreover, PEF treatments can potentially alter the apparent charge of proteins by influencing their ionic interactions, leading to changes in their structural and functional characteristics [20,46]. Numerous published review articles have explored the influences of PEF processing on food and its potential applications [10,20,21,28,29,34,39,47–58]. This literature review aims to 1) Concisely contrast PEF with other well-known processing methods; 2) Elaborate on the principles and underlying concepts that govern PEF technology; 3) Examine the impact of PEF on the structural and techno-functional characteristics of dairy and plant proteins, such as solubility, foaming, emulsifying, and gelling properties.

2.2 PEF *vs* other processing technologies

In addition to PEF, several emerging technologies, such as cold plasma processing [59–61], microwave treatment [62–65], high-pressure processing [66–69], and ultrasound [70–73] have been utilized to modify the techno-functional and structural properties of food proteins. The effects of these technologies on proteins, processing parameters, and mechanisms are summarized in **Table 1**. However, due to its sustainable approach and wide range of applications, PEF has attracted considerable interest in the food and biotechnology industries [74]. PEF has been used for improving the functional properties of proteins [21], protein extraction from algae, winemaking, and biogas production [74], enhancing drying and extraction kinetics [75], improving the quality of potato chips [76], and freeze-dried fruits [77] as well as microbial inactivation [78].

PEF has many advantages compared to other processing techniques [79]; these advantages include suitability for processing heat-sensitive foods, better nutrients, flavors, and color retention, environmentally friendly nature, low energy consumption, waste-free process, and short processing times. However, some disadvantages of PEF technology include the presence of bubbles during PEF treatment, which can lead to non-uniform treatment and operational problems. Furthermore, PEF units for commercial use are not widely available in many regions around the world [79].

Table 1 Brief comparison among different emerging processing techniques and their effects on proteins' structure and techno-functional properties, reprinted from (Taha et al. [1]).

Processing technology	Processing parameters	Mechanism	Effects on protein structure	Effects on proteins' techno-functional properties
PEF	- Treatment duration, temperature, frequency, electric field strength (EFS), pulse duration, and pulse wave shape [80].	- Polarization of protein molecules and the production of free radicals can cause structural and functional changes in proteins [20].	Depends on the EFS and the type of proteins. The secondary structure and exposure of hydrophobic groups on the surface of protein molecules changed significantly [44].	Different pulse waveforms and types of proteins can have varying effects on the solubility of proteins. Enhancement of emulsifying and foaming characteristics [81].
Ultrasound	Temperature, time, energy density (J/mL), intensity, acoustic energy, frequency, and amplitude [82]	Acoustic cavitation (the creation and collapse of air bubbles) generates chemical reactions and physical issues that cause the structure and technological qualities of proteins [83].	Alterations occurred to the secondary and tertiary structures. Surface hydrophobicity and free sulfhydryl groups increase [73].	Proteins' emulsifying and gelling capabilities were enhanced [84].
High pressure processing	Temperature, pressure, and treatment duration [67]	The entry of water into the protein matrix can cause protein unfolding [49].	Depending on the used circumstances and protein system. Mainly Denaturation and aggregation of proteins occurred [85].	Depends on the applied pressure. Emulsifying and Foaming capabilities enhanced. Solubility of proteins improved [86].

Processing technology	Processing parameters	Mechanism	Effects on protein structure	Effects on proteins' techno-functional properties
Microwave	Temperature, time, frequency, and power [62].	The exposed proteins interact with electromagnetic energy at the molecular level. During the treatment, electromagnetic energy generates heat through the motion of molecules [83].	- Secondary structure changes. Protein aggregation [87].	Gelling properties improved [88].
Cold-plasma processing	Voltage, frequency, time, and temperature [89]	Several high-energy radicals, such as hydroxyl radicals, superoxide nitric oxide, and atomic oxygen break the covalent bonds and promote several chemical reactions [90].	The high-energy reaction may disrupt peptide bonds and oxidize amino acid side chains. Additionally, they may enhance protein-protein interactions. -Changes were identified in the secondary structures[91].	The improved emulsifying and gelling characteristics of proteins have resulted in increased water- and oil-holding capacities [61].

2.3 Fundamentals of PEF technology: Device components and pulse generation

A closed-loop that facilitates the movement of electricity is known as an electric circuit. Electric current (I) refers to the flow of electrons through the circuit and is measured in amperes (A). This flow can be determined using the equation $I = V/R$, where the current is driven by the electric pressure measured in volts (V), and R (in ohms) is the resistance to the current flow. The resistance opposes the flow of electric current [92].

The contemporary method of PEF processing involves directly applying electrical pulses to food material positioned between the two electrodes for a duration of ms to ns at a range of electric field strength (EFS)[93]. Multiplying the effective pulse duration by the number of applied pulses yields the processing time for the PEF. The voltage generator and electrode geometry control the time course and magnitude of the PEF process.

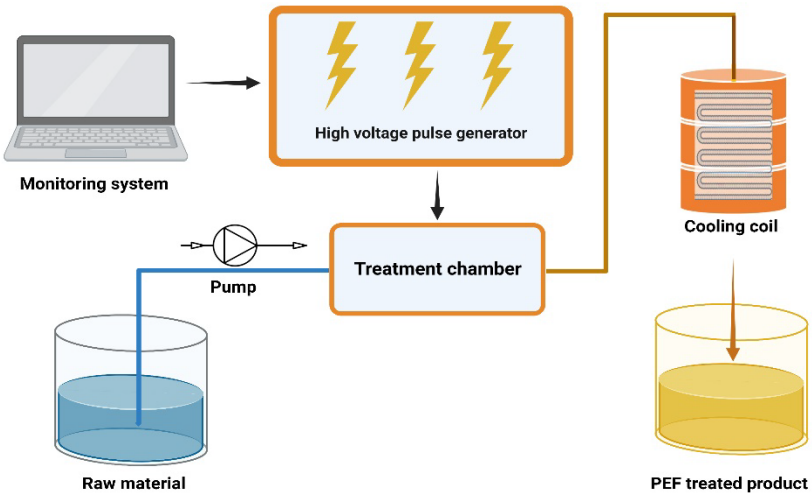

Figure 1. A diagram of a possible continuous PEF device used to treat food samples.

The conventional PEF apparatus includes a high voltage pulse generator, a treatment chamber with an appropriate cuvette, and the required monitoring and regulating tools. **Figure 1** depicts a diagram of a continuous PEF device used for food treatment. The equation ($I=V/R$) can be used to compute the electric current, or flow of electrons across the circuit, which is expressed in amperes (A). Voltage is the term for the force or source of electricity that

drives the flow of current (V, measured in volts). Ohms (R), a unit of electrical resistance, represents the resistance of an electric circuit. The electric field is affected by the voltage that is supplied, the separation between the two electrodes, as well as pulse width and waveform. E is the electric field intensity (V/m), u(t) is the voltage applied over time (V), and d is the distance between the electrodes (m) **Equation (1)** [94].

$$E(t) = {}^{1}/_{d} * \int_{0}^{t} u(t)\ dt \qquad (1)$$

Different circuit components are used in a variety of circuit types (pulse generators) in PEF devices to carry out the necessary functions. A schematic representation of a PEF device used for food processing is shown in **Figure 2**. A capacitor is charged to create the electrical pulses, and a switcher or trigger that regulates the decay in an electronic circuit discharges the capacitor [95]. The elements and their functions that make up PEF systems are listed in **Table 2**. The PEF devices used for food processing have a number of electric components in their electric circuit. The capacitors are charged by a pulse generator that can be an alternating current (AC) turned to a direct current (DC) using a rectifier. The pulse generator is also used to discharge high voltage from capacitors through a pulse-forming network (PFN) in the form of a pulse with a specific pulse width and shape (**Figure 2**).

Table. 2 Functions of main PEF devices components, reprinted from (Taha et al. [1]).

Component	Description & Function(s)	References
High-Voltage Pulse Generator	• Utilizing a power supply to generate high voltage DC at a particular intensity. • Utilizing a PFN to discharge the high voltage as pulses of specific shapes and widths.	[93]
Resistors	Delay the current flow and reduce the voltage.	[96]
Capacitors	Energy (voltage) storage.	[97]
Switchers	Connect or disconnect electric current and regulate the release of stored energy.	[34]
Treatment chambers	Specific containers are used to hold food samples during PEF treatment at mainly have two electrodes.	[94,98]

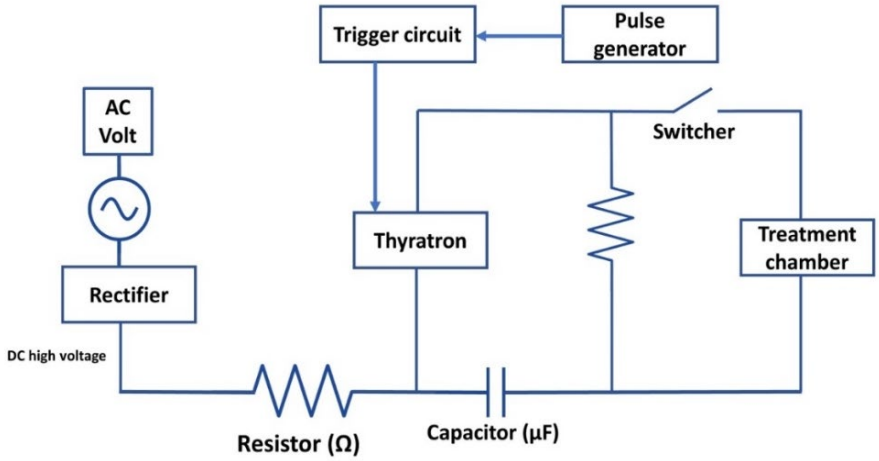

Figure 2 A schematic diagram illustrating an exemplar electric circuit within a Pulsed Electric Field (PEF) device employed in food processing. Reprinted from (Taha et al. [1]).

A capacitor is a type of electrical component that stores energy for use later in an electric circuit to produce electric pulses (PEF systems). There are many kinds of capacitors on the market, including mica, paper, ceramic, electrolytic, and non-polarized capacitors [99]. Recently, a lot of electronic applications have been using electrochemical double-layer capacitors (EDLC), also known as electrochemical capacitors (ECs), or supercapacitors [97]. Typically, capacitors are made up of two parallel conductive (metal) electrodes that are separated by non-conducting materials (dielectrics), for instance, liquid gel, mica, ceramic, plastic, or waxed paper, similar to how electrolytic capacitors are made. The capacitor prevents direct current from passing through it because there are dielectric materials sandwiched between two conducting ones. As a result, a voltage will be stored as an electrical charge in the conductive metal plates [97]. The size, quantity, and resistance of the charging resistor are some of the variables that affect how much power is required to charge the capacitor [100]. It was determined that charging a larger capacitor required more energy and time than charging a smaller capacitor. The capacitor's capacitance $C_0\,(F)$ can be computed using the **Equation (2).** Where σ (S/m) is the conductivity of the food sample, d (m) is the distance between the two electrodes, τ (s) is the pulse duration, A (m^2) is the area of the electrode surface, and $R\ (\Omega)$ is the resistance [93].

$$C_0 = \frac{\tau}{R} = \frac{\tau\sigma A}{d} \qquad (2)$$

As indicated in **Equation (3)**, the energy stored (Q) in a capacitor is computed using the charged voltage (V) and values of capacitance (C_0) [93].

$$Q = 0.5\, C_0\, V^2 \quad (3)$$

The switching device, known as a switcher, is an essential component of the effectiveness of the PEF system. In order to disconnect or connect the current and release the energy stored in the capacitor, the PFN is essential in the circuit. ON/OFF (totally controlled) and ON (semi-controlled) switchers are the two most common types of switches. A switcher is chosen for a circuit based on its ability to function at high voltage and its repetition rate. In semi-controlled switches, the capacitors must be depleted entirely to turn off the switcher (including Ignitron, Gas Spark Gap, Trigatron, and Thyratron). These switches can affordably regulate high voltages. The primary disadvantages of these switches are their short lifespan and low repetition rate. The wholly controlled switches (including the gate tum off (GTO) thyristor, insulated gate bipolar transistor (IGBT), and symmetrical gate commutated thyristor (SGCT) may regulate the pulse production process and are turned off and on with either a partial or complete discharge of the capacitors. The introduction of semiconductor totally controlled switches boosted the longevity and enhanced the performance of switches [34,93]. The pulse shape is affected by the relative electrical value of each PFN system element. A simple resistance-capacitance (RC) circuit, for example, will lead to the production of a pulse shape that degrades in an exponential manner. Instead, complex PFN systems have the potential to produce instantaneous reversal pulses, in addition to square and bipolar pulses (**Figure 3**). The production of exponential decay pulses requires only ON switchers, during which the capacitor will be fully discharged. The fully regulated discharge of a capacitor, which may be accomplished with the help of ON/OFF switchers, can be used to generate square wave pulses [98].

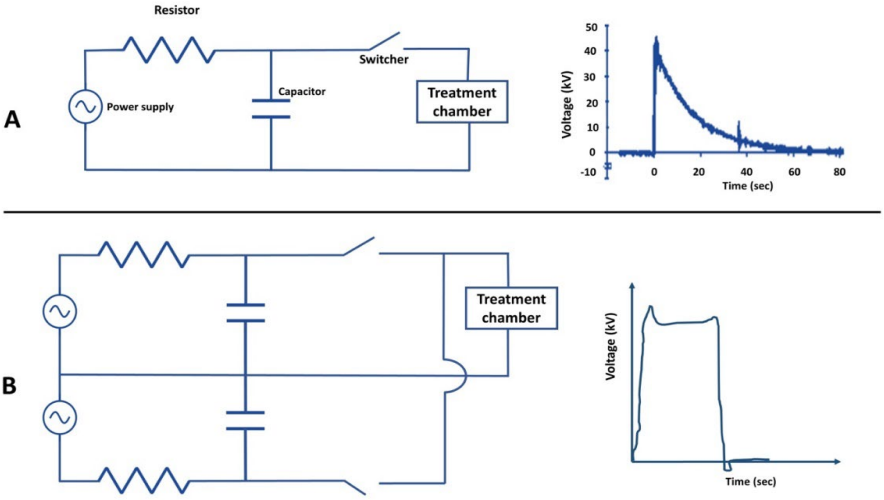

Figure 3 Electrical circuit types and their pulses' shapes: (A) The exponentially decaying pulse of the simple resistance-capacitance (*RC*) circuit; (B) The square pulse shape of the complex electric circuit. Reprinted from (Taha et al. [1]).

A resistor is an essential component of electrical circuits. It is used to force voltage reduction and control current flow. Electric resistance theory is comparable to water flow in pipes; the resistor (wire in the electric circuit) could be considered a narrow pipe that reduces the water flow rate [96]. When the current flow is reduced, the resistor absorbs the electrical energy and dissipates it as heat. The capacitors are classed according to the materials used in their manufacture: wire-wound, semiconductor film or cermet (metal-oxide or metal), and carbon-based capacitors. The link between current (*I*), voltage (*V*), and resistance (*R*) was defined by Ohm's law of resistance; one ohm (Ω) equivalents a volt per ampere [96,101].

For the purpose of subjecting food samples to an electric field, distinct treatment chambers are built. Static chambers are utilized for lab-scale or batch processing, while continuous chambers are more suited for addressing industrial-scale requirements. Batch chambers have various advantages at the lab-scale, including the ability to treat small sample volumes, efficient temperature control via electrode cooling, and the capability to slow down repetition rates. Continuous chambers, on the other hand, are essential for supporting high-volume capacity and can be integrated into the currently existing food processing lines [94,98]. The treatment chambers must be constructed from a material that is either autoclavable or washable. Currently, three basic types of treatment chambers have been established, characterized

by the arrangement of electrodes in various geometries: parallel plate, coaxial, and co-linear chambers [52,98]. Batch processing uses parallel and coaxial plates due to their efficiency. These plates suit batch processing treatment chambers. Co-linear chambers treat food samples in continuous processing machines (**Figure 4**).

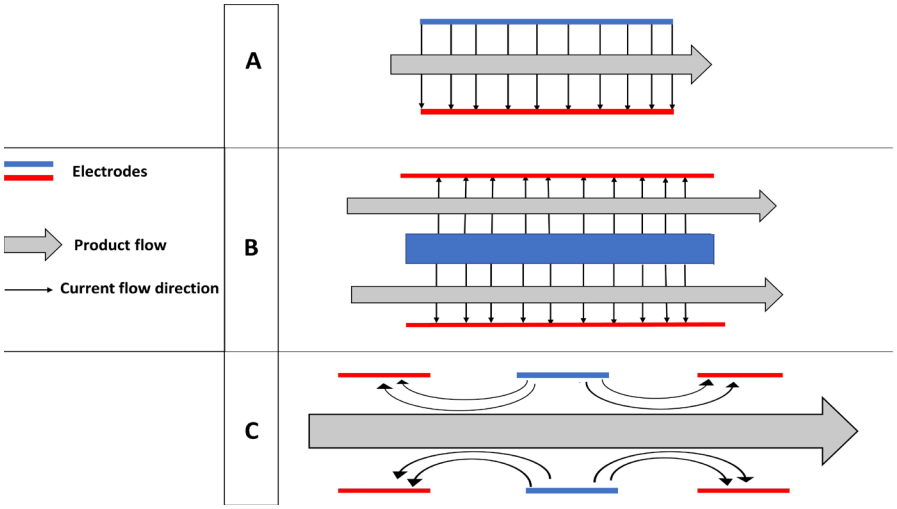

Figure 4 The schematic illustration shows the many types of treatment chambers found in PEF devices. A) parallel plate chambers; B) coaxial plate chambers; C) co-linear plate chambers. Reprinted from (Taha et al. [1]).

Several businesses have recently made significant progress in creating new PEF devices specifically developed for industrial applications. For their operation, the large-scale PEF devices currently in use primarily rely on Marx generators, where electric pulses are continuously applied. In Marx generators, a set of capacitors are sequentially charged in parallel and discharged in a manner that produces a high power conversion rate. On the other hand, a pulse transformer and a low-voltage switch are used in transformers. The majority of PEF devices have average power output that usually ranges from 20 to 400 kW [102].

Treatment chamber designs are made to meet the requirements of certain applications. Belt and pipe systems are the two main varieties of treatment chambers. Processing solid products like potatoes or shellfish typically uses belt systems. The solid food products are moved through the treatment chamber by a device resembling a conveyor belt so they can be exposed to the proper electric field. However, processing liquid goods is done using pipe systems. The liquid food products pass through pipes in these chambers,

allowing effective treatment and electric field exposure. Depending on the type of food product being processed, the treatment chamber type is chosen; belt systems are best for solids, while pipe systems are made for liquids [103].

Numerous aspects of the product and the technique influence the efficacy of PEF processing. The chemical makeup of the food, pH level, rheological characteristics (such as viscosity and consistency), temperature, and electrical conductivity of the product being handled are all important product aspects. Similarly, different process variables greatly impact how PEF treatment turns out. The electric field intensity used during treatment, the quantity of pulses delivered, the frequency at which the pulses are applied, the pulse shape, the length of each pulse (pulse width), the kind of treatment chamber utilized, the flow circumstances within the chamber, and the flow rate of the product through the chamber are some of these parameters. The effectiveness and desired results of PEF treatment on food products are determined by the interaction between these products and process parameters [104]. Due to many circumstances, comparing PEF treatment data from different research groups is difficult. This review discusses these factors. We will examine how PEF affects milk protein structure and function. These results will help us understand how PEF therapy impacts milk protein properties and functions.

2.4 Effects of PEF on the structure of dairy and plant proteins

Figure 5 summarizes casein and whey protein subunits. It shows that casein has 4 major subunits: αs1-casein, αs2-casein, β-casein, and kappa-casein. Whey proteins contain α-lactalbumin (α-LA), bovine serum albumin (BSA), β-lactoglobulin (β-LG), lactoferrin, and minor amounts of immunoglobulins and glycomacropeptide [105,106]. The structure of milk proteins often changes following heat treatment, causing the proteins to unfold. This unfolding is driven by the dissolution of covalent bonds within the protein structure. Intermolecular sulfhydryl (-SH) groups are then exposed to the surface, forming new disulfide bonds which are responsible for aggregation.

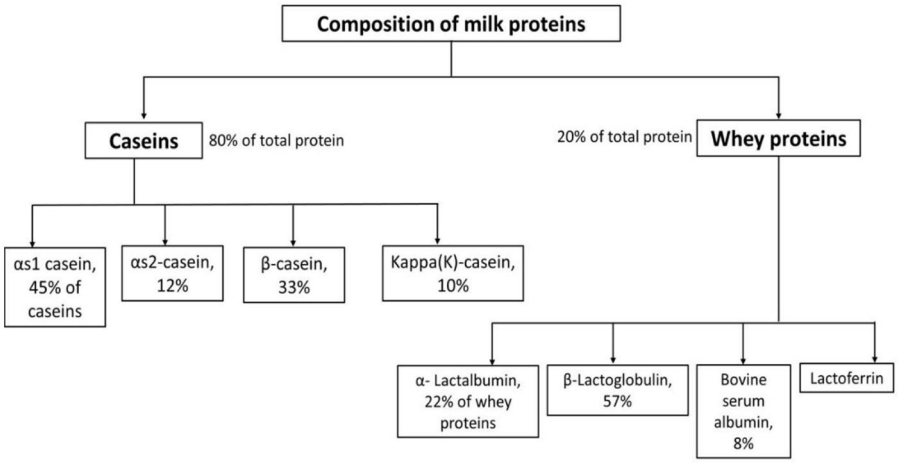

Figure 5 A diagram represents bovine milk composition (data summarized from Abd El-Salam et al. [105] and Onwulata et al. [106]). Reprinted from (Taha et al. [1]).

Additionally, α-LA is less vulnerable to heat processing than β-LG because free thiol groups are not present in α-LA [20]. Studies revealed that PEF could alter the structure of milk proteins, particularly at higher EFS and various temperatures [10]. PEF devices generate energy that may affect the structure of protein molecules. In particular, this energy may cause amino acid residues and/or free sulfhydryl (-SH) groups to be exposed. The energy generated by PEF may also disturb the non-covalent interactions that help to form the protein's structure, such as hydrogen bonds and hydrophobic interactions [20]. It has been discovered that PEF treatment modifies the amino acids' charge density, particularly at carboxyl (-COOH) and amine ($-NH_4^+$) groups. In turn, this can influence the catalytic activity of peptides [107]. Growing interest has been directed to whey proteins because of their industrial applications and nutritional benefits.

The available research studies regarding the impact of PEF on whey proteins structures are inconsistent **(Table 3)**. Sui et al. [108] studied the influences of PEF processing at various temperatures (19.2-211 s, 30-75 ˚C, 30-35 kV/cm) on the functional and structural properties of whey protein isolates (WPI). The study found that PEF processing had no effect on surface hydrophobicity, protein unfolding, or the concentration of free-SH groups [108]. In contrast, Xiang et al. [9] noticed that PEF treatment increased both extrinsic fluorescence intensity and surface hydrophobicity of WPI using a unique treatment chamber with varied electrode spacing. Similarly, the natural structure of β-LG was altered by PEF treatment at 12.5 kV/cm for 10 pulses,

and protein aggregation was produced, according to Perez et al. [8]. The discrepancies in the results could be explained using various experimental setups, such as variations in the treatment chambers, EFS, frequency, and temperatures used in the investigations [34]. Bovine lactoferrin was PEF treated at a variety of temperatures ranging from 30 to 70 ˚C [37]. At the same temperatures, samples treated and untreated with PEF were compared. As a result of the PEF treatment (35 kV/cm, 19.2 s, 30-70 ˚C), the results showed that the lactoferrin concentration remained constant. Furthermore, there is no obvious change between PEF-treated and control lactoferrin, as revealed by the gel profiles of SDS-PAGE. In contrast, increased temperatures were found to increase the hydrophobicity of the surface. Notably, there were no appreciable variations in the surface hydrophobicity of control and PEF-treated lactoferrin [37]. Bekard et al. [109] applied Circular Dichroism (CD) spectroscopy to examine the influences of low EFS on the conformational state of BSA. According to the study, BSA's tertiary structure changed after being exposed to low EFS (500 V/m) for three hours at temperatures between 22.7 and 24.2 °C. The hydrogen bonds are crucial for sustaining the native structure of BSA; the disruptions in these bonds could cause these alterations [109]. In a study by Sharma et al. [110], milk samples were heated (55 ˚C for 24 seconds) before being exposed to a PEF for 34 microseconds at strengths ranging from 20 to 26 kV/cm. The study's conclusions showed that higher EFS significantly increased the surface hydrophobicity of proteins. Furthermore, it was shown that the thermal treatment between 30 and 55 °C led to the dissociation of β-LG dimers into monomers [111]. The dissociation of β-LG dimers in milk samples has been demonstrated to possibly be aided by the combination of thermal pre-treatment and PEF, exposing hydrophobic and free sulfhydryl (-SH) groups [110]. A comparison was made between traditional heat treatment and moderate electric field (MEF) at temperatures ranging from 50 to 90 ˚C[112]. The researchers found that, compared to traditional thermal treatment at the same temperature, MEF showed increased content of random coil and α-helix structures and reduced concentration of β-sheet structures at 70 and 80 ˚C treatments. The combined effects of thermal treatment and the electric field on the conformational state of β-LG probably contributed to these observed structural alterations.

Table 3. The impact of PEF treatment on the structural characteristics of dairy proteins. Reprinted from (Taha et al. [1]).

Dairy protein	PEF conditions	Structural changes	Reference
Whey proteins	35.5 kV/cm for 300 -1,000 µs. frequency of 111 Hz and 7 µs Pulse duration.	Significant variations in serum albumin, α-LA, and β-LG concentrations between PEF-treated samples.	[113]
WPI	12-20 kV/cm, 10-30 pulses	• More exposed hydrophobic groups. • WPI fraction partial denaturation.	[9]
WPI	30-35kV/cm, 60 mL/min flow rate, 30-75 ˚C and pulse duration of 19.2-211 µs.	• There were no noticeable differences between the PEF and non-PEF control samples in the SDS-PAGE gel pattern. • After PEF treatment, there was no discernible change in surface hydrophobicity.	[114]
Lactoferrin	35 kV/cm, 60 mL/min flow rate, 2 µs pulse width, and a pulse frequency of 200 -100 Hz.	• There are no significant changes between the surface hydrophobicity values of PEF-treated and untreated lactoferrin. • No significant difference in the surface hydrophobicity.	[37]

Dairy protein	PEF conditions	Structural changes	Reference
β-LG	12.5 kV/cm, 40 μF of capacitance for 1-10 pulses with 15s interval between pulses.	β-LG was partially denatured by PEF.	[8]
Whole milk	20-26 kV/cm, pulse width of 20 μs, pulse duration 34 μs, bipolar square wave pulses.	Milk proteins' surface hydrophobicity rose as the EFS increased.	[110]
Sodium caseinate	60 Hz sine wave alternating current, 10-150 V/cm for 5s to 2h.	Sodium caseinate's secondary structure was changed by MEF, which also caused the protein molecules to unfold.	[44]
β-LG	20 kHz frequency for 5-7 minutes at 20 V/cm during holding and 80 V/cm during heating.	β-LG secondary structural alterations	[112]
BSA	EFS of 78, 150, 300 and 500 V/m for 3h.	The tertiary structure of BSA was altered by a low EFS.	[109]

Caseins (80% of total milk protein) are an important protein source in human nutrition and have received little attention regarding the impact of PEF on their structure. Subaşı et al. [44] examined the influence of MEF treatment (at 230 V/cm) on sunflower protein and sodium caseinate. FTIR results revealed that MEF treatment could cause alterations in the secondary structure of sodium caseinate, resulting in protein unfolding. This action is most likely due to the MEF-induced polarization of the protein molecule's surface, which enhances the exposure of hydrophobic groups [8,44].

Based on the available literature, the PEF influence on the structures of milk proteins can be stated as follows: PEF treatments with low EFS had no discernible influence on the structure of milk proteins. High EFS, conversely, can drastically affect the proteins' structure, notably whey proteins.

According to the information provided in **Figure 6**, exposing milk proteins to high EFS causes energy absorption by polar groups within the proteins. This energy absorption can produce free radicals, which can disrupt numerous protein-protein interactions, including disulfide and hydrogen bonds, Van der Waals forces, and electrostatic and hydrophobic interactions. Furthermore, PEF can influence the strong dipole moment of the polypeptide chains, resulting in an increased dielectric constant of proteins. These structural alterations in proteins may facilitate protein molecule unfolding and expose hydrophobic and sulfhydryl (-SH) groups. When the duration of PEF treatment is extended, it may result in the development of protein aggregates as unfolded protein molecules crosslinked via covalent and hydrophobic contacts [8,20,21]. It is vital to note that during PEF treatment, temperature has a major impact on the denaturation of protein molecules. Therefore, it is advisable to carry out research on PEF's impact on protein structures in temperature-controlled environments. **Table 4** shows how PEF treatment changed the structural makeup of plant proteins. For example, PEF treatment at EFS ranging from 30 to 50 kV/cm caused alterations in the secondary structure of soy protein isolate (SPI). Due to the development of hydrophobic contacts and disulfide (S-S) bonds, this treatment caused SPI to denature and aggregate [7,115]. Significant alterations in the secondary and tertiary structures of sunflower protein were seen when it was subjected to MEF (150 V for 20 s) at temperatures below 45 °C. The protein's hydrophobic connections were discovered to be affected by PEF treatment, which also facilitated amino acid side chain crosslinking [44]. Similar findings were confirmed with canola and pea proteins [116,117]. In general, it has been verified that PEF treatment has a significant effect on the structure of plant proteins. These structural alterations may affect the technological and

functional characteristics of these proteins. Due to the altered protein structure brought on by PEF treatment, features like solubility, emulsification, foaming, gelation, and rheological behavior may change. Therefore, PEF treatment has the ability to affect how plant proteins function and is used in different food and industrial processes.

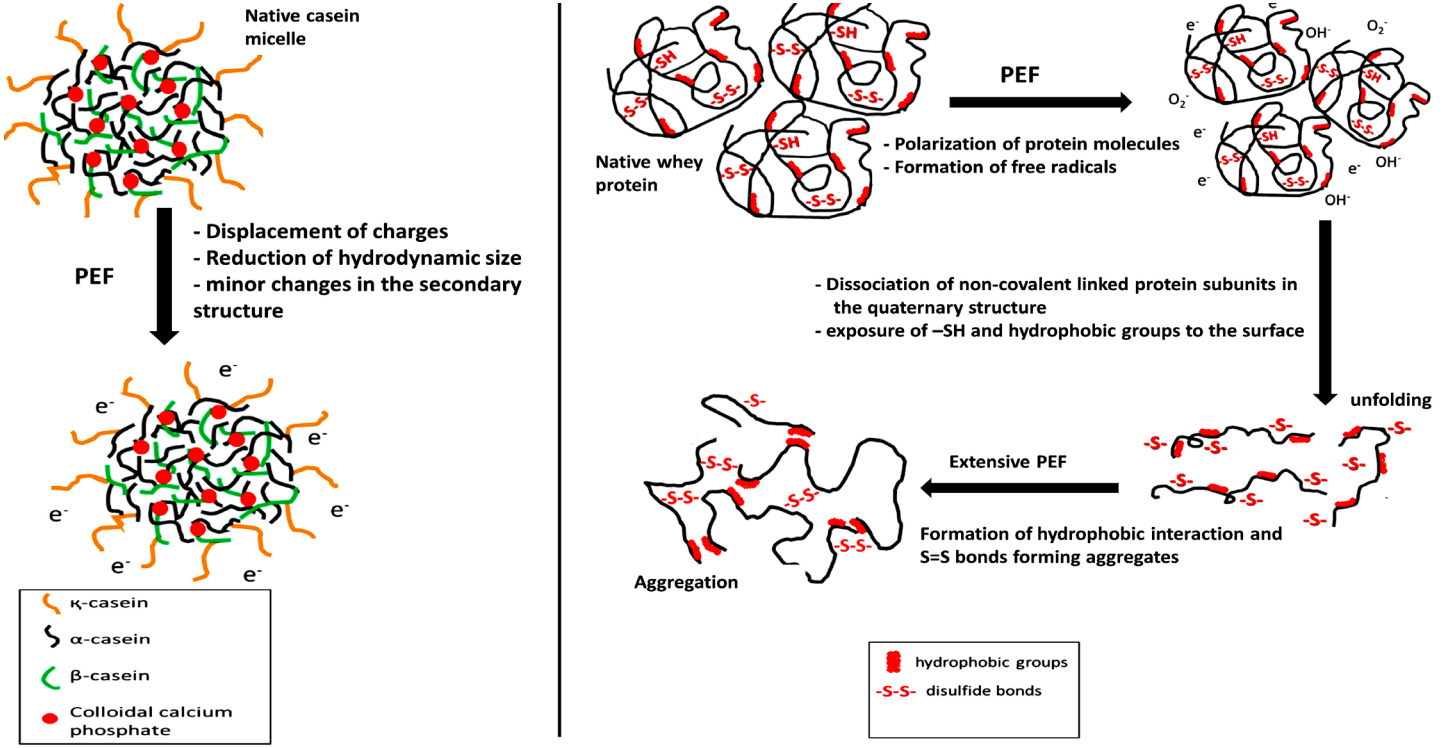

Figure 6 Schematic diagram represents the mechanism of PEF effects on milk protein structural properties (whey proteins and caseins). Reprinted from (Taha et al. [1]) and modified from [20] with permission (License number: 5607640132535).

Table 4. Influences of PEF on the structure of plant proteins. Reprinted from (Taha et al. [1]).

Plant protein	PEF conditions	Structural changes	Reference
Soy protein isolate (SPI)	0-40 kV/cm, pulse width of 2 ms, 500 pulse per second (pps), 0-547 μs treatment duration.	- PEF led to minor modifications in the secondary structures. - SPI aggregated and became denaturized after PEF treatment.	[7]
SPI	0 to 50 kV/cm, a pulse width of 40 μs, a frequency of 1 kHz, and a flow rate of 10 mL/min.	- Reduced hydrogen bonding strength and altered polar group vibration caused by PEF resulted in an increase in anti-parallel β-sheets and a decrease in β-turns.	[118]
Sunflower protein	At a temperature of 25–45 °C, 10-150 V/cm for 5s–2h.	Sunflower protein's secondary and tertiary structures were changed by MEF at 150 V for 20s.	[44]
Canola protein	600 Hz pulse frequency, 8 s pulse width, and a voltage range of 10 to 35 kV.	- PEF produced protein molecule aggregation. - PEF boosted α-helices and β-sheets while decreasing β-turns and random coils.	[116]
Pea protein isolate	Frequencies from 50 Hz to 20 kHz) and EFS of 5, 10 and 20 V/cm).	- When exposed MEF (20 V/cm at a frequency of 50 Hz), the α-helix collapsed into a β-sheet structure. - Exposure of aromatic amino acids to the solvent.	[117]

2.5 The impact of PEF treatment on the techno-functional characteristics of plant and dairy proteins

The techno-functional characteristics of milk proteins refer to their physicochemical qualities that influence their behavior in food systems [119]. Changes in protein structure can affect their functional characteristics [26]. Techno-functional abilities, such as solubility, gelation, emulsification, and foaming abilities, are essential for many applications in the food industry [120]. Consequently, this part will investigate the impact of PEF on the functional characteristics of milk proteins. **Table 5** summarizes the key studies exploring the effects of PEF on the functional properties of milk proteins, while **Table 6** reviews the studies concentrating on the PEF's impacts on the functional characteristics of plant proteins.

Table 5. Effects of PEF on the techno-functional properties of dairy proteins. Reprinted from (Taha et al. [1]); an open access article.

Dairy protein	PEF conditions	Changes in protein functionality	Reference
Raw milk	30 kV/cm EFS, 50±1 ˚C outlet temperature, 80-120 pulse numbers, 2 μs pulse width, and 2 Hz pulse frequency.	Rennet coagulation time (RCT) is greater for unpasteurized milk than for pasteurized milk.	[121]
WPI	25 kHz frequency, 15–22 V/cm heating phase, 4–8 V/cm holding phase.	The MEF produced a gel structure that was weaker than the traditional heat treatment.	[122]
β-LG	20 kHz at a frequency of 20 V/cm during holding and 80 V/cm during heating.	At pH 7, MEF and thermal treatment (up to 60 C) affected the free SH group relativity in a similar manner. At higher temperatures, the free SH group relativity of conventionally heat-treated materials was greater than that of MEF-treated samples.	[112]
WPI	30-75°C, 19.2-211 s, and 30-35 kV/cm	• Emulsions stabilized with PEF-treated and heat-treated (72˚ C for 15s). • WPI exhibited comparable droplet diameters and, consequently, emulsifying properties. • While increasing the period of heat treatment to 10 minutes, the droplet size of emulsions stabilized by heat-treated WPI increased significantly.	[114]

Dairy protein	PEF conditions	Changes in protein functionality	Reference
		• The gel strength of PEF-treated WPI was less than that of untreated samples. Increasing the time of PEF decreased gel strength further.	
β-LG	12.5 kV/cm EFS and 40 μF of capacitance.	PEF enhanced the gelling rate of β-LG (at 72 ˚C) when less than six pulses were applied.	[8]
WPI	50 to 90°C, 2 to 8, and 15 to 55 kV/cm	When treated at 35 kV/cm, the gelling characteristics of WPI enhanced, but reduced when treated at 45 kV/cm.	[123]

Protein solubility

Protein samples are separated by centrifugation to determine their solubility, and the amount of soluble proteins is then measured in relation to the total protein concentration. Investigating the behavior and functional characteristics of proteins in many situations, including food systems, is facilitated by measuring protein solubility [124]. Numerous intrinsic factors influence protein solubility, including the capacity of proteins to dissolve in a solvent or media. The composition of the amino acids found in the protein sequence is a crucial consideration. The solubility behavior of different amino acids can be affected by their individual chemical characteristics, such as polarity and hydrophobicity. In addition, protein molecular weight is another essential factor since larger proteins often have less solubility than smaller ones. Proteins' solubility is also influenced by their surface properties. By encouraging interactions with the solvent, hydrophilic groups, such as charged or polar residues, can improve solubility. Furthermore, hydrogen bonding is important for the solubility of proteins. To understand and control protein solubility, it is crucial to know the complex interplay of these intrinsic variables. Protein solubility can be adjusted for various purposes in industries, including biotechnology, pharmaceuticals, and food science by modifying elements like amino acid content, molecular weight, surface characteristics, and hydrogen bonding [67,125]. The protein solubility can also be affected by numerous external parameters, such as pH, ionic strength, temperature, and the presence of solvents [126]. In many food applications of proteins; for example, as emulsifiers or foam stabilizers, protein solubility is a critical component as it influences the development of well-dispersed colloidal systems [127]. Investigations of the effects of PEF treatments on protein solubility are summarized in the following paragraph.

According to studies using a PEF system (at 25 kV/cm) with square-wave pulses, PEF reduced the solubility of soluble egg white proteins (by 7.84 %)[128], gluten concentrate (from 25 to 22.4 %), rice concentrate (from 16.4 to 9.2 %), and pea concentrate (from 23.2 to 17.2 %) [129]. Protein unfolding, the creation of insoluble protein molecules, and the occurrence of intermolecular interactions, such as disulfide (S-S) bonds, are all responsible for the decline in solubility. However, Li et al. [7] noticed that PEF treatment (30 kV/cm) with a bipolar waveform increased the solubility of SPI. A small reduction in solubility only occurred at EFS greater than 30 kV/cm. Additionally, compared to control samples (43.25 %), PEF treatment at 35 kV/cm for 8 s enhanced the solubility of canola protein to 50.07 % [116]. These findings emphasized that the specific protein type and the used electric

field conditions impact the effect of PEF treatment on protein solubility. However, considering the particular parameters (EFS, pulse shape, treatment duration, treatment chambers, etc.) used in the treatment procedure, more research is needed to fully understand the variables influencing the desirable solubility changes of milk proteins after PEF treatment.

Table 6. PEF effects on the functional properties of plant proteins. Reprinted from (Taha et al. [1]).

Plant protein	PEF conditions	Protein functionality changes	References
SPI	500 pulses per second (pps) pulse frequency, 2 ms pulse width, and EFS of 0-40 kV/cm for 0-547 μs.	- PEF reduced the surface hydrophobicity and solubility.	[7]
Canola protein	600 Hz pulse frequency, 8 μs pulse width, and a voltage range of 10 to 35 kV.	The solubility, emulsifying and foaming capabilities of canola protein were all enhanced after PEF treatment.	[116]
Sunflower protein	At 25–45 °C, 10-150 V/cm for 5s–2h.	- MEF treatment at 20V decreased the interfacial tension at the air/water interface.	[44]
Pea protein isolate	(50 Hz and 20 kHz) and voltages (5, 10 and 20 V/cm).	- Pea protein was subjected to a MEF treatment (50 Hz and 20 V/cm), which improved the gelling characteristics and raised the protein's surface hydrophobicity.	[117]

Gelling properties

Disulfide linkages and -SH groups substantially impact the ability of proteins to form gels. The capacity of milk proteins to form gel-like structures determines the quality of numerous dairy products such as desserts,

yogurt, and cheese [130]. According to studies, PEF treatment can improve the ability of some proteins to gel. When exposed to fewer than six PEF pulses, Perez et al. [8] found that β-LG gelled quicker at 72 °C. The effects of PEF at 20 and 30 kV/cm and various outlet temperatures on the rennet coagulation properties of raw milk were examined by Yu et al. [121]. Compared to pasteurized milk samples, they noticed that PEF-treated milk at 20 °C had firmer curds. A decreased rennet coagulation time (RCT) in the PEF-treated milk samples also suggests enhanced gelling qualities [121]. However, it should be noted that the protein type and the used electric field parameters both affect how the PEF treatment affects gelling qualities. According to Jin et al. [123], gelling characteristics of WPI increased after PEF treatment at 35 kV/cm but reduced following PEF treatment at 45 kV/cm.

The increased gelling qualities of milk proteins during PEF treatment can be attributed to several variables (**Figure 7**). First, it is possible that milk proteins unfolding and -SH group exposure can create new S-S bonds and boost gel formation. Furthermore, the polarization of protein molecules following PEF treatment might facilitate the electrostatic interactions that further promote gelation [8]. It is worth mentioning that depending on the protein type and the PEF conditions, the impact of PEF on gelling properties can change. In contrast to untreated samples, Sui et al. [37] showed that WPI treated with PEF at 30 kV/cm displayed lower gel strength. Additionally, the gel strength of WPI sample samples decreased as PEF treatment time increased. In the study published by Rodrigues et al. [122], it was concluded that WPI samples treated with conventional heat exhibited stronger gel strength compared to those treated with MEF treatment (15-22 V/cm). The observed disparity in gel strength might be attributed to the presence of electrostatic repulsion between protein molecules under neutral pH conditions, reducing the size of protein aggregates[131]. Applying the electric field during PEF treatment could disrupt non-covalent protein interactions, influencing the gel characteristics [122]. At lower EFS (25 kV/cm), the water-holding capacity (WHC) of PEF-treated canola protein increased, but it decreased at higher EFS (35 kV/cm) [116]. Similarly, pea protein isolate treated with a lower EFS produced weaker, more elastic, and cohesive gels with a higher WHC [117]. Inconsistencies in gelling property results among studies could be attributed to differences in PEF parameters, such as voltage, pulse waveform shape, and treatment chamber type. These parameters can have a substantial impact on protein interactions and structural alterations, resulting in various gel characteristics and WHCs. Although the precise effects depend on the protein type and the electric field conditions used, our

findings highlighted the potential of PEF treatment to improve the gelling properties of some proteins. Additional studies are required to fully understand and maximize the impact of PEF on the gelling characteristics of different protein systems.

Emulsifying and foaming properties

The stability of emulsions is essential for prolonging the shelf life of emulsion-based foodstuffs (i.e., margarine, milk, butter, mayonnaise, and ice cream). Diverse emulsifiers are utilized to lessen interfacial tension and improve emulsion stability in order to increase emulsion stability [82]. With their surface-active properties, proteins are frequently used as natural emulsifiers [11,132]. Diverse processing methods, including high-pressure [67], sonication [82,133], cold plasma [60], and microwave [62], have been investigated for their ability to enhance the emulsifying capabilities of proteins. However, PEF effects on the foaming and emulsifying capabilities of dairy proteins are poorly understood. Sui et al. examined the influences of PEF combined with heat treatment on the emulsifying capabilities of WPI in their study [108]. The droplet diameters of emulsions stabilized by heat-treated (72 ˚C for 15s) and PEF-treated (30 kV/cm) WPI were reported to be around 4 μm. In contrast, the droplet size of WPI-stabilized emulsions heated for 10 minutes was substantially bigger at 18.3 μm. This indicates that PEF treatment enhanced the emulsion stability comparable to heat treatment. Sun et al. [134] investigated the influences of PEF treatment (15-30 kV/cm) on the emulsifying capabilities of WPI-dextran conjugates. The investigation revealed that the untreated conjugates had a lower emulsifying activity index (EAI) compared to the PEF-treated conjugates. This suggests that PEF treatment improved the emulsifying qualities of the WPI-dextran mixture. It was observed that PEF treatment accelerated the glycosylation reaction between dextran and WPI. The effectiveness of enhancing emulsion stability has been confirmed by the incorporation of both proteins and polysaccharides. The hydrophilic regions of polysaccharides can align themselves towards the aqueous phase, while the hydrophobic segments of proteins can adhere to the surface of oil droplets, thereby offering steric stability and limiting the coalescence of droplets [82].

Zhang et al. [81] studied canola proteins and noticed that PEF-assisted extraction of protein and oil from canola seeds increased the foaming and emulsifying capabilities of the resultant proteins. The PEF treatment improved the foaming and emulsifying abilities of plant-based proteins by increasing their solubility and exposing their hydrophobic groups. To completely comprehend the impact of PEF treatment on the emulsifying and foaming

capabilities of both dairy and plant proteins, additional research is required. It has been proposed that the modifications in protein structures caused by PEF treatment contribute to the enhancement of protein functioning. As seen in **Figure 7,** Protein molecules may polarize and unfold in response to PEF treatment, exposing their hydrophobic groups [21]. In addition, PEF treatment at a particular EFS can reduce the particle size and increase the protein solubility. These modifications can decrease interfacial tension at the water/ oil interface, hence improving the stability of protein-stabilized emulsions and the emulsifying ability of food proteins [135].

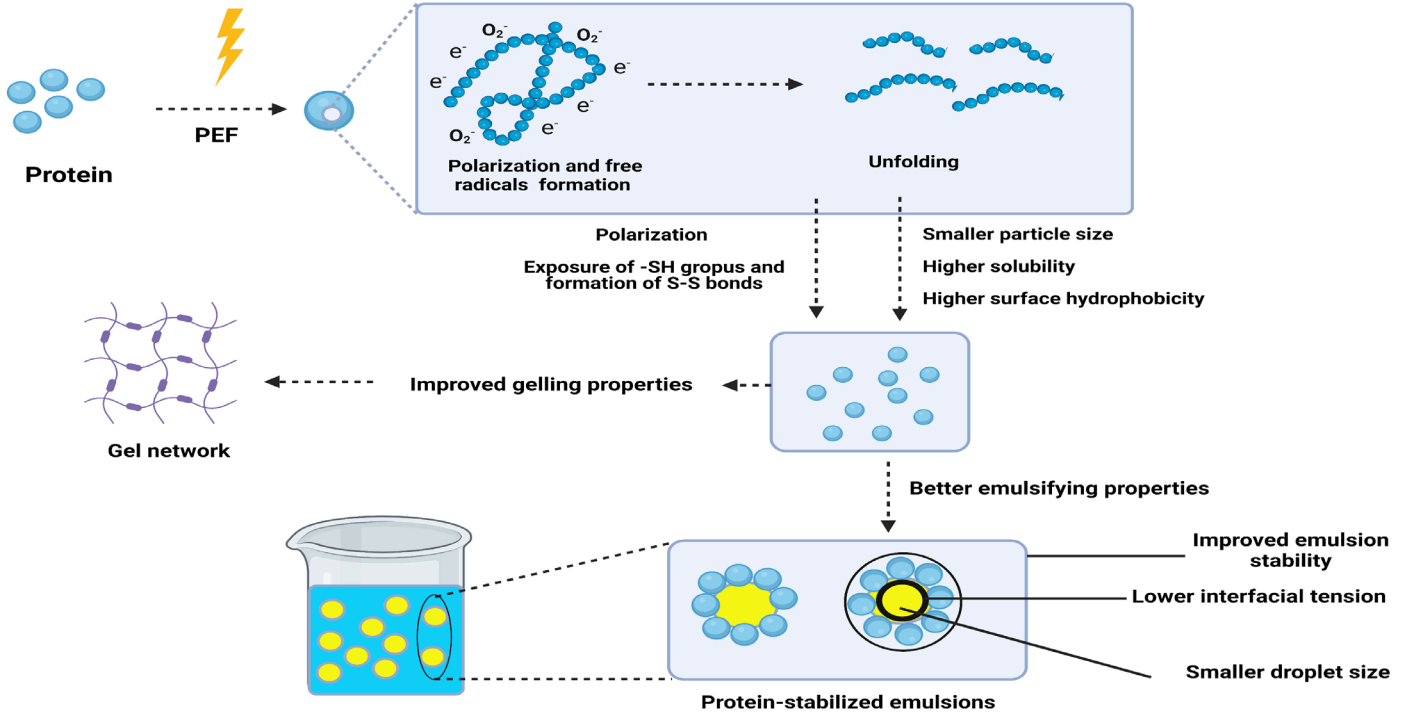

Figure 7 Schematic diagram represents a proposed mechanism of PEF effects on the gelling and emulsifying properties of proteins. This figure was created using BioRender (https://biorender.com/) with publication permission. Reprinted from (Taha et al. [1]).

CHAPTER 3: METHODS

3.1 PEF treatment of BSA/starch mixtures

The BSA/starch mixes were made by dissolving soluble starch (2 mg/mL) in distilled water and heating the mixture to around 50 °C until the starch was fully dissolved. The solution was allowed to cool to ambient temperature once it became transparent. The soluble starch solution was subsequently mixed with BSA (2 mg/mL) for an additional hour at room temperature [141]. A Mettler Toledo conductometer with an InLab 738-ISM sensor was used to measure the electrical conductivity of the BSA and BSA/starch mixtures. Before applying the PEF treatment, the reported electrical conductivity values for the BSA and BSA/starch mixtures were 1.430 and 1.240 mS/cm [133]. A 4 mm gap electroporation cuvette (Model No. 640, BRT HARVARD APPARATUS®, Holliston, USA) was next used to hold 0.9 mL of the dispersion. A pulse generator manufactured at the State Research Institute, Center for Physical Sciences and Technology (FTMC), Vilnius, Lithuania, was used to treat the dispersions in triplicates. Our recent publication [142] provides comprehensive technical details surrounding the pulse generator (Figures **8 and 9**). Each sample was treated for 10 pulses during the PEF treatment, with a pulse duration (τ) of 50 μs. **Table 7** presents the EFS and sample codes. Both before and after the PEF treatment, the samples' pH levels were examined. The pH values were somewhat lower, but they were still within the neutral range (6.98–7.34), and the shift was not statistically significant [133]. During the PEF treatment, a FLIR one pro infrared camera (Teledyne FLIR LLC, Oregon, US) was utilized to track temperature changes. The camera was connected to an Android smartphone.

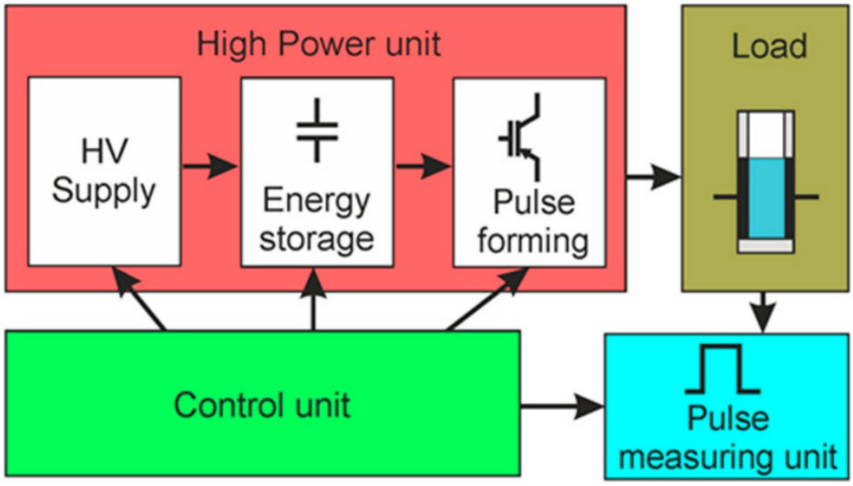

Figure 8 Block diagram simplification of the square-wave pulse generator. HV: High voltage; reprinted from [142].

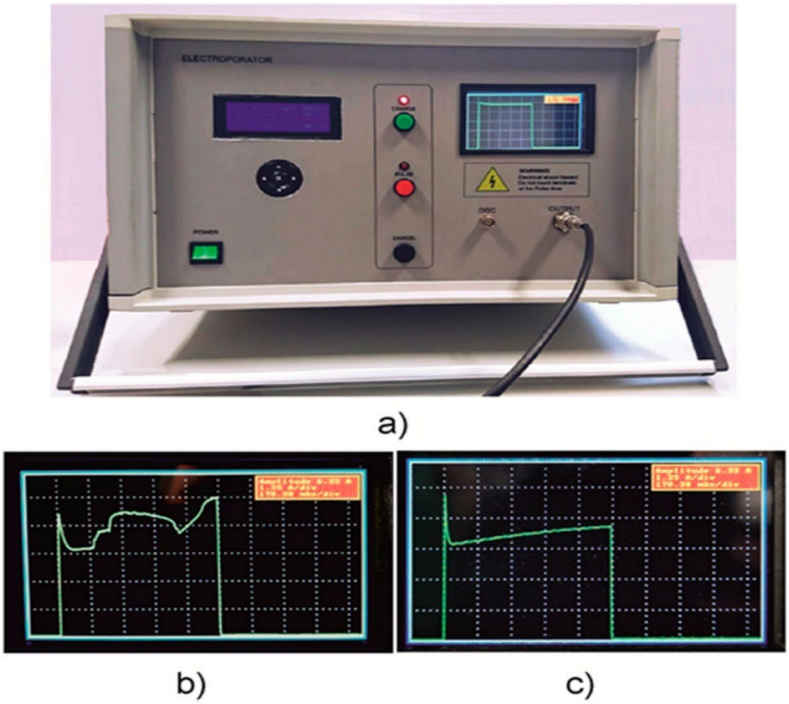

Figure 9 A) An image of the compact square-wave generator. (B, C) Images of the display depicting when the sparking in the cuvette occurs (B) and when the current during the pulse grows due to the cuvette's substance heating (C), reprinted from [142].

Table 7 The calculated EFS and the abbreviations of samples' names, temperature, and pH values. Reprinted from [143].

Sample code	BSA (mg/mL)	Soluble starch (mg/mL)	Applied voltage (V)	EFS (kV/cm)	pH	Temperature (° C)
B	2	-	-	-	7.34±0.03[a]	22.5±0.2
BS	2	2	-	-	7.02±0.05[a]	22.5±0.2
BS-PEF 1	2	2	1500	3.5±0.3	7.00±0.03[a]	23.5±0.3
BS-PEF 2	2	2	2000	4.5±0.5	7.00±0.02[a]	24.4±0.5
BS-PEF 3	2	2	2500	5.7±0.5	6.98±0.04[a]	24.7±0.5
BS-PEF 4	2	2	3500	8.1±0.7	7.00±0.03[a]	25.8±0.4

3.2 PEF treatment of casein micelles (CSMs)

To prepare the protein suspension, a 1% (w/v) protein solution was prepared in potassium phosphate buffer (0.1 M, pH = 7) and continuously stirred overnight for optimal dispersion. Subsequently, 0.5 mL of the protein suspension was transferred to the Fisher electroporation cuvette with a 2 mm gap (Thermo Fisher Scientific Inc., USA). The samples' conductivity was determined to be 6.5 mS/cm through measurement. The following settings were used for the PEF treatment: applied voltages of 2, 4, and 6 kV (equivalent to electric field intensities of 10, 20, and 30 kV/cm, respectively) for 10 pulses. The corresponding current values for these voltage settings were 360, 680, and 1060 A. The pulse duration was determined to be 480 ns based on the time constant of the exponential decay pulse shape (**Figure 10**).

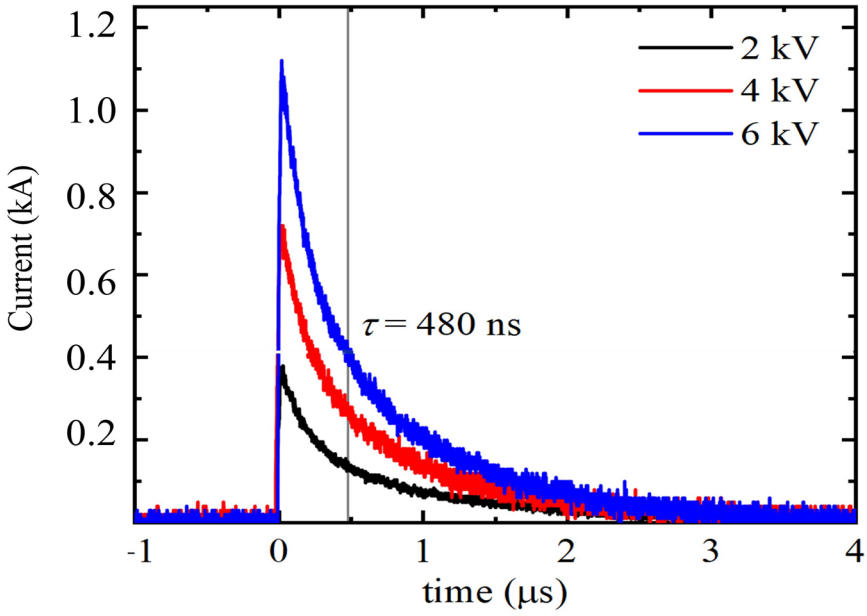

Figure 10 The generated electric pulses showing the pulse duration and the applied current. Reprinted from our open-access article [198].

At the Center for Physical Sciences and Technology (FTMC), Vilnius, Lithuania, a specifically built generator was used to produce the PEF that was used in this study. The generator has a high voltage source with a 20 kV maximum output, a capacitor bank with a 100 nF capacitance, and a 30 kV maximum voltage. It should be noted that a 2 mm cuvette can generate an electric field as high as 100 kV/cm.

The cuvette holding the sample was placed in a container with two flexible metal contacts to administer the PEF treatment. A shunt resistor was connected in series to measure the current flowing through the cuvette, and a high-voltage divider was used to measure the voltage. The generated pulse had an exponential structure, and its time constant was expressed as " $\tau=RC$ " where "R" stands for the capacitor's capacitance and "C" for the equivalent circuit resistance. The duration of the PEF treatment, which is dependent on the resistance of the solution being treated, may be easily controlled thanks to this design. **Figure 11** represents the electric circuit used in the electric field generating system.

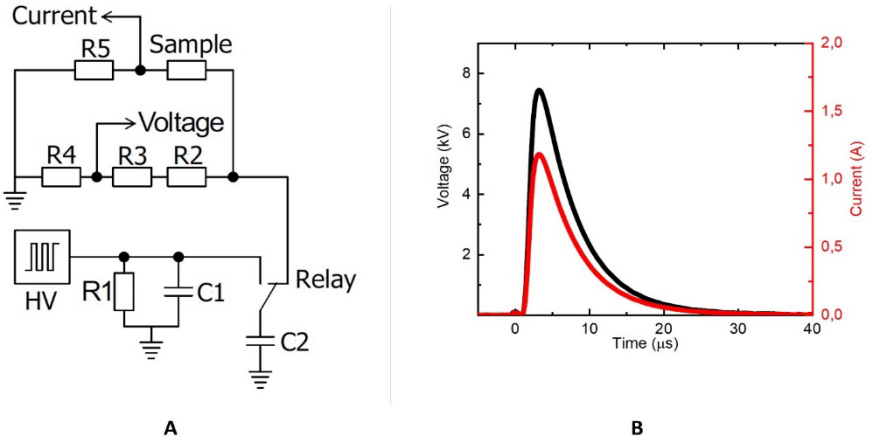

Figure 11 (A) Schematic diagram of the homemade electroporator electrical circuit, (B) generated electric pulse. R1= 55 MΩ; C1=C2= 100 nF; R2=R3=500 kΩ; R4= 47 kΩ; and R5= 0.1 Ω. Reprinted from our open access article [198].

3.3 PEF treatment of BSA and BSA/EGCG mixtures

10 mg/mL of BSA was prepared using distilled water and stirred for 30 min. The electric conductivity of the solution was adjusted to 2.5 mS/cm to comply with the resistance requirement of the nsPEF generator. Subsequently, 0.5 mL of the protein suspension was transferred to the Fisher electroporation cuvette with a 2 mm gap (Thermo Fisher Scientific Inc., USA). The following settings were used for the PEF treatment: applied voltages of 4, 6, 8, and 10 kV (equivalent to electric field intensities of 8, 12, 16, and 20 kV/cm, respectively) for a single pulse with a pulse duration of 90 ns. Then, in another set of experiments, 3 pulses were applied to BSA/EGCG mixtures. The

detailed diagram of the nsPEF generator is shown in **Figure 12**. **Figure 13** represents the summary of the experimental design.

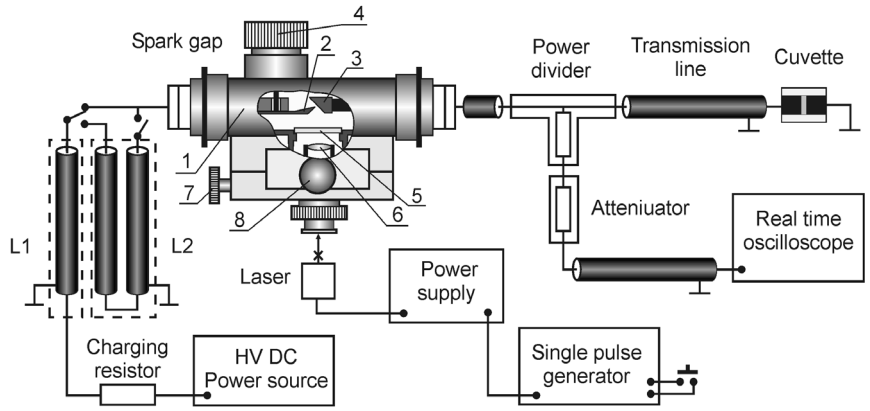

Figure 12 The detailed diagram of the nsPEF generator design; source: [231] with permission.

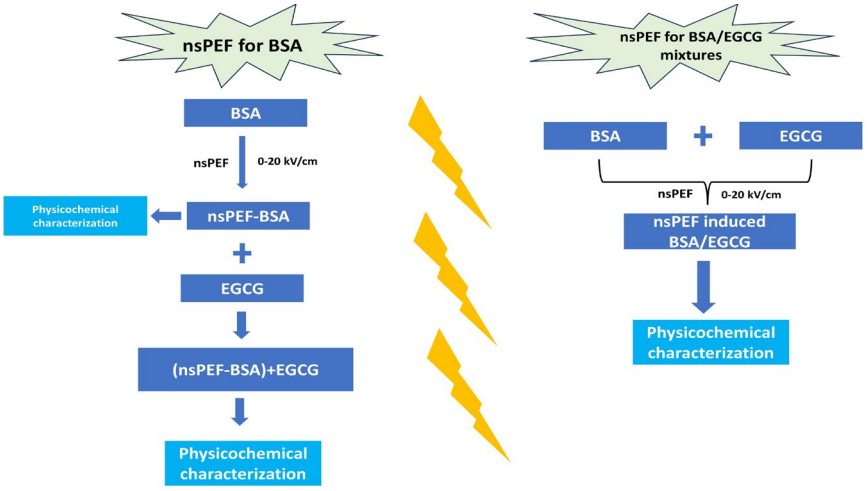

Figure 13 Schematic diagram representing the study design of this section.

3.4 Characterization of BSA/starch conjugates and their stabilized emulsions

Browning intensity (A420 nm) and UV–vis spectra

Using a UV-visible spectrophotometer (Halo RB-10, Dynamic Scientific Ltd., Livingston, United Kingdom), the absorbance of Maillard reaction products at 420 nm was measured in order to assess the degree of browning.

In addition, using the same spectrophotometer, the UV-Vis spectra were recorded between 260 and 340 nm [140,144].

Grafting degree

Using the OPA (1,2-Phthalic dicarboxylate) technique [145], Glycated BSA's grafting degree (DG) was measured. By dissolving 80 mg of OPA in 2 mL of methanol and adding it to 50 mL of 0.1 M borate buffer (pH=9.7), the OPA reagent was produced. This mixture was added to 200 µL of β-mercaptoethanol and 5 mL of a 20% (w/w) solution of SDS. Using distilled water, the final volume was brought to 100 mL. After production, the OPA reagent was immediately employed. For DG measurement, 4 mL of the OPA reagent was added to 200 µl of the BSA/starch conjugates and incubated for 2 minutes at 35 °C. A UV-vis spectrophotometer was then employed to measure the absorbance of the reaction mixture at 340 nm. Distilled water was utilized as a blank, and BSA/starch samples without PEF treatment served as the reference standard. Using the following formula, the DG (%) was determined:

$$DG\ (\%)=\frac{A_B - A_{BS}}{A_B} \times 100 \qquad (4)$$

Where A_{BS} stood for conjugates of BSA and starch conjugates while A_B for native BSA absorbance.

Surface hydrophobicity (H_o) measurement

Using 1-anilino-8-naphthalenesulfonate (ANS) as a fluorescent probe, the hydrophobicity (Ho) values of BSA and BSA/starch conjugates were measured. For each sample, 3 mL of the solution (0.02, 0.1, 0.2, 0.5, and 1 mg/mL of protein) was added to 60 µL of an ANS solution containing 8.0 mM. The samples were then incubated for 30 minutes in the darkness. The fluorescence intensities were thereafter assessed utilizing a PerkinElmer LS 50B spectrometer (PerkinElmer, Waltham, MA, USA) equipped with a 5 nm slit width at excitation and emission wavelengths of 390 nm and 470 nm, respectively. Determining the slope between fluorescence and protein concentration enabled calculating the Ho value [146].

Intrinsic fluorescence emission spectroscopy

Using phosphate buffer (0.1 M, pH 7.0), The concentration of BSA and BSA/starch conjugate samples were adjusted to 0.5 mg/mL. The spectra of intrinsic fluorescence were measured with a PerkinElmer spectrometer (LS 50B). Each sample (3 mL) was placed into a 10 mm quartz cuvette. The fluorescence emission spectra were collected between 290 and 450 nm, and

the excitation wavelength was 280 nm. Both the emission and excitation slits were set at 10 nm [147].

Particle size

The particle size (zeta average) was assessed using dynamic laser light scattering (DLS) using a Malvern Zetasizer analyzer (Nano ZS, Malvern Instrument Co., Ltd., Worcestershire, UK) before and after PEF treatment at a temperature of 25 ºC. The conjugates and dispersant had refractive index values of 1.45 and 1.33, respectively [148].

Protein Solubility

The solubility of proteins was determined by modifying the method of Zheng et al. [72]. 1 mL (protein content of 2 mg/mL of BSA, P_C) was centrifuged at 12,000 g for 25 min in 1.5 mL microcentrifuge tubes. The concentration of proteins in the supernatant (P_S) was determined using the Bradford protein assay. Using **Equation 4**, the protein solubility (%) was determined.

$$\text{Protein solubility}(\%) = \frac{P_S}{P_C} \times 100\% \quad (5)$$

Emulsion preparation

0.5 mL of sunflower oil (10%, v/v) was added to 4.5 mL of BSA/starch conjugates or BSA samples and was vortexed to prepare coarse emulsions. The emulsification procedure was done with an ultrasonic processor (Sonics VC 505, Sonics & Materials Inc, Newtown, USA). The ultrasound machine with a 13 mm probe diameter, 20 kHz frequency and a maximum power of 500 W. 5 mL of the samples were sonicated for 1 minute at a 35 % amplitude in an ice bath for the emulsification procedure. During the sonication process, a 2-second on, 2-second off pulse duration was used. Off-pulse time was not considered; only the effective processing time was counted. Using **Equation 6** and the approach provided by Koh et al. [181], the energy density (J/mL) was estimated. The energy density range was 700–750 J/mL in this study.

$$\text{Energy density (J/ml)} = \frac{\text{Power drawn (W) X Time (s)}}{\text{Volume (mL)}} \quad (6)$$

Emulsion characterization

Droplet size characterization

The emulsion sample concentrations were diluted 1:50 with distilled water. A Malvern Zetasizer analyzer was then used to determine the droplet sizes of

the emulsions (Nano ZS, Malvern Instrument Co., Ltd., Worcestershire, UK). The tests were performed at a temperature of 25 ˚C and a scattering angle of 90˚.

Adsorbed protein (AP %)

The examination of AP (%) surrounding oil droplets was performed based on the approach reported by Taha et al. [170]. 1 mL of each emulsion sample was centrifuged for 30 minutes at 10,000g and 25 °C at a speed of 10,000g. Subsequently, 0.22 m filters were used on the supernatant to remove any remaining particles. The Bradford assay [182] was used to quantify the protein content (Fc) in the filtered supernatant. Using **Equation 7**, the percentage of AP was then computed.

$$AP(\%)=\frac{P_C - F_C}{P_C}\times 100\% \qquad (7)$$

Confocal Microscopy

The microstructural properties of the emulsions were studied using a Nikon Ti2-E inverted microscope (Nikon, Tokyo, Japan) with a 40x objective lens. Each emulsion sample (1 mL) was mixed with 20 µL of FITC (Fluorescein isothiocyanate) solution for protein staining (excitation wavelength: 488 nm, emission wavelength: 515 nm) and 20 µL of Nile Red solution for oil staining (emission wavelength: 605 nm, excitation wavelength: 543 nm) [23]. After that, on a microscope slide, 5 µL of each emulsion sample was placed before being covered by a glass coverslip. NIS-Elements application (NIS-Elements, Nikon, Tokyo, Japan) was utilized to capture and process the micrographs.

Differential scanning calorimetry (DSC)

Differential scanning calorimetry (DSC) study was carried out to assess the stability of the emulsions under freezing conditions. When evaluating the performance of emulsion-based frozen goods, DSC analysis is a crucial tool for understanding the emulsions' thermal properties [183]. A DSC 8500 instrument (Perkin Elmer, USA) was used to perform the DSC measurements. A typical aluminium pan was filled with between 3.7 and 4.3 mg of each emulsion sample, which was then sealed within and covered with a lid for the analysis. At first, the temperature was lowered from 40°C to -40°C at a rate of 10°C/min. For five minutes, the samples were maintained at -40 °C to guarantee thermal equilibrium. The temperature was then elevated from -40°C to 40°C at a rate of 10°C / min. In order to maintain an inert atmosphere

throughout the analysis, The blanket gas was nitrogen, flowing at a rate of 40 mL/min (20 mL/min in each furnace).

Emulsion stability at the isoelectric point (p*I*) condition:

Following the emulsion preparation process, HCl and NaOH solutions with a concentration of 0.1 M were used to get the emulsion sample pH values to 4.6 ± 0.1. This pH value corresponds to the isoelectric point of BSA, as reported in previous studies [184,185]. Subsequently, the microstructure, AP %, and droplet sizes of the emulsions were examined to assess their stability under these p*I* conditions.

Emulsion stability under different ionic strengths:

NaCl powder was added to the emulsions to reach the final concentrations of 150 and 300 mM. These specific concentrations were determined based on our previous study [132]. The impact of varying ionic strength on emulsion stability was then investigated by analyzing the emulsions' microstructure, AP %, and droplet sizes.

3.5 Characterization of PEF-treated CSMs

Surface hydrophobicity (H_0) measurement, intrinsic fluorescence emission spectroscopy, particle size, ζ-potential, and protein solubility were characterized according to the methods described in **section 3.4**.

Turbidity

The CSMs solution was diluted (1:10), and the adsorption values were measured at 600 nm using a UV–visible spectrophotometer (Halo RB-10, Dynamica Scientific Ltd., Kirkton Campus, Livingston, UK) [199].

Fourier transform infrared spectroscopy (FTIR)

The infrared spectra of freeze-dried CSMs, BSA and BSA/EGCG samples were obtained using an infrared spectrometer (Spectrum 100, PerkinElmer, Norwalk, CT, USA). 2 mg of each sample were scanned 32 times with a resolution of 4 cm^{-1} over a range of 400 to 4000 cm^{-1}. The IR spectra of both untreated and PEF-treated CSM were obtained.

The amide I region (1600-1700 cm-1) was particularly interesting to analyze the secondary structural changes in proteins. The Peakfit software (version 4.12, Seasolve Software Inc., CA, USA) was employed to identify any hidden peaks within this region. This analysis provided valuable insights into the modifications occurring in the secondary structure of the proteins.

Raman spectroscopy

Raman spectra were recorded using an Echelle-type spectrometer RamanFlex 400 (PerkinElmer, USA). The excitation source was a 785 nm laser, and a thermoelectrically cooled CCD detector (-50 ºC) along with a fiber-optic cable was used. The laser beam, with a power of 100 mW, was focused on the surface of CSM powder samples dispersed on a Tienta steel substrate (SpectRIM, Merck, USA). The measurements were performed at room temperature with an acquisition time of 1800 s. The ratio of the double peaks observed near 850 cm^{-1} and 830 cm^{-1} (I_{850}/I_{830}) was calculated to investigate the hydrogen bonding microenvironment of phenolic hydroxyl groups [72].

Scanning electron microscopy (SEM):

To examine the morphology of both control and PEF-treated CSMs, a Hitachi SU-70 SEM device (Minato-ku, Tokyo, Japan) was utilized. The CSM powder samples were gold-sputtered to create a thin coating before imaging. The SEM analysis was conducted at an accelerated voltage of 2 kV, and micrographs were captured at magnifications of 250 and 2,000X.

3.6 Characterization of nsPEF-treated BSA and BSA/EGCG mixtures

Surface hydrophobicity (H_0) measurement, intrinsic fluorescence emission spectroscopy, particle size, ζ-potential, Raman spectroscopy, FTIR, and UV-vis spectroscopy were performed as described in **sections 3.3-3.5**.

Circular Dichorism (CD)

The far-UV spectra of BSA (0.1 mg/mL) were obtained using Jasco J-150 (Jasco Co., Japan) at room temperature. The average of 2 scans was collected at a wavelength range from 190-260 nm. The contents of secondary structures were calculated using the DichroWeb online platform for CD spectra deconvolution by applying the CDSSTR analysis program [232,233].

Molecular dynamic and docking simulation.

In order to further personalize the forces that drive the binding between BSA and EGCG, a docking experiment was conducted using the libDock-protocol in Discovery Studio (DS, ver. 2.5) and the libdock-algorithm, which was available from Accelrys Software Inc. (San Diego, CA, US). The X-ray crystal structure of BSA was made available by the RCSB Protein Data Bank

(PDB: 3v03, Resolution: 2.7 Å) (http://www.rcsb.org/pdb). As a ligand, EGCG (PubChem CID: 65064, https://pubchem.ncbi.nlm.nih.gov/compound/65064) was used. To fit into the receptor pocket, the docked conjugate was adjusted for unique and continuous hydrophobicity, van der Waals bonds, H-bonds, electrostatics, and entropy. To reflect a molecule's most beneficial binding mode, the docked model with the greatest scoring (i.e., lowest docking energy) was chosen from the docking data. Solvent-available surface area (SASA) was calculated after molecular dynamic simulation (MD) runs were maintained every 10 ns for a total of 80 ns. First, the EGCG geometry was optimized using the M062X operation and the 6-31G (d, p) support provided by the Gaussian 09 program. Atomic charges were re-expressed using the RESP algorithm, and solvent realization was carried out using the IEF-PCM test. EGCG was double-minimized, located randomly around RCSB (20 Å), and executed [234].

Statistical analysis

Data are presented as the mean and standard deviation and were collected from studies carried out in triplicate. The statistical analysis was done using the SPSS program (IBM SPSS Statistics, version 25, SPSS Inc., Chicago, IL, USA). A one-way ANOVA was utilized, followed by Duncan's test ($p<0.05$), to assess the statistical significance of mean differences.

CHAPTER 4: PULSED ELECTRIC FIELD-ASSISTED GLYCATION OF BOVINE SERUM ALBUMIN/STARCH CONJUGATES

- Effects of PEF (3.5 - 5.7 kV/cm, 50 μs) on the glycation between BSA and soluble starch were investigated.
- BSA/soluble starch glycation was facilitated by PEF treatment.
- PEF affected the physicochemical properties of BSA/soluble starch conjugates.

4.1 Introduction

Recently, the application of green technologies in the food sector as a strategy to improve sustainability and environmental friendliness has received considerable interest. PEF is one such technique that has been extensively studied and provides excellent prospects for many food processing applications. PEF processing has been predominantly applied for enzyme and microbial inactivation, allowing the nutritional value of PEF-processed food products to be preserved [33,136]. PEF treatment involves exposing food samples to high EFS in short pulses, typically between microseconds and milliseconds. This exposure to electric fields induces a range of chemical and physical changes in the food matrix proteins [10]. Numerous investigations have revealed that PEF treatment can alter the functional and structural characteristics of dietary proteins efficiently [20,21,137].

The production of free radicals is one of the main mechanisms through which PEF affects protein structure. During PEF processing, polar groups within proteins are exposed to high EFS, producing free radicals. Protein-protein interactions (including hydrophobic interactions, electrostatic interactions, disulfide bridges, Van der Waals forces, and hydrogen bonds) can be disrupted by these free radicals [21,138]. In addition, it was confirmed that PEF treatment altered the surface charge of proteins. This change in charge results from alterations in the ionic interactions of proteins, which can have a substantial impact on their structural and functional properties [20,46]. These alterations in charge distribution can affect protein solubility, aggregation, and molecule-to-molecule interactions within the food system. Understanding the structural and functional changes generated by PEF treatment in dietary proteins remains an active research topic. However, the studies to date imply that PEF can significantly change protein functioning and, consequently, the quality of food products. Continued research into the specific impacts of PEF parameters, including EFS, pulse shape, duration, and the design of the treatment chamber, is required to optimize PEF settings for changing the structural and technological properties of target proteins [20,21,137].

There have been few investigations into the impact of PEF on protein-polysaccharide conjugates and their physicochemical characteristics [134,139,140]. However, it has not been determined how specifically PEF-induced electrochemical alterations will affect the physicochemical characteristics of BSA/soluble starch conjugates. This study aims to

investigate how PEF treatment alters the physicochemical characteristics of BSA/starch conjugates. By analyzing the interactions between proteins and polysaccharides during PEF treatment, this research can help to improve knowledge of the underlying mechanisms.

4.2 Materials

Soluble starch from potato (Product Number: S-9765), BSA, Coomassie blue dye (G250), sodium dodecyl sulphate (SDS), and sodium azide were purchased from Sigma Aldrich (St. Louis, Missouri, USA). According to the supplier's information, starch possesses the following structure and properties: physical form: amorphous powder; 78 % amylopectin, 20 % amylose; ash content 0.4 %; pH=6.0-7.5 at 25 ˚C, 2% in solution). Merck supplied ethanol 100%, methanol, phosphoric acid, and hydrochloric acid (Darmstadt, Germany). β-mercaptoethanol, sodium hydroxide, and sodium chloride were obtained from AppliChem GmbH (Darmstadt, Germany). 1,2-Phthalic dicarboxaldehyde (98 %, OPA) was acquired from ACROS Organics, Fisher Scientific GmbH, Schwerte, Germany. MP Biomedicals was the source of Nile red dye (Illkirch, France). Fluorescein isothiocyanate acquired from Fluorochem Ltd. (Hadfield, UK). 8-Anilino-1-naphthalenesulfonic acid (ANS) was bought from Cayman Chemical Company (Michigan, USA). ANIRA UAB (Kaunas, Lithuania) produced sunflower oil that was acquired from a local market in Vilnius, Lithuania.

4.3 Results and Discussions

4.3.1 Protein-polysaccharides interactions

By comparing the absorbance (A_{420}) of PEF-treated and reference samples [149], the PEF effects at various EFS on the rate of glycation were determined. The A_{420} value indicates the progress of browning intensity during the last stages of the Maillard reaction [140,150]. The A_{420} values enhanced with increasing the EFS, with the greatest values seen in the BS-PEF 3 group **(Table 8)**. This significant rise indicated an increase in the Maillard reaction's intensity. At greater EFS (>8.1 kV/cm), the A_{420} values decreased. The increased browning intensity indicates that the Maillard process is approaching its terminal phases. The observed rise in A_{420} values indicates that PEF treatment may enhance the browning process caused by the Maillard reaction. This result is likely because of the polarization and breakdown of protein-protein connections within BSA molecules following PEF treatment,

promoting the interaction between soluble starch and BSA molecules [20]. Guan et al. [139] showed that PEF-induced BSA-dextran conjugates had higher browning intensity following treatment at 10 and 20 kV/cm, 30 mL/min a flow rate in a continuous PEF system, and τ of 7.35 ms. The decrease in A_{420} values at EFS larger than 5.7 kV/cm can be attributed to the crosslinking of amino groups and intermediate products of the Maillard reaction. Exposing lactose/peanut protein mixtures to a dielectric barrier discharge reactor with a discharge strength of 90 W for more than 3 minutes hindered the development of primary or intermediate products, consequently lowering browning intensity and intermediate products [151].

The UV-Vis spectra of BSA and BSA/soluble starch conjugates treated with PEF were observed between 260 and 340 nm (**Figure 14A**). Maximum absorbance was reported for all treatments at wavelengths between 277.5 and 278 nm, corresponding to the π→π* transition of BSA [152,153]. Following PEF treatment, the absorbance intensity rose, with BS-PEF 3 having the greatest absorbance value of 1.33±0.07 at 277.5 nm. These results imply that a ground-state combination and a Schiff base of BSA/starch are formed [145]. Similar results were reported with gum acacia/WPI conjugates, where UV-vis absorbance values rose with prolonged sonication times [154].

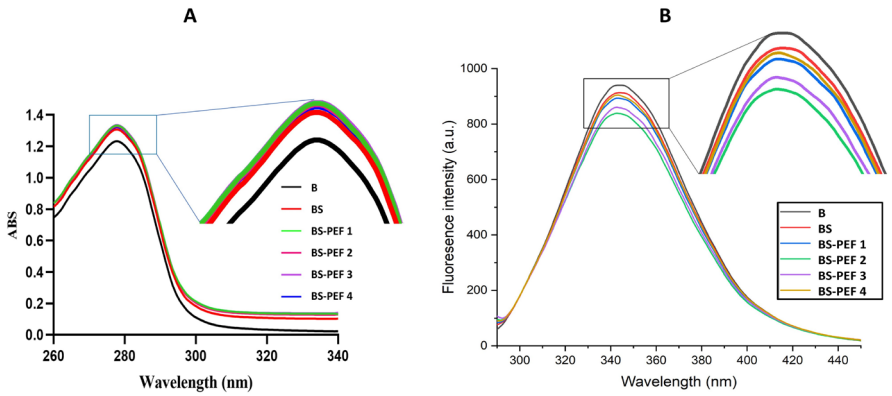

Figure 14 The UV-vis absorption spectra (A) and fluorescence emission spectra (B) of BSA and BSA/Starch conjugates before and after PEF treatment. This figure is reprinted from [143].

Table 8. Browning intensity (A_{420}), Surface hydrophobicity (Ho), z-average, and PDI of BSA without PEF (B) BSA/starch mixture without PEF (BS) and PEF-treated BSA/Starch conjugates (BS-PEF 1 – BS-PEF 4) at different EFSs. Reprinted from [143].

	Browning Intensity (A_{420})	Ho	Z-average (nm)	PDI
B	-	311.3±5.6 [a]	120.1±19.1[a]	0.24±0.04[c]
BS	0.17±0.02[b]	304.4±3.1 [a,b]	26.3±4.9[b]	0.29±0.03[b,c]
BS-PEF 1	0.23±0.03[a,b]	298.4±2.2 [b,c]	19.4±0.1[b]	0.32±0.06[b]
BS-PEF 2	0.27±0.02[a,b]	292.7±3.1[c]	38.3±8.3[b]	0.36±0.03[a,b]
BS-PEF 3	0.34±0.03[a]	291.7±1.4 [c]	160.8±22.4[a]	0.39±0.07[a,b]
BS-PEF 4	0.30±0.03[a,b]	296.6±1.2 [b,c]	211.2±19.4[a]	0.44±0.08[a]

The DG is indicative of the Maillard process and the presence of free amino acids. Higher concentrations of free amino acids in the system facilitate the glycosidic bond formation between the carbonyl groups of polysaccharides and amino groups in amino acids [155]. While the BSA/starch mixtures are being stirred, the glycation degree could occur in the case of BS samples. Wang et al. [156] observed that swirling WPI/pectin mixtures can cause a degree of glycation, even in the absence of heat treatment.

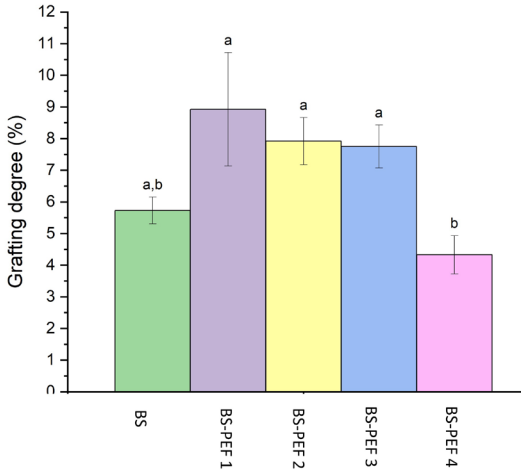

Figure 15 PEF treatment effects on the grafting degrees of BSA and BSA/Starch conjugates.

The findings verify that PEF treatment considerably enhanced the degree of grafting. As indicated in **Figure 15**, lower EFS (3.50.3 kV/cm) resulted in the maximum DG. This rise could be due to the PEF treatment-induced unfolding of BSA molecules, which exposes amino acids to the carbonyl groups of starch molecules. However, the grafting degree steadily declined when samples were exposed to PEF treatments with EFS of more than 3.50.3 kV/cm. Yu et al. [156] observed comparable outcomes with peanut protein/lactose conjugates, in which a short-duration cold plasma treatment improved the DG but decreased when treated for a longer time. Identical tendencies were also seen with (2.5-12.5 kGy) gamma-irradiated soy protein/maltose conjugates [157]. Qu et al. [158] noticed a similar pattern with dextran-rapeseed protein isolate conjugates, where the DG rose with moderate ultrasonic treatment (28 kHz frequency at 65.8 W/L power) but declined with higher ultrasound frequencies (>28 kHz). This decline may be attributable to decreased free amino acids following glycosylation, resulting in a lower DG [151]. The breakdown of conjugates at high EFS or the agglomeration of

protein molecules could be another factor leading to the decline in the DG [159]. At high EFS, PEF can cause the formation of protein aggregates with fewer free amino acids, hence delaying protein-polysaccharide interactions and decreasing the degree of grafting. This conclusion is consistent with those found for particle size and solubility (**Section 3.3.2**).

4.3.2 Particle size and protein solubility

The protein solubility and particle size of BSA/starch conjugates were investigated as indications of their functional characteristics. **Table 8** demonstrates that the averages of particle sizes of BS samples were smaller than those of B samples. In addition, the particle sizes reduced even further following PEF treatment, with the smallest particle size being seen at PEF 3.5±0.3 kV/cm. The conjugated starch in BSA/starch conjugates may reduce the aggregation of BSA. The presence of more hydrophilic soluble starch conjugated to BSA may stabilize a higher surface area, hence decreasing the particle size of conjugates [148]. This result is consistent with our DG observations (**Figure 11**). Nonetheless, the particle sizes gradually grew when the EFS (>3.50.3 kV/cm) rose. The secondary structure of BSA molecules may change as a result of the PEF treatment as it may alter the hydrogen bonds arrangements [20]. Higher EFS can further disrupt protein-protein interactions, resulting in protein unfolding and subsequent aggregation [21]. Similar findings were reported in investigations utilizing gum Arabic-zein, and pectin-soy protein isolate conjugates treated with ultrasound [145,160].

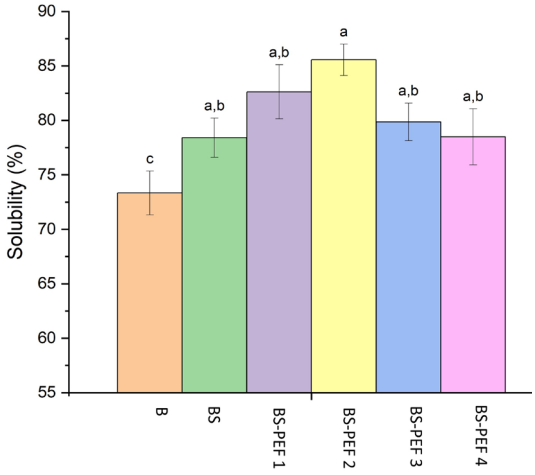

Figure 16 Solubility of native BSA (B), BSA/starch mixture without PEF (BS) and PEF-treated BSA/Starch conjugates (BS-PEF 1 – BS-PEF 4).

Protein solubility can be affected by various factors, such as amino acid composition, the exposure of hydrophobic and hydrophilic groups, the molecular weight, and the number of hydrogen bonds [67,125]. According to **Figure 16**, solubility increased dramatically following PEF treatment, reaching its maximum at 4.5±0.5 kV/cm. PEF treatment has the ability to increase the dielectric constant and produce molecular polarization of proteins, thus altering electrostatic protein-protein interactions [161]. This result is congruent with the findings of Dong et al. [162], who hypothesized that free radicals generated by PEF (18 kV/cm) could disrupt electrostatic interactions and non-covalent bonds, increasing the contact between myofibrillar proteins and water. In addition, the partial unfolding of proteins induced by PEF treatment may expose additional hydrophilic groups, enhancing protein solubility [163]. However, solubility steadily reduced as the EFS increased (>4.5 kV/cm). Li et al. [7] observed that the solubility of soy protein reduced with increasing EFS over 30 kV/cm. Among partially unfolded polypeptides, higher EFS can increase the formation of more disulfide (S-S) bonds and hydrophobic interactions [40,161], formating insoluble protein aggregates. These observations correspond to the particle size information reported in **Table 8**. The greater surface area of particles with smaller sizes is responsible for the increased protein-water interactions. Therefore, the smaller BSA particles can lead to fewer protein aggregates in the pellet after centrifugation, improving protein solubility [164].

4.3.3 H_o analysis and Intrinsic fluorescence

During the conjugation process, the intrinsic tryptophan (Trp) fluorescence spectra of BSA were observed to monitor alterations in the tertiary structure. The maximum fluorescence intensity of BSA and BSA/soluble starch conjugates was achieved at wavelengths between 342 and 344 nm, as shown in **Figure 14B**. The BSA/soluble starch mixes had a lower fluorescence intensity than the BSA sample. In addition, the intensity dropped following PEF processing at 3.5 and 4.5 kV/cm, with a minor blue shift. This reduction in fluorescence intensity is due to starch's shielding effects during the Maillard reaction. The greater DG and Maillard reaction degree at lower EFS can increase the shielding effect and decrease the fluorescence intensity. Following ultrasonic treatment, Ma et al. [165] detected a reduction in the fluorescence intensity of pectin/soy protein isolate conjugates. In addition, the presence of soluble starch in this research prevented the ANS fluorescent probe from accessing the hydrophobic areas of BSA molecules. The

fluorescence intensity increased at EFS greater than 4.5 kV/cm, possibly due to decreased protein aggregation and Maillard reaction degree. These results agreed with the solubility, DG, and particle size findings.

The BSA H_0 values provide insight into the effect of starch conjugation on the protein structure. The H_0 values declined gradually as the EFS increased **(Table 8)**, showing that the tertiary structure of BSA was altered [166]. The generation of less hydrophobic glycation products and the Maillard reaction might alter the structure of BSA and reduce the exposure of hydrophobic groups [165]. Additionally, the hydrophilic hydroxyl groups in starch may increase the hydrophilicity of BSA upon conjugation, leading to a decline in H_0 values [167]. The slight increase in H_0 at higher EFS (8.1 kV/cm) may be attributable to decreased protein aggregation and Maillard reaction intensity. Due to the partial loss of shielding effects of starch, the protein molecules' aggregation, and the decrease in DG at higher EFS could enable the exposure of previously covered hydrophobic groups on the protein surface.

4.4 Conclusion

The Maillard reaction between soluble starch and BSA has been successfully facilitated using PEF treatment. The physicochemical characteristics of BSA/ soluble starch conjugates are significantly influenced by applying various EFSs during PEF treatment. Regarding the BSA/starch conjugates, PEF treatment enhanced the degree of grafting, protein solubility, and browning at EFSs between 3.5 and 5.7 kV/cm. Additionally, the conjugate particle sizes, surface hydrophobicity, and fluorescence intensity were decreased. However, the protein solubility, DG, and particle sizes of BSA/starch conjugates decreased when the EFS exceeded 5.7 kV/cm. These results demonstrate the potential of PEF treatment to alter and improve the properties of food ingredients by highlighting the impact of various EFSs on the physicochemical properties of BSA/soluble starch conjugates.

CHAPTER 5 PHYSICOCHEMICAL PROPERTIES OF O/W EMULSIONS STABILIZED BY PEF-INDUCED BSA/SOLUBLE STARCH CONJUGATES.

- Emulsions were prepared using PEF-induced BSA/soluble starch as an emulsifier.

- The utilization of PEF enhanced the stability of emulsions stabilized BSA/starch conjugates.

- Moderate EFS resulted in improved emulsifying properties of BSA/starch conjugates and better stability of emulsions.

5.1 Introduction

Emulsions have numerous uses in food products, such as processed cheese, mayonnaise, and ice cream, as well as in drug delivery systems, cosmetics, and pharmaceuticals [168,169]. Emulsifiers are required to produce stable emulsions that can keep their stability for a longer time, as emulsions are naturally thermodynamically unstable [82]. Besides their nutritional value and biodegradability, proteins are frequently utilized as emulsifiers due to their ability to interact with both the water and oil phases due to their amphiphilic nature [11]. Protein-stabilized emulsions are nevertheless sensitive to aggressive environmental factors like temperature, ionic strength, and pH [132,170]. Consequently, several studies have been performed to enhance the stability of protein-stabilized emulsions under such challenging conditions [82,145,171–173].

Protein-polysaccharide conjugation is a common method for improving the stability of protein-stabilized emulsions under a variety of environmental conditions [174,175]. These conjugates are produced by non-covalent and covalent interactions, which result in synergistic effects between proteins and polysaccharides, modifying the interfacial properties of the adsorbed layers. Strong attractions can arise between positively charged proteins and negatively charged polysaccharides, especially under acidic conditions (pH < isoelectric point) [176]. Under different conditions, it has been demonstrated that these protein/polysaccharide conjugates increase the stability of protein emulsions. Ultrasound has been utilized to facilitate the protein-polysaccharide conjugation and Maillard reaction. as an environmentally friendly processing approach [165,177]. Studies have demonstrated that ultrasound can alter the structure of citrus pectin and soy protein, improve electrostatic interactions, and enhance the emulsifying properties of their conjugates [178]. This enhancement is due to ultrasound-induced graft reaction acceleration and the improvement of the conjugates' surface hydrophobicity [179,180]. As a novel green technology, it would also be beneficial to investigate how PEF-induced changes in BSA/soluble starch conjugates could affect the stability and physicochemical characteristics of BSA/starch conjugate-stabilized emulsions.

In this work, it was hypothesized that using BSA/starch conjugates as emulsifiers will increase the emulsions' stability by facilitating the Maillard reaction between BSA and soluble starch. There is a lack of knowledge on the effects of PEF treatment on the emulsifying properties of BSA/soluble starch conjugates. This study aims to investigate the emulsifying capabilities of PEF-

induced BSA/starch conjugates and enhance BSA-stabilised emulsions' stability. Additionally, this research can help PEF technology improve and be used in the food industry as a green, sustainable method.

5.2 Results and Discussions

5.2.1 Droplet size and morphology of emulsions

Smaller droplets typically contribute to greater emulsions' stability compared to larger droplets, making the size of emulsion droplets an essential predictor of their stability and physicochemical characteristics [168]. In our investigation, it was discovered that emulsions stabilized by BSA/starch conjugates that had undergone PEF treatment had smaller droplet sizes than emulsions stabilized by native BSA. The emulsions containing the BS-PEF 1 and BS-PEF 2 conjugates had the smallest droplet sizes among the PEF-treated conjugates, with 411.5 and 440.6 nm, respectively (**Table 9**). The conjugates' particle sizes decreased after PEF treatment (**Table 8**), facilitating their quick movement toward the water/oil interface during emulsification. These results were consistent with the DG findings (**Figure 11**), which showed that PEF treatment at lower EFS increased the conjugation between BSA and starch. The improved conjugation may help create a strong interfacial layer, encouraging the production of smaller droplet sizes in the emulsions [186].

In soy protein isolate-lentinan conjugates, an increase in the solubility of SPI can improve the conjugates' emulsifying capabilities, according to Wen et al. [187]. As demonstrated in **Table 8 and Figure 15**, bigger particle sizes and lower DG values for the conjugates were seen in our investigation when greater EFSs were used during PEF treatment. When EFSs were more than 3.5 kV/cm, the emulsion droplet sizes stabilized by PEF-treated conjugates gradually increased. The results from the CLSM micrographs shown in **Figure 17** where BS-PEF 1 emulsions had smaller droplet sizes, which is consistent with this trend. In addition, as shown in **Table 9**, the PEF-treated conjugates (BS-PEF 2, BS-PEF 3, and BS-PEF 4) had reduced amounts of AP (%) surrounding the oil droplets. This is explained by the increased particle sizes and protein molecule aggregation seen in the BS-PEF 4 and BS-PEF 3 conjugates (**Table 8**), which led to less protein being adsorbed and bigger droplet sizes in the emulsions.

Table 9 Adsorbed protein (AP%) and averages droplet size of BSA and BSA/starch conjugates-stabilized emulsions. Reprinted from [143].

	BSA/starch conjugates- emulsions (BSE)	
	z-average (nm)	**AP (%)**
B	620.76±39.48[a]	26.57±1.20[a]
BS	571.33±21.75[a]	26.66±1.94[a]
BS-PEF 1	411.53±28.53[c]	27.22±1.69[a]
BS-PEF 2	440.6±30.45[c]	24.21±1.10 [a]
BS-PEF-3	460.83±40.27[b,c]	19.79±3.96[a]
BS-PEF 4	506.06±13.31[b]	22.38±2.88[a]

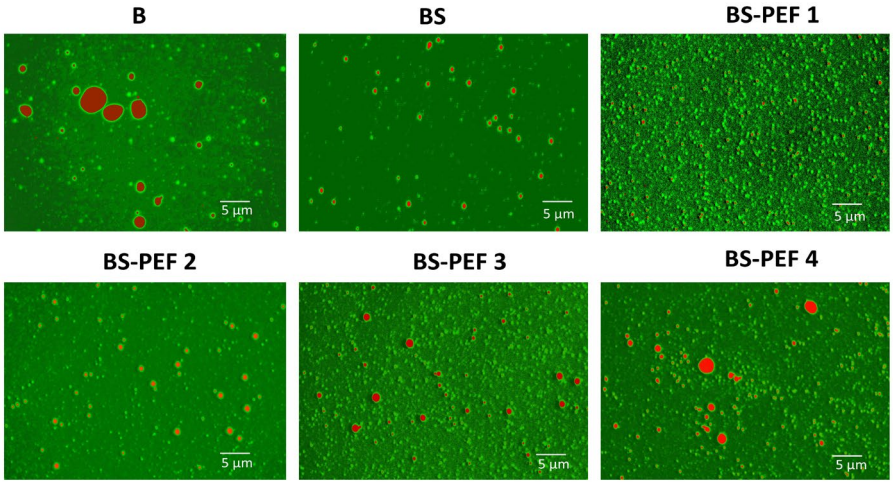

Figure 17 CLSM images of emulsions stabilized with BSA and BSA/starch conjugates with and without PEF treatment. This figure is reprinted from [143].

5.2.3 DSC analysis

DSC is commonly used to assess emulsion freezing stability. The heat flow changes throughout the cooling and heating cycles reveal emulsions' freezing behavior and stability. Sealing emulsion samples in aluminium pans, gradually cooling them to the proper freezing point, and noting thermal transitions during heating is the analysis. DSC data can be used to determine the emulsion's stability during freezing, storage, and thawing. DSC analysis has helped formulate stable emulsion-based products for freezing or low-temperature storage by examining the effects of many components [188,189].

DSC thermograms were used to examine the freezing behavior of emulsions stabilized by native BSA, PEF-treated BSA/starch conjugates, and untreated BSA/starch conjugates (**Figure 18**). The endothermic peaks, which depict the melting behavior of emulsions, did not alter significantly (**Figure 18**), indicating that ice crystal formation predominantly affected the freeze-thaw stability of these emulsions [183]. Peak temperatures for the exothermic peaks, which correspond to the creation of ice crystals, ranged from -12.7 to -15.5 °C. Notably, emulsions' freezing points were lowered after PEF treatment of BSA/starch mixes. The lowest freezing temperature among the emulsions was for BS-PEF 3 (-15.5 °C), whereas the highest freezing temperature was for B emulsions (-12.7 °C), showing that PEF treatment of BSA/starch conjugates may effectively suppress ice crystal formation [190]. According to the browning intensity and DG, the alterations in the exothermic peaks can be linked to the development of more complex BSA/starch conjugates following PEF processing (**Table 8**). In addition, Phase separation in B and BS emulsions may result in a higher volume of water than emulsions stabilized by PEF-treated conjugates, resulting in crystallization at higher temperatures [191]. These results show the efficiency of PEF in modifying ice crystal formation and provide information on the PEF effects on the freezing behavior of BSA/starch conjugate-stabilized emulsions.

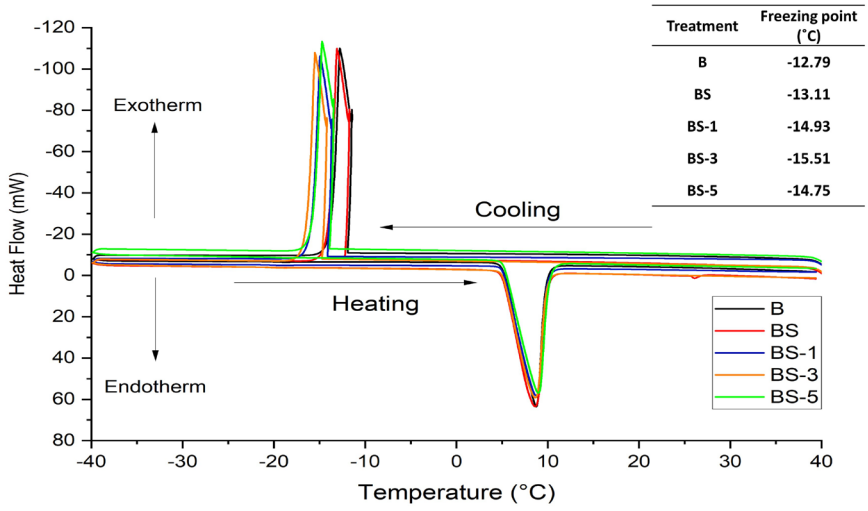

Figure 18 DSC thermograms of BSA and BSA/starch conjugates (with and without PEF treatment)-stabilized emulsions. This figure is reprinted from [143].

5.2.4 Effect of ionic strengths

In many food applications, salt is frequently added to emulsion-based food products. This approach can cause changes in the conformational structure of protein molecules when used as emulsifiers, resulting in protein aggregation. The stability and physicochemical characteristics of protein-stabilized emulsions may then be affected. This study investigated how changing NaCl concentrations (C_{NaCl}) affected the size of emulsion droplets. It was shown that BS-PEF 3 and BS-PEF 1 emulsions had the least average droplet sizes at a C_{NaCl} concentration of 150 mM, whereas B and BS-PEF 4 emulsions had the highest average droplet sizes (**Figure 19 A**). Similarly, with a C_{NaCl} concentration of 300 mM, the smallest average droplet size was seen in the BS-PEF 1 emulsion, whereas the smallest average droplet size was seen in the BS-PEF 4 emulsion (**Figure 19 A**). These results support those of Zha et al. [186], who showed that conjugating gum Arabic conjugated with pea protein isolate could decrease particle sizes and improve emulsion stability at various salt concentrations. The increased amount of AP (%), as seen by the average droplet diameters, may be responsible for the improved emulsion stability (**Figure 19 B**). This higher AP (%) improves stability by preventing oil droplet flocculation and coalescence. The enhanced BSA-starch conjugation under weaker electric fields may contribute to preventing protein molecule aggregation, ultimately improving emulsion stability.

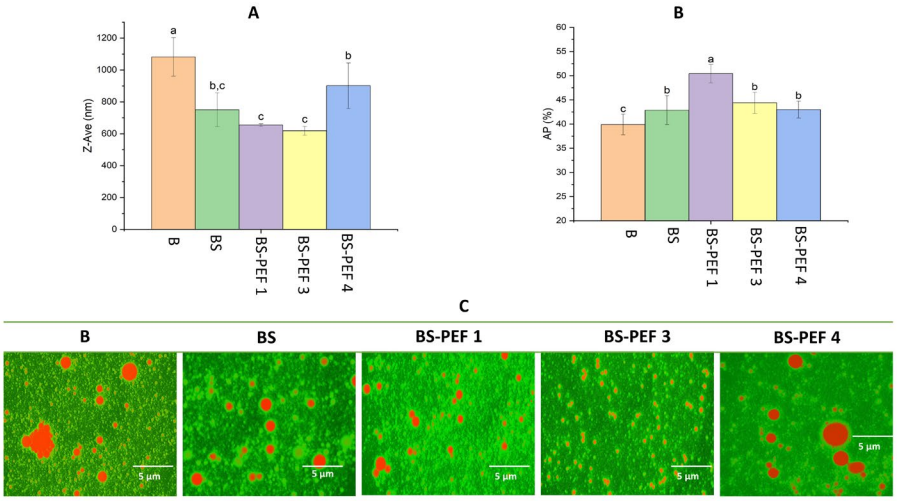

Figure 19 Droplet sizes averages (A), Adsorbed protein (AP%) (B), and CLSM images (C) of emulsions stabilized with BSA and BSA/starch conjugates (with and without PEF treatment) at NaCl concentration of 150 mM. These figures are modified from [143].

Protein and soluble starch both play a unique role in stabilizing the emulsion systems. Protein increases stability by electrostatic repulsion, while starch improves the steric repulsion of oil droplets [82]. BSA and soluble starch combined as emulsifiers could increase emulsion stability over a range of ionic strengths. The amount of AP (%) increased when NaCl was added to the emulsions. This result matches those of a recent study, which proved that adding NaCl increased the AP (%) in emulsions stabilized by soybean and whey proteins [132]. The droplet size average and AP (%) findings were further corroborated by the confocal laser scanning microscopy (CLSM) pictures of emulsions with C_{NaCl} concentrations of 150 and 300 mM (**Figure 19 C** and **20 C**). In particular, the micrographs showed that BS-PEF 3 and BS-PEF 1 emulsions had smaller droplets (indicated by red cores) and higher intensities of protein films around the oil droplets (represented by green perimeter). These findings suggest that the synergistic effects of BSA, starch, and the presence of NaCl all work together to strengthen the protein film that forms around the oil droplets, improving the emulsion stability.

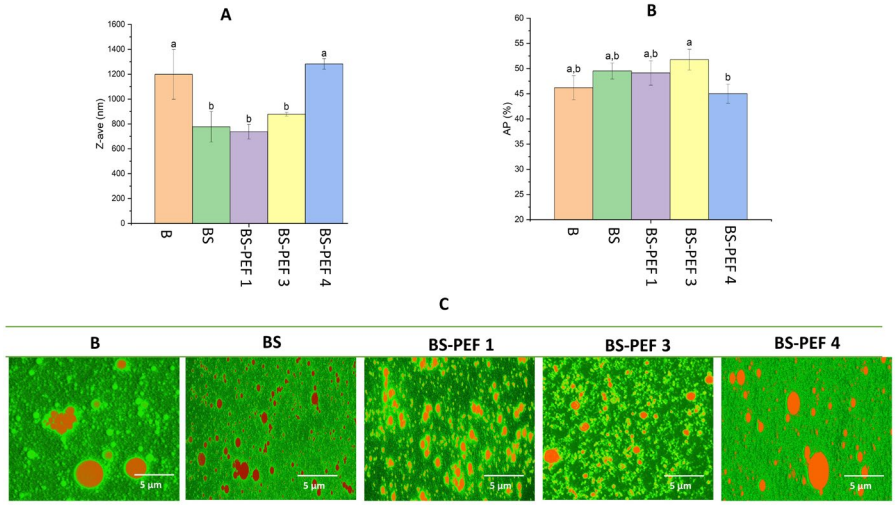

Figure 20 Droplet sizes averages (A), Adsorbed protein (AP%) (B), and CLSM images (C) of BSA and BSA/starch conjugates (with and without PEF treatment)-stabilized emulsions at NaCl concentrations of emulsions to 300 mM. These figures are modified from [143].

5.2.5 Effect of pH

When compared to emulsions prepared at neutral pH, pH 4.6 emulsions showed larger droplet sizes and greater AP (%) (**Figure 21**). Compared to emulsions stabilized by native BSA, those with BSA/starch conjugates had

smaller droplet sizes. Interestedly, the PEF-treated emulsions (BS-PEF 3 and BS-PEF 1) showed the smallest average droplet diameters and the highest AP (%). These results were further substantiated by CLSM pictures, which demonstrated that at pH 4.6, B and BS-PEF 4 emulsions had larger droplet sizes than other emulsions. Similar findings were made for emulsions stabilized by starch/WPI conjugates at their p*I* (5), which showed bigger droplet sizes than emulsions at neutral pH [172]. As seen in the B emulsion, the coalescence of oil droplets in our study may have resulted from the BSA molecules' tendency to aggregate at pH 4.6. (**Figure 21**). BSA and starch may have formed a combination that prevented BSA from aggregating at pH 4.6, improving the stability of BSA/starch-stabilized emulsions. Since BSA molecules' surface charges are neutral at pH 4.6, there is insufficient electrostatic repulsion at the oil/water contact to prevent the aggregation of oil droplets. But, through a combination of steric and electrostatic repulsion mechanisms, starch and BSA/starch conjugates may have helped to stabilize the emulsion system [82,179].

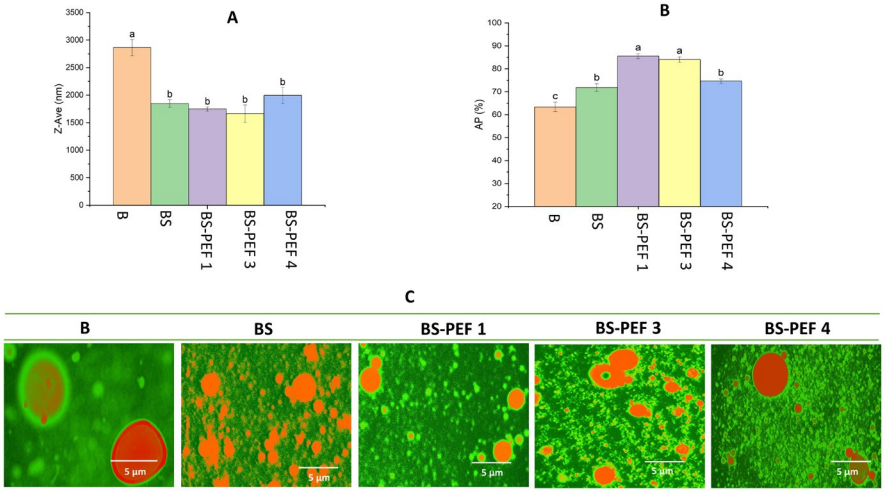

Figure 21 Droplet sizes averages (A), Adsorbed protein (AP%) (B), and CLSM images (C) of BSA and BSA/starch conjugates (with and without PEF treatment)-stabilized emulsions at pH values of emulsions to 4.6. These figures are modified from [143].

5.3 Proposed mechanism of PEF-assisted glycation of BSA/starch conjugates and their emulsifying properties.

Figure 22 illustrates the effect of PEF treatment on BSA molecules, primarily inducing polarization and generating free radicals. These free radicals can disrupt various protein-protein interactions, such as hydrophobic and electrostatic interactions, van der Waals forces, disulfide, and hydrogen bonds. Consequently, the unfolding of BSA molecules is facilitated [20,21]. The particle sizes (**Table 8**), solubility (**Figure 16**), and DG (**Figure 15**) demonstrate that PEF increased BSA solubility, reduced the particle size of BSA molecules, and generated more free amino acids. Zeng et al. [192] noticed that PEF treatment of starch reduced the molecular weight and relative crystallinity of rice starch when subjected to specific PEF conditions (<50 °C at 30-50 kV/cm for 40 s). These modifications in both starch and BSA likely facilitated starch/BSA conjugation following PEF treatment. The improved emulsifying properties of PEF-induced starch/BSA conjugates can be attributed to the following reasons:

BSA molecules contribute to emulsion stability through electrostatic repulsion, while starch provides steric repulsion [82]. Therefore, the co-adsorption of starch and BSA forms a double layer at the water/oil interface, enhancing the emulsions' stability under harsh environmental conditions, such as pH variations, temperature fluctuations, and changes in ionic strength [176].

Following PEF treatment, smaller particle sizes are obtained, encouraging conjugates to accumulate at the oil/water interface during emulsification. Then, the interfacial tension is decreased by this accumulation, leading to smaller oil droplet sizes and improved emulsion stability [170].

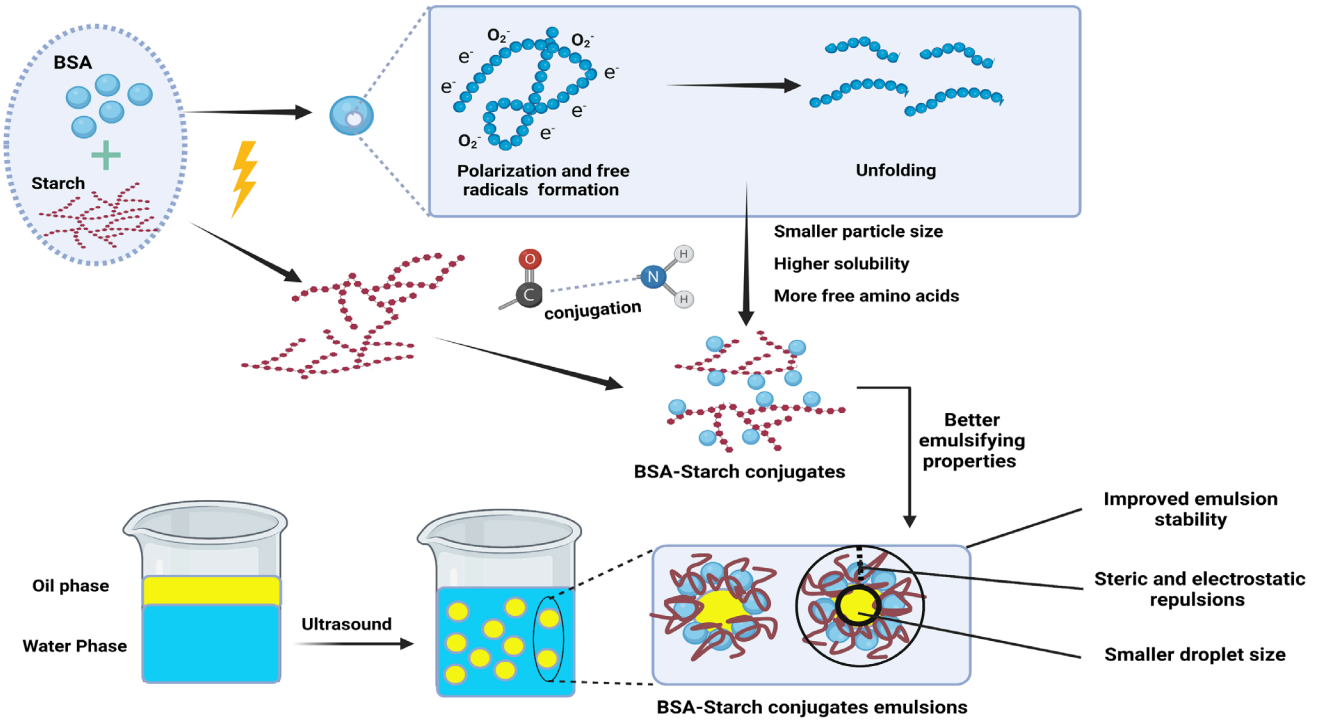

Figure 22: Proposed mechanism of PEF-assisted glycation of BSA/starch conjugates, as well as their emulsifying capabilities. This figure was reprinted from [143].

5.4 Conclusion

Emulsions stabilized by PEF-induced conjugates in the 3.5–5.7 kV/cm EFS range showed reduced droplet sizes and exhibited superior stability across various environmental conditions, such as freezing, fluctuating ionic strengths, and pH variations. Emulsions stabilized by PEF-induced conjugates at EFS> 5.7 kV/cm, on the other hand, exhibited greater droplet sizes and less stability when exposed to these environmental factors. Accordingly, it is advised to use mild to moderate PEF treatment to enhance the emulsifying abilities of soluble starch/BSA complexes. However, the underlying processes by which PEF treatment generates these observed effects on the gels generated by protein/polysaccharide conjugates and their impact on the bioaccessibility of gels enriched in bioactive phytochemicals need to be clarified. Finding the ideal PEF treatment parameters for future investigations might also be accomplished by investigating the effects of a wide range of EFS and pulse numbers.

CHAPTER 6 EFFECTS OF PULSED ELECTRIC FIELD ON THE PHYSICOCHEMICAL AND STRUCTURAL PROPERTIES OF MICELLAR CASEIN

- Impacts of PEF treatment (0-30kV/cm, 480 ns) on CSMs were studied.

- PEF treatment was found to induce changes in the particle sizes, surface hydrophobicity and protein solubility.

- It was also noticed that PEF can alter the secondary structure and disulfide linkages in CSMs.

6.1 Introduction

Pulsed electric field (PEF) as a promising green technology in different food applications has received significant interest [34,103]. By subjecting food materials positioned between two electrodes to millisecond- to nanosecond-long electric field pulses [103], PEF processing has been utilized mainly for enzyme and microbe inactivation in food systems [55]. Interestingly, investigations have demonstrated that PEF treatment can produce structural changes and influence the technological properties of food proteins [1]. Numerous food products rely on bovine milk proteins (whey proteins (20 %) and caseins (80 %)) as vital raw materials [6]. However, proteins frequently have functional restrictions, such as large molecular weight, reduced solubility, and moderate electrostatic repulsion [170]. Therefore, it is necessary to improve the functional performance of proteins, such as their foaming, gelling, and emulsifying capacities [20]. To achieve enhanced functionality, proteins must undergo conformational modifications. To address this issue, the effects of PEF treatment (19.2-211 μs, 30-35 kV/cm) and various heat treatments (30-75 ˚C) on the structural and functional properties of WPI were investigated [108]. The results showed that the PEF treatment had no significant effect on the free-SH group concentration, surface hydrophobicity, or unfolding of proteins. Surprisingly, emulsions formed from PEF-induced WPI (30 kV/cm) had comparable droplet diameters (4 μm) to those derived from heat-induced WPI (72 ˚C for 15 seconds) [108]. However, it is important to note that lower EFS (22.7-24.2 ˚C, 500 V/m) produced structural alterations in bovine serum albumin (BSA), possibly as a result of the breakage of its native hydrogen bonds [109]. Rodrigues et al. [193,194] also investigated the effects of a moderate electric field (MEF) on the structures of whey proteins and -lactoglobulin. Their findings revealed that MEF (range from 0 to 10 V/cm) enhanced the hydrophobicity of β-lactoglobulin's surface and altered its Trp fluorescence spectra and secondary structure. Notably, when MEF was combined with heat treatment (up to 70 ˚C), the structural alterations in β-lactoglobulin were amplified. In addition, the combination of MEF and ohmic heating in WPI reduced viscosity and led to the production of smaller aggregates with less thiol group concentration [193,194].

Caseins, which account for approximately 80% of total milk protein, consist of various subunits, including αs1 (45% of total casein), αs2 (12%), β (33%), and kappa (k, 10%) caseins [106]. These proteins are widely utilized as raw ingredients in numerous food products. Ultrasound and high-pressure

treatments have been employed to modify the technological and structural characteristics of caseins. For instance, ultrasonication at a frequency of 20 kHz and a power density of 0.75 W/ml has been shown to reduce the particle size and enhance the solubility (greater than 95%) of casein powders (MCP) [195]. In another study, sonication at 30% amplitude and 20 kHz resulted in decreased solubility, particle size, and improved thermal stability of casein micelles within the pH range of 4 to 8 [196]. Ultrasound-induced alterations in protein tertiary structures exposed hydrophobic residues to the protein molecule surface, thereby increasing protein flexibility and reducing interfacial tension at the oil/water interface, ultimately enhancing emulsifying properties [82]. On the other hand, high-pressure treatment at lower pressures (100-200 MPa) did not significantly impact the structure of casein micelles, whereas, at higher pressures (> 400 MPa), hydrophobic interactions were disrupted, leading to a reduction in the average size of casein micelles [197].

Few research was done on the structural and functional properties of CSMs after PEF treatment. As a result, the main goal of this work was to evaluate the structural changes that occurred in CSMs after receiving high-intensity PEF treatment at voltages between 0 and 30 kV/cm. This study will advance knowledge of PEF's effects on casein micelles' functional capabilities by exploring how it affects the structural characteristics. The results of this study will offer insightful information on the prospective uses of PEF technology in changing the structural characteristics of casein micelles and may have implications for the creation of cutting-edge methods for food processing and new product formulations.

6.2 Materials

Casein micelles (CSMs, 92% protein) were purchased from VWR Chemicals (Leuven, Belgium). β-mercaptoethanol, sodium hydroxide, and sodium chloride were acquired from AppliChem GmbH (Darmstadt, Germany). Sodium dodecyl sulphate (SDS) and Coomassie blue dye-(G250), were obtained from Sigma Aldrich (St. Louis, Missouri, USA). 8-Anilino-1-naphthalenesulfonic acid (ANS) was purchased from Cayman Chemical Company (Michigan, USA). Hydrochloric acid, phosphoric acid, methanol, and ethanol absolute were obtained from Merck (Darmstadt, Germany).

6.3 Results and Discussions

6.3.1 PEF effects on the particle size and ζ-potential

The particle size of proteins plays a crucial role in determining their solubility and other functional properties. **Table 10** presents the effects of PEF on the particle size and ζ-potential of CSMs. Upon PEF treatment, the particle size enhanced from 266.8 to 276.2 nm at an EFS of 10 kV/cm. However, the particle sizes decreased as the EFS was further increased to 20-30 kV/cm. The size distribution of both untreated and PEF-treated CSMs was bimodal, similar to that found in β-casein by Li et al. [200]. Peak values were obtained between 30-100 nm (peak 1) and 200-1000 nm (peak 2). The observed shift in the peaks of CSMs treated at 10 kV/cm suggests an increase in particle size, indicating the assembly of bigger aggregates (**Figure 23**). A similar observation was reported for soy protein isolate treated with MEF (8-10 V/cm) [201]. This phenomenon could be attributed to the aggregation or partial unfolding of CSMs [44,143]. It is worth noting that using EFS beyond 10 kV/cm led to the production of smaller particle sizes compared to both the native protein and PEF-treated CSMs at 10 kV/cm. PEF treatment can reduce protein size by disrupting hydrogen bonding, electrostatic interactions, and hydrophobic interactions [202]. However, further investigations are required to verify and better understand the underlying causes behind the increase in particle size at 10 kV/cm and the subsequent decrease at higher PEF strengths. The ζ-potential offers valuable insights into the electric properties exhibited by proteins. The experimental findings indicated that the absolute ζ-potential value exhibited an increase from 26.6 mV (native CSMs) to 30.1 mV subsequent to treatment at 10 kV/cm. An analogous augmentation in the absolute ζ-potential magnitude was seen in soy protein isolates following treatment with MEF at an EFS of 4 V/cm [201]. This increase in ζ-potential could be attributed to the unfolding of CSMs, exposing more buried polar groups on the surface and increasing the surface charges.

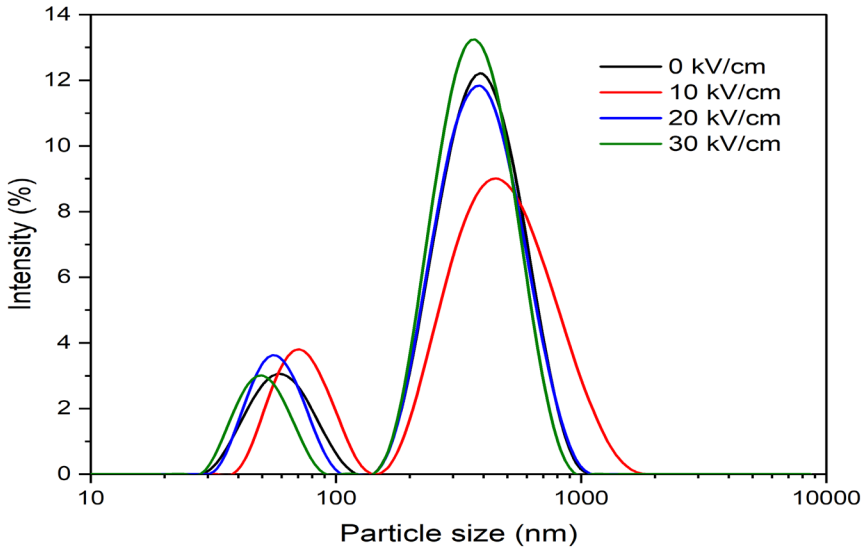

Figure 23 Particle size distribution (PSD) of native (0 kV/cm) and PEF-treated CSMs at an EFS of 0-30 kV/cm. Reprinted from our open access article [198].

Table 10 Particle size (z-average), PDI, ζ-potential, turbidity, protein solubility, and surface hydrophobicity (Ho) and temperature of native (0 kV/cm) and PEF-treated casein micelles at electric field strength of 0-30 kV/cm. Reprinted from our open access article [198].

	Z-average (nm)	PDI	ζ-potential (mV)	Turbidity	Protein solubility	Surface hydrophobicity (Ho)	Temperature (˚C)
0 kV/cm	266.8±2.3^{b}	0.52±0.03 ^{b}	-26.6±0.2 ^{b}	0.137±0.001^{c}	84.9±0.3^{b}	164.9±1.3^{a}	20.3±0.3
10 kV/cm	276.2±3.1^{a}	0.61±0.01 ^{a}	-30.1±0.3 ^{a}	0.152±0.002^{a}	87.1±0.2^{a}	166.0±2.4^{a}	21.1±0.4
20 kV/cm	258.2±2.9^{c}	0.56±0.01 ^{b}	-29.3±0.8 ^{a}	0.141±0.002^{b}	86.4±0.3^{a}	160.6±2.7^{b}	22.3±0.3
30 kV/cm	257.5±3.3^{c}	0.59±0.02 ^{a,b}	-29.5±0.5 ^{a}	0.143±0.003^{b}	86.6±0.4^{a}	159.4±1.3^{b}	24.2±0.5

6.3.2 Protein solubility and turbidity

Protein solubility is a significant element that affects their functional properties, such as their gelling, emulsifying, and foaming capacities [203]. Several factors, such as the molecular weight, amino acid profile, hydrogen bond concentration, and the presence of hydrophobic and hydrophilic groups on the surface, can influence a protein's solubility [67,143]. Protein solubility improved following PEF treatment at 10, 20, and 30 kV/cm from 84.9 to 87.1, 86.4, and 86.6 %, respectively (**Table 10**). The use of PEF promoted the establishment of hydrophobic contacts between unfolded proteins, creating more soluble protein aggregates [40]. Increased protein solubility following PEF treatment may be attributable to molecular polarization and enhanced dielectric constant resulting from PEF treatment at high EFS. Also, it has been claimed that PEF treatment (18 kV/cm) of myofibrillar protein generates free radicals that can disrupt electrostatic interactions and non-covalent bonds and improve protein solubility [162].

Turbidity is a measure of the size, amount, and aggregation of suspended proteins [204]. In our investigation, CSMs treated with 10 kV/cm exhibited a considerable increase in turbidity compared to untreated samples (**Table 10**). Increased aggregation and particle size may increase light absorption and scattering, resulting in an improvement in turbidity [205]. These results suggest that a PEF treatment at 10 kV/cm may accelerate the development of hydrophobic contacts and new intermolecular disulfide (S-S) bonds [40,206]. The increased turbidity of protein suspensions might be attributed to the formation of aggregates and the rise in particle size, which led to an increase in diffuse light reflection [201]. These results are consistent with those of particle size, as provided in **Table 10**.

6.3.3 Tertiary structure and surface hydrophobicity (Ho)

The intrinsic fluorescence spectra of proteins can provide insights into changes in the microenvironment polarity of aromatic amino acids [207]. In our study, we obtained the fluorescence spectra of CSMs before and after PEF treatment to investigate alterations in the tertiary structure [208]. The fluorescence intensity significantly rose from 829.5 to 855.6 when subjecting the CSMs to an EFS of 10 kV/cm. However, a slight decline in fluorescence intensity was seen as the EFS exceeded 10 kV/cm (**Figure 24**). An increase in fluorescence intensity indicates that tryptophan (Trp) residues are positioned

in a hydrophobic or non-polar environment, while a decrease in fluorescence suggests exposure to a hydrophilic polar environment [209].

The observed enhancement in peak intensity subsequent to PEF treatment at an EFS of 10 kV/cm may be related to the conversion of active residues into a comparatively more hydrophobic environment within the recently developed aggregates [210]. The application of PEF treatment at an EFS of 10 kV/cm has the potential to cause alterations in the conformation of protein structures. This phenomenon can result in the increased exposure of aromatic amino acids on the surface of the protein. Furthermore, it was observed that the λ_{max} value saw a modest blue-shift from 345.5 nm (native protein) to 344.5 nm (at 10 kV/cm), suggesting an increase in the hydrophobic nature around the fluorophore [211]. The PEF treatment has potentially exposed hydrophobic areas by inducing partial unfolding, as indicated by previous research [212]. Around a pH of 7, it is observed that certain hydrophobic amino acids exhibit negative charges on their surface. Consequently, the elevation in the absolute ζ-potential value after PEF treatment can be attributed to the enhanced exposure of additional hydrophobic areas [213]. The augmentation of the absolute ζ-potential value [170] can be attributed to the existence of uncovered hydrophobic regions accompanied by an elevation in the number of negatively charged amino acids. The aforementioned findings are consistent with the outcomes derived from the measurements of ζ-potential as presented in **Table 10**, as well as the study conducted using Raman spectroscopy.

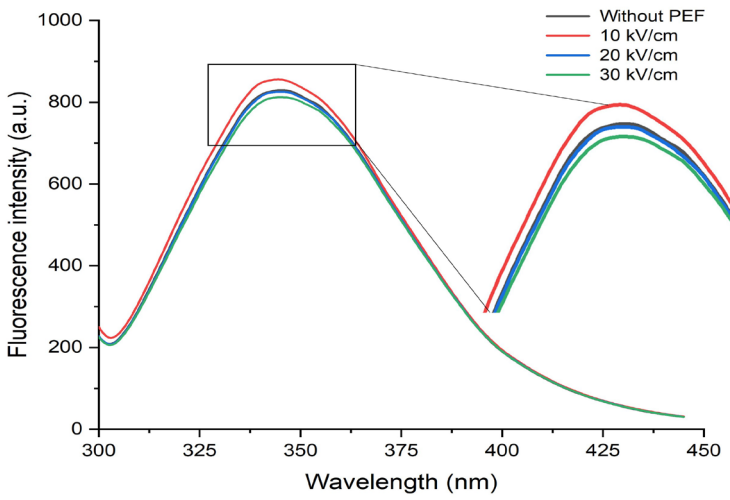

Figure 24 Fluorescence emission spectra of native (0 kV/cm) and PEF-treated casein micelles at electric field strength of 10-30 kV/cm. Reprinted from our open access article [198].

6.3.4 Microstructure

Figure 25 depicts the surface morphology of natural casein and casein subjected to PEF treatment. The untreated and 10 kV/cm treated CSMs exhibited condensed structures characterized by significant aggregates, and their surfaces exhibited an unbroken appearance free of visible cracks or fissures. On the other hand, SEM images of CSMs samples treated with PEF revealed surface structures that were visibly disturbed, displaying obvious cracks and fissures. As the EFS was raised from 10 to 30 kV/cm, the intensity of these disturbances became more evident. The SEM pictures of the casein sample treated with PEF at higher EFS exhibited more pronounced alterations to the surface structure of the protein. These alterations were characterized by the presence of smaller aggregates and the emergence of sheet-like structures. In comparison, the native casein sample and the casein sample treated with 10 kV/cm electric field strength had less severe disruptions. The obtained SEM micrographs provide evidence that the application of PEF treatment resulted in notable alterations in the surface structure and morphology of CSMs. The observed level of disruption on the protein surface exhibited a positive correlation with the application of higher voltage PEF treatments, indicating that higher EFSs induce more pronounced alterations in the protein's structural integrity.

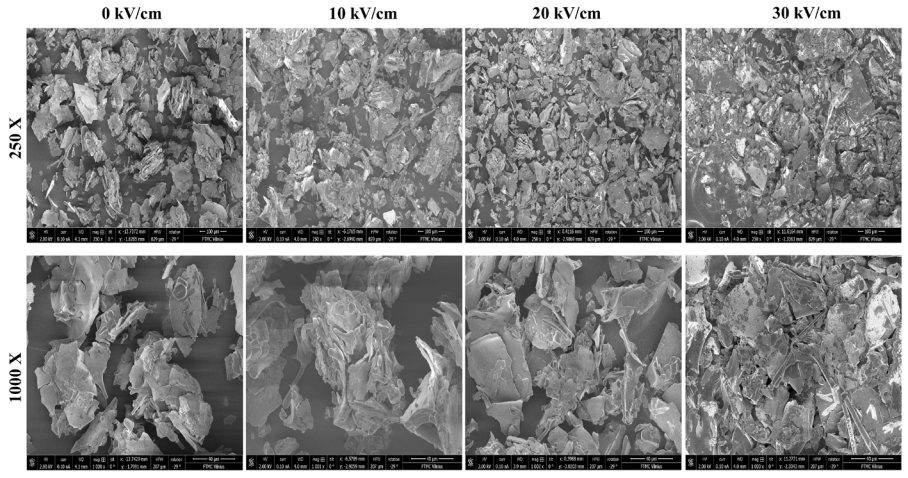

Figure 25 SEM images of native (0 kV/cm) and PEF-treated casein micelles at an electric field strength of 10-30 kV/cm. Reprinted from our open access article [198].

6.3.5 Secondary structure

Fourier Transform Infrared Spectroscopy (FTIR) is a widely used method for analyzing protein secondary structures [214]. By examining the vibrational changes in protein chemical interactions, FTIR data can provide valuable information about the protein's structure. In the case of polypeptides, the amide I band, which typically ranges from 1600 to 1700 cm^{-1}, is particularly informative as it reflects the C=O stretching vibrations of the protein backbone [215]. The FTIR spectrum shown in **Figure 26** presents the IR spectra of the control (native) and PEF-treated CSMs samples. The region between 1050 and 1100 cm^{-1} contains peaks attributed to the phosphate stretching of colloidal calcium phosphate. Upon PEF treatment, these peaks gradually disappear, indicating changes in the protein structure. These changes may be associated with the unfolding of casein, dissociation of colloidal calcium phosphate, and shielding of calcium ions [216].

The second derivative method was employed to assess the casein samples' secondary structure, and the obtained FTIR spectra were subjected to peak deconvolution using Peakfit software [217]. The amide I region's hidden peaks were automatically identified, and their positions were fitted using a Gaussian model to estimate the presence of different secondary structures. The area of each fitted peak was then calculated as a percentage of the total area of the amide I peak. Comparing the secondary structures of native casein PEF-treated casein (10-30 kV/cm), several notable changes were observed (**Table 11**). The α-helix content experienced a significant decrease, dropping from 33.5% in native casein to approximately 20.5% in PEF-treated casein. Additionally, an extra peak appeared in the α-helix region of the FTIR-fitted peaks for native casein [218]. The β-turn content increased from 16.6% in native casein to 18.5-20.9% in PEF-treated casein. Similarly, the β-sheet content increased from 30.5% in native casein to 37.5-39.7% in PEF-treated casein. Conversely, the random coil content decreased from 12.7% in native casein to 10.8% at 10 kV/cm but increased to 15.8% at 30 kV/cm [218].

These findings indicate that PEF treatment-induced changes in the secondary structure of casein. The creation of new secondary structures and partial unfolding of the protein is suggested by the decrease in α-helix content and the increase in β-turn and β-sheet contents [219]. Protein-protein interactions, such as Van der Waals, hydrogen and disulfide bonds, as well as hydrophobic and electrostatic interactions, might be blamed for these structural alterations. The amount of β-sheets and surface hydrophobicity may increase as hydrophobic groups on the protein surface are exposed [1,218]. It

is worth noting that no significant changes in β-sheet and α-helix contents were observed among the different PEF-treated casein samples at varying voltage levels [129]. This indicates that the secondary structure changes induced by PEF treatment may not exhibit a gradual increase with higher voltage treatments. In addition, the study suggests that PEF treatment at lower voltage levels can induce both chemical (e.g., aggregation and secondary structure changes) and physical (e.g., increase in particle size) alterations. Conversely, smaller soluble particles were produced at higher EFS levels, but the secondary structures of the proteins were not significantly affected compared to treatments at lower EFSs.

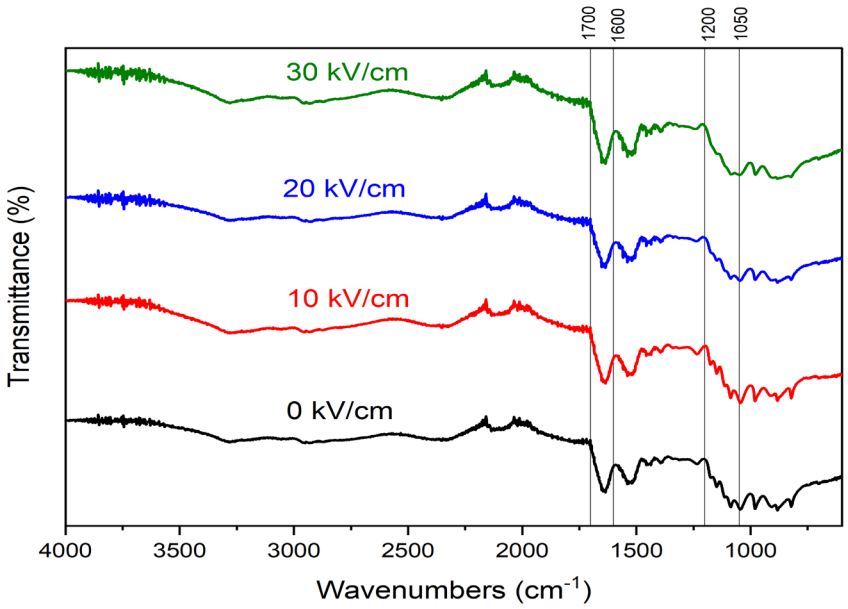

Figure 26 FTIR spectra of native (0 kV/cm) and PEF-treated casein micelles at an electric field strength of 10-30 kV/cm. Reprinted from our open access article [198].

Table 11. Total percentages area of secondary structures in Amide I region (1600-1700 cm^{-1}) in the FTIR spectra of native (0 kV/cm) and PEF-treated casein micelles at an electric field strength of 10-30 kV/cm. Means with different letters (a, b, c) in each column indicate statistically significant differences among protein samples following Duncan's analysis ($p < 0.05$). Reprinted from our open access article [198].

	Peak area (%)				
	Side chain	**Intramolecular & Aggregated β-sheet**	**Random coil**	**α-helix**	**β-turn**
0 kV/cm	6.5±1.2^{a}	30.5±2.1^{c}	12.7±2.3^{c}	33.5±2.4^{a}	16.6±2.1^{c}
10 kV/cm	7.9±0.9^{a}	39.7±2.5^{a}	10.8±1.7^{d}	20.5±1.9^{b}	20.9±2.6^{a}
20 kV/cm	7.7±1.3^{a}	37.5±1.9^{b}	14.7±1.6^{b}	20.8±1.5^{b}	19.1±1.8^{b}
30 kV/cm	7.4±0.8^{a}	37.6±2.8^{b}	15.8±1.9^{a}	20.5±2.2^{b}	18.5±2.1^{b}
Band frequency (cm^{-1})	1605-1611	1618-1630 &1685-1690	1630-1645	1652-1666	1670-1675

6.3.6 Raman spectroscopy analysis:

Figure 27 presents the Raman spectra of CSMs before and after PEF treatment. The changes in frequency and scattering intensity in the Raman spectrum can provide insights into the conformational changes of CSMs [160]. One notable observation in the Raman spectra is the sharp increase in intensity of the Raman band at 430-550 cm^{-1} after PEF treatment. This band is attributed to the disulfide ν(S-S) bond [72,220]. The appearance of this band indicates potential changes in the disulfide bonds within the protein structure. The spectral modes related to cysteine disulfide bonds are typically found in the 450-700 cm^{-1} range, with the exact frequency strongly dependent on the conformation of the CCSSCC moiety [221]. It is important to note that the S-S bond isomerization reaction may contribute to these changes, although there could also be some contribution from Amide VI.

Another interesting feature is the mode near 710 cm^{-1}, which corresponds to the stretching vibration of the C-S bond in the trans conformation (νT(C-S)). The intensity of this mode is increased in the 10 kV/cm samples compared to native CSMs [222]. This suggests alterations in the conformation of the C-S bonds within the protein structure due to PEF treatment. The dips observed near 1074 and 1448 cm^{-1} can be associated with changes in the vibrational intensity of C-C and C-N stretching, as well as CH2 deformation [160]. Additionally, the negative-facing mode at 1722 cm^{-1} corresponds to the carbonyl vibration (ν(C=O)). These changes in vibrational intensity indicate modifications in the chemical environment and interactions within the CSMs. Furthermore, a dip at 856 cm^{-1} is related to one of the doublet modes of tyrosine [160]. This mode is further analyzed in more detail in **Figure 28**, likely providing additional information about the specific changes occurring in the tyrosine residues within the protein structure.

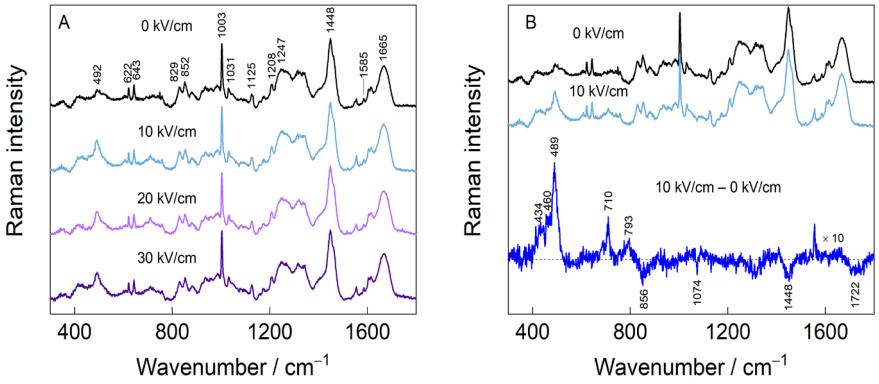

Figure 27 Raman spectra in the fingerprint region (A) of native (0 kV/cm) and PEF-treated casein micelles at an electric field strength of 10–30 kV/cm, and (B) the difference between native and 10 kV/cm-treated CSMs. Reprinted from our open access article [198].

The presence of tyrosine (Tyr) can be determined by observing its ring breathing mode Y1, which presents as a Fermi doublet at about 850 and 830 cm^{-1}. This characteristic feature serves as an indicator of the hydrogen bonding state and allows for the investigation of the hydrophobic or hydrophilic environment in close proximity to the Tyr side chain. A value ranging from 0.7 to 1.0 for the intensity ratio (I_{850}/I_{830}) indicates that Tyr is situated inside a hydrophobic environment. When the ratio (I_{850}/I_{830}) falls within the range of 0.90 to 1.45, it suggests the presence of Tyr in polar environments [72]. As illustrated in Figure 26, the increase of the EFS resulted in a reduction in the value of the (I_{850}/I_{830}) ratio. The results of this study suggest that the application of PEF treatment led to the burial of a greater number of Tyr residues within a hydrophobic environment, primarily as a result of intermolecular interactions [160,223]. The Raman data reveals that the most significant alterations caused by PEF treatment are observed in the disulfide linkages of the protein, affecting both the structure of S–S and S–C bonds. A certain degree of burying of the tyrosine sidechain was also observed.

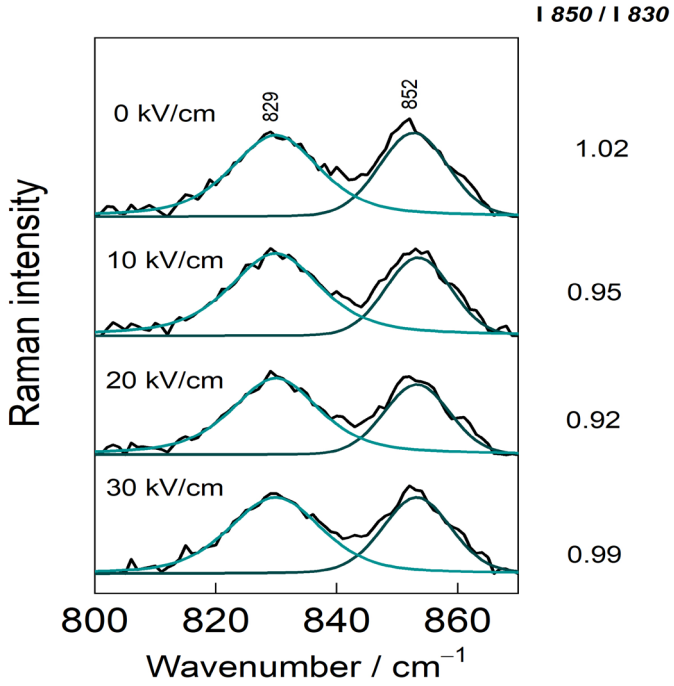

Figure 28 The Raman spectra within the range of 820-860 cm^{-1} and the relative integral intensity ratio at 850 and 830 cm^{-1} were analyzed for both native (0 kV/cm) and PEF-treated CSMs under an EFS ranging from 10-30 kV/cm. Reprinted from our open access article [198].

6.4 Conclusion

The application of PEF treatment proved to be effective in modifying the physicochemical and structural properties of casein micelles (CSMs). The treatment resulted in increased β-sheet contents, absolute ζ-potential values, and protein solubility. Additionally, PEF treatment reduced surface hydrophobicity, α-helix content, and particle sizes of the CSMs. Notably, no significant differences were observed in the physicochemical properties of CSMs treated at higher voltages (20-30 kV/cm) compared to those treated at 10 kV/cm. These findings suggest that using a moderate electric field (MEF) treatment could be a more energy-efficient approach when aiming to modify the structure of casein. Further research is recommended to investigate the impact of PEF treatment on the interfacial, emulsifying, and gelling properties of casein.

CHAPTER 7 NANOSECOND PULSED ELECTRIC FIELD PROMOTE THE BINDING BETWEEN BSA AND EPIGALLOCATECHIN GALLATE (EGCG)

- Nanosecond PEF (nsPEF, 0-20 kV/cm, 90 ns) was applied to investigate its effects on the BSA/EGCG binding.
- nsPEF altered the structure and physicochemical properties of BSA molecules.
- nsPEF promoted the BSA/EGCG binding.
- Molecular docking simulation confirmed that binding between BSA and EGCG molecules can occur at specific locations mainly via hydrogen bonding.

7.1 Introduction

Recently, there has been a growing interest in exploring the response of biomolecules to external stimuli, driven by its implications for diverse industries such as food, biotechnology, and pharmaceuticals. Among these stimuli, nanosecond pulsed electric field (nsPEF) has emerged as a promising technique to alter protein structures and techno-functional properties [10]. However, the influences of nsPEF on protein structure, specifically bovine serum albumin (BSA) and its interaction with epigallocatechin gallate (EGCG), a bioactive polyphenolic compound found in green tea, remain largely unexplored.

Proteins' structural characteristics severely affect their functionality, stability, and interactions with other molecules [224]. Extensive research has been conducted on the impact of physical and chemical factors such as ultrasound, temperature, pH, and high pressure on protein conformation [66]. Due to the possible health advantages of EGCG and its capacity to form complexes with proteins [225,226], studying the binding relationship between BSA and EGCG is also of considerable interest. The ability of BSA to bind and transport a variety of substances has been well investigated [227,228]. As a polyphenol, EGCG is sensitive to pH, light, and heat treatments. These characteristics significantly limit its applications [229]. Understanding the structural alterations brought on by this electrical treatment and how nsPEF affects the binding of BSA and EGCG may help to improve the stability and bioavailability of bioactive chemicals. In a recent study, Chen et al. [230] studied the influences of PEF treatment (0-25 kV/cm for 40 μs) on the binding ability of pea protein isolate (PPI) with EGCG. The authors applied multi-spectral techniques and computer simulation to confirm that PEF treatment increases the binding affinity between PPI and EGCG, hence potentially enhancing the functional characteristics and food industry applications of PPI. However, the effects of short (in the nanosecond range) duration PEF treatment are yet to be studied.

This study was carried out using spectroscopic, biophysical, and computer simulation methods. The secondary structure of BSA after exposure to short duration (90 nanoseconds, 90 ns) PEF treatment was examined using circular dichroism (CD) spectroscopy, fluorescence spectroscopy to study the modifications to BSA's secondary and tertiary structure and the possible changes of BSA/EGCG binding affinity. The modifications in BSA aggregation brought on by nsPEF are also characterized by dynamic light

scattering (DLS). Molecular dynamics simulation is used to identify the active sites on the BSA and EGCG and confirm their interaction. The study aimed to study the effects of nsPEF in altering the structure and physicochemical properties of BSA and its binding with EGCG. The results of this study could significantly impact the design of novel functional food ingredients or drug delivery systems, as well as the creation of creative protein modification methodologies.

7.2 Materials

BSA was obtained from Sigma Aldrich (St. Louis, Missouri, USA). 1,2-Phthalic dicarboxaldehyde (98 %, OPA) and EGCG (purity 95%)were acquired from ACROS Organics, Fisher Scientific GmbH, Schwerte, Germany.

7.3 Results and Discussions

7.3.1 Physicochemical properties of nsPEF-treated BSA and (nsPEF BSA)+EGCG

Table 12 represents the particle sizes, ζ-potential, and surface hydrophobicity of nsPEF-treated BSA. The particle sizes of BSA increased after applying nsPEF. The increase in the particle size values could be due to the partial aggregation of BSA molecules after nsPEF treatment. Similarly, in our recent study, 10 kV/cm PEF treatment resulted in larger particles of CSMs [198]. Moreover, the absolute ζ-potential value of BSA enhanced after PEF treatment and reached the maximum value (28.9 mV) at 16 kV/cm. The partial unfolding of BSA, followed by the exposure of more buried polar groups after nsPEF treatment, could intensify the amount of negative charges at the surface. Similar findings were observed with CSMs [198] and pea protein isolate [230]. Surface hydrophobicity reflects the amount of hydrophobic amino acid residues exposed on the surface, which impacts the intermolecular interaction. The surface hydrophobicity of BSA gradually improved after nsPEF treatment and reached its peak at 16 kV/cm, then decreased at 20 kV/cm. The destroyed hydrophobic groups and unfolding of BSA molecules after PEF treatment resulted in the exposure of hydrophobic groups and increased surface hydrophobicity values [198,229].

EGCG tea polyphenol (1 mmol/L) was added to nsPEF-induced BSA (1:1) to investigate the impact of nsPEF treatment on the binding and interaction between BSA and EGCG. The particle size (z-average), ζ-potential, and

surface hydrophobicity of (ns-PEF BSA) after adding EGCG (**Table 12**). Adding EGCG increased the particle sizes compared to native and nsPEF-induced BSA. For example, the particle size value raised from 29.4 nm (nsPEF BSA at 8 kV/cm) to 167.9 nm after adding EGCG to nsPEF BSA at 8 kV/cm (**Table 12**). This rise in particle sizes revealed the occurrence of the covalent binding between BSA and EGCG. The chain reaction between EGCG and BSA and the formation of a biopolymer could be the reason for the increased particle sizes [235,236]. However, the particle sizes of EGCG+nsPEF-induced BSA gradually decreased with the increase in the EFS (**Table 12**). Surface hydrophobicity represents the measurement of the hydrophobic groups (at the exterior sides of proteins) binding to the ANS probe. Thus, the drop in surface hydrophobicity values indicates the binding of the EGCG to the hydrophobic amino acids on the surface of BSA molecules. This can block the binding of the ANS fluorescence probe to the hydrophobic groups [237]. Surface hydrophobicity declined after adding EGCG polyphenol to native and nsPEF-induced BSA. The covalent interaction between EGCG and BSA decreased the surface hydrophobicity of BSA [238,239].

The fluorescence intensity of nsPEF-treated BSA and (nsPEF BSA)+EGCG complexes was measured and presented in **Table 13**. At lower EFS (8kV/cm), the fluorescence intensity of both nsPEF-treated BSA and (nsPEF BSA)+EGCG increased but then decreased at higher EFS. Similar findings were reported in our recent study with CSMs [198]. Moreover, compared to nsPEF-treated BSA, (nsPEF BSA)+EGCG had a lower fluorescence intensity and redshift towards higher wavelengths was observed. This change indicates a potential connection between tryptophan and the interaction of EGCG and BSA, reducing the fluorescence intensity [236].

Table 12 Particle size (z-average), ζ-potential, and surface hydrophobicity (Ho) of native (0 kV/cm), and nsPEF-treated BSA (ns-PEF BSA) added to EGCG at EFS of 0–20 kV/cm.

	nsPEF BSA			(nsPEF BSA) + EGCG		
	z-average (nm)	ζ-potential (mV)	Surface hydrophobicity (Ho)	z-average (nm)	ζ-potential	Surface hydrophobicity (Ho)
0 kV/cm	23.8±2.1^{b}	-10.1±2.8^{a}	345.3±1.7^{c}	170.3±2.4^{a}	-19.5±2.7^{a}	221.1±2.8^{c}
8 kV/cm	29.4±1.8^{a,b}	-27.4±3.5^{b}	354.4±2.1^{a}	167.9±1.9^{a}	-20.7±1.2^{a}	225.4±1.6^{c}
12 kV/cm	34.7±2.5^{a}	-27.7±2.4^{b}	365.7±1.1^{a}	163.4±2.3^{a}	-24.3±0.5^{b}	245.2±3.1^{b}
16 kV/cm	39.4±1.4^{a}	-28.9±3.1^{b}	369.4±1.6^{a}	129.2±1.8^{b}	-25.1±1.5^{b}	253.4±1.4^{a}
20 kV/cm	36.2±2.2^{a}	-27.2±2.2^{b}	359.2±3.4^{b}	132.6±1.7^{b}	-24.5±0.9^{b}	250.2±0.8^{a,b}

Table 13 Fluorescence intensity of native (0 kV/cm), and nsPEF-treated BSA (ns-PEF BSA) added to EGCG at EFS of 0–20 kV/cm. WL; Wavelength; FL, Fluorescence.

	nsPEF-BSA		(nsPEF-BSA)+EGCG	
	WL (nm)	FL intensity	WL (nm)	FL intensity
0 kV/cm	344.5	518.1	358.4	232.7
8 kV/cm	345.1	526.7	358.9	231.9
12 kV/cm	344.8	513.3	356.3	234.6
16 kV/cm	344.2	505.1	358.1	242.5
20 kV/cm	345.8	520.8	358.2	237.2

Circular dichroism (CD) was used to study the changes in the secondary structure of native BSA compared to nsPEF-treated BSA. **Figure 29** shows the nsPEF-induced changes in the secondary structure of BSA. It was observed that α-helix content increased from 65.5% (native BSA) to 76.3% after nsPEF treatment at 20 kV/cm. Moreover, β-sheets, β-turns and unordered structures decreased after nsPEF treatment. Zhang et al. [240] studied the effects of ultrasound treatment on the secondary structure of BSA. Similar to our findings, they noticed that the sonication of BSA increased the α-helix content from 63.6% before sonication to 74.03% after sonication at 59 kHz frequency.

50.9

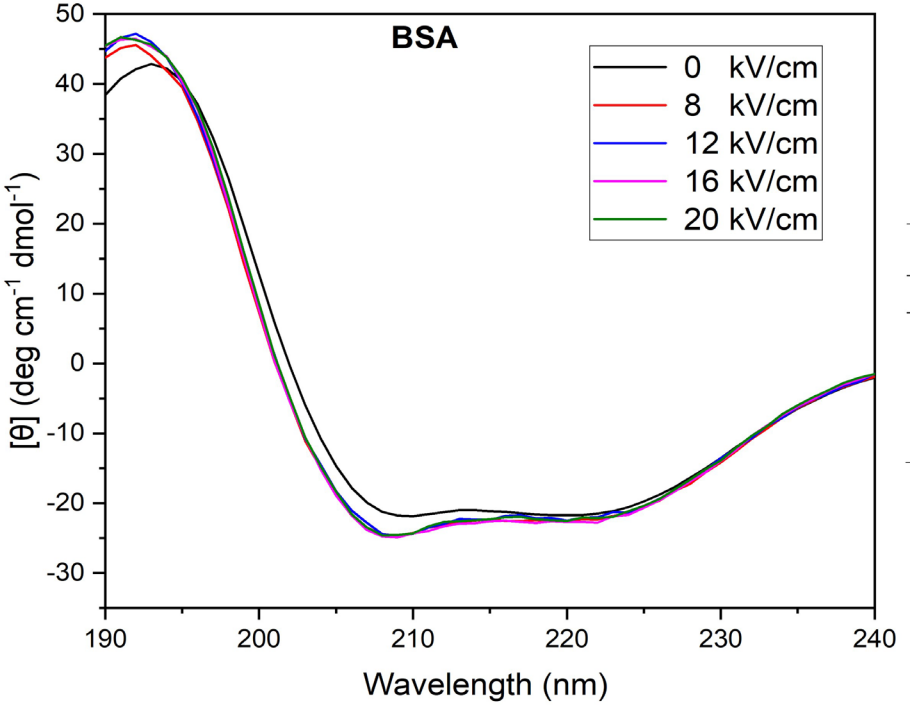

	Seconadry structures (%)			
	α-helix	**β-sheet**	**β-turns**	**Unordered**
0 kV/cm	65.5±1.3	5.3±0.6	8.4±1.2	20.8±1.1
8 kV/cm	71.3±2.0	3.1±0.6	7.2±0.8	18.4±0.9
12 kV/cm	75.2±1.1	4.2±0.4	5.1±0.1	15.5±0.8
16 kV/cm	75.4±1.4	5.1±0.9	5.2±0.3	14.3±0.5
20 kV/cm	76.3±1.6	3.1±0.3	5.5±0.8	15.1±0.5

Figure 29 CD spectra and secondary structure contents (%) of native and nsPEF-induced BSA.

7.3.2 Physicochemical properties of nsPEF-induced (BSA+EGCG).

In this section, EGCG (1 mmol/L) was mixed with BSA (2%, w/v) (1:1) to reach a final concentration of 1% BSA and 0.5 mmol/L EGCG. NsPEF then treated the mixture of 3 pulses. As shown in **Table 14**, nsPEF treatment boosted the particle sizes of BSA molecules, and the highest increase was observed with BSA/EGCG mixture treated at 8 kV/cm. This rise in the particle sizes occurred mainly due to the covalent binding between BSA and EGCG, partial unfolding, and the formation of BSA/EGCG biopolymer [235,236]. From these results, it could be concluded that nsPEF treatment could facilitate EGCG and BSA binding, probably because of the partial unfolding and the exposure of polar groups to the protein surface [1,10]. The absolute ζ-potential values significantly improved from 8.7 mV for the BSA/EGCG mixture before treatment (BE-0) to 33.7 mV following nsPEF treatment at 8 kV/cm **(Table 14)**. nsPEF treatment could enhance the polarization of protein molecules, exposing more negative groups to the surface. Similar findings were reported by Tan et al. [241] who found that high hydrostatic pressure treatment increased the absolute ζ-potential values of blueberry pectin and cyanidin-3-glucoside/blueberry pectin mixtures. The surface hydrophobicity significantly declined after adding EGCG to BSA, possibly due to the fluorescence quenching after EGCG and BSA binding. The values were further declined after applying nsPEF. The unfolding of BSA could expose more active sites to the surface, increasing the BSA/EGCG binding. This could increase the fluorescence quenching, lowering surface hydrophobicity [237].

Table 14 Particle size (z-average), ζ-potential, and surface hydrophobicity (Ho) of nsPEF(BSA+EGCG). B:BSA; BE:BSA+EGCG; 0-20 kV/cm: EFS.

Samples	z-average (nm)	ζ-potential	Surface hydrophobicity (Ho)
B-0	21.3 ± 1.3^{d}	-8.9 ± 1.6^{a}	342.3 ± 7.7^{a}
BE-0	34.7 ± 5.1^{c}	-8.7 ± 0.9^{a}	295.6 ± 4.1^{b}
BE-8	69.6 ± 4.2^{a}	-33.7 ± 6.1^{c}	269.3 ± 3.6^{c}
BE-12	50.9 ± 3.5^{b}	-33.1 ± 5.6^{c}	278.5 ± 2.8^{c}
BE-16	50.2 ± 1.8^{b}	-30.5 ± 1.3^{c}	265.2 ± 2.7^{c}
BE-20	25.9 ± 1.6^{d}	-21.8 ± 2.4^{b}	250.2 ± 3.8^{d}

UV-vis spectroscopy is widely used to investigate the structural changes of proteins upon complex formation and ligand binding. **Figure 30** shows the UV-vis spectra of BSA, BE, and BE (8-20 kV/cm). The highest points of absorption for BSA, BE, and BE (8-20 kV/cm) were in the range of 285-290 nm, which can be associated with the π-π* transition of the aromatic amino acids. The application of nsPEF treatment and mixing EGCG with native BSA amplified the intensity of the absorption peak. This suggests the formation of complexes through interaction, introducing a new π-π* transition [242]. New peaks appeared around 320-330 nm for all BE samples. These findings confirmed that the interaction between EGCG and BSA induced peptide chain stretching and protein structure alterations. Furthermore, these results verified that the binding of EGCG to BSA involved static quenching because dynamic quenching usually does not cause modifications in the absorption spectrum [243,244].

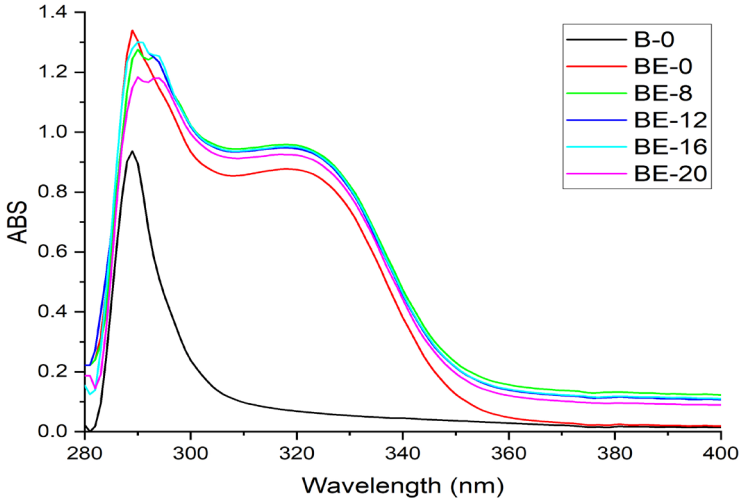

Figure 30 UV-vis spectra of BSA, BSA/EGCG without nsPEF treatment, and BSA/EGCG mixtures nsPEF-treated at 8-20 kV/cm.

Raman spectroscopy was applied to confirm the changes in the structure of BE (8-20 kV/cm). As illustrated in **Figure 31**, the intensity of the Raman signal within the 450–500 cm^{-1} range showed an increase following nsPEF. This range represents vibrations connected to the disulfide ν(S–S) bond [72,220]. Spectral modes connected to cysteine di-sulfide interactions are visible between 500–700 cm^{-1}, with the exact frequency mainly depending on the CCSSCC segment configuration [221]. This could occur probably due to the S–S bond isomerization reactions. Another peak around 710 cm^{-1} can be linked to the C–S stretching vibration bond in trans conformation, νT(C–S).

Notably, this band intensity is heightened after nsPEF treatment when compared to the native BSA [222].

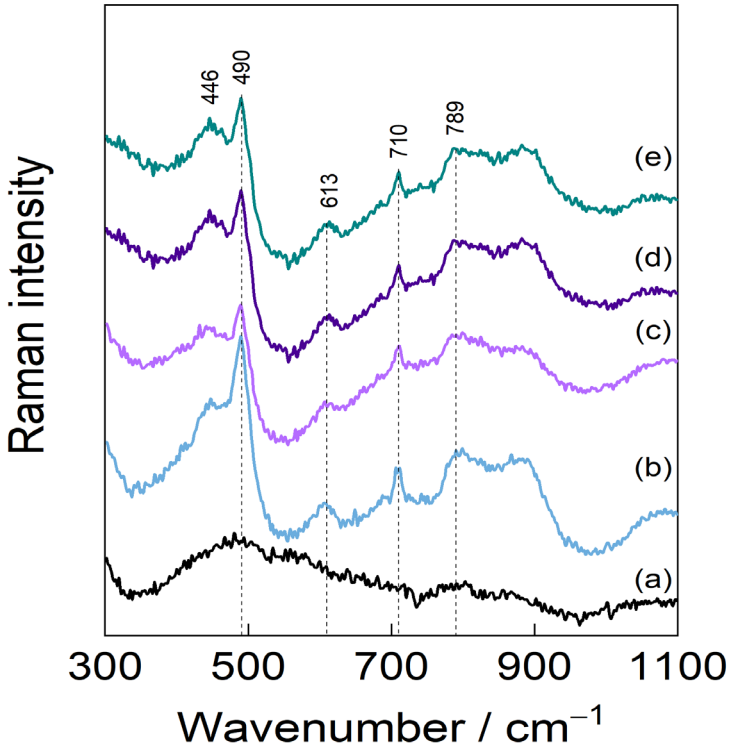

Figure 31 Raman difference spectra constructed by subtracting the BSA-EGCG-0 spectrum from BSA-0 (a), BSA-EGCG-8 (b), BSA-EGCG-12 (c), BSA-EGCG-16 (d), BSA-EGCG-20 kV/cm (e).

Tyrosine (Tyr) doublet, at about 850 and 830 cm^{-1}, is used as an indicator for hydrogen bonding configurations and provides information about the hydrophobic or hydrophilic environment surrounding the Tyr side chain [72]. **Figure 32** shows that a rise in the EFS causes a fall in the I_{850}/I_{830} ratio. These findings imply that intermolecular interactions play a significant role in increasing Tyr residues' seclusion inside a hydrophobic environment following nsPEF treatment [160,223]. This indicated that Tyr phenolic groups participated in the formation of new hydrogen bonds. The decrease in the I_{850}/I_{830} ratio was also observed due to the protein/anthocyanin interaction [245,246]. Raman evidence confirms that nsPEF causes the protein's disulfide connections to alter significantly, impacting both the S-S and S-C bond structures. The tyrosine side chain was also found to be partially buried as a

result of nsPEF and EGCG binding. Thus, it could be concluded that nsPEF changed the structure of BSA and thus facilitated the binding with EGCG.

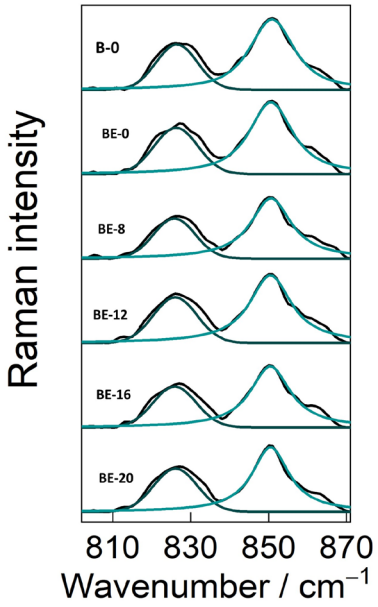

	I_{850} / I_{830}	A_{850}/A_{830}
B0	1.55	2.04
BE-0	1.55	1.93
BE-8	1.51	1.94
BE-12	1.49	1.86
BE-16	1.50	1.83
BE-20	1.50	1.70

Figure 32 Raman spectra in the Tyr doublet range; I, Intensity; A, Absorbance.

FTIR spectroscopy is a noninvasive and rapid technique for acquiring biochemical fingerprints and detecting structural changes in proteins. FTIR can provide insight into the molecular structure and composition via functional groups and secondary protein structures [247]. The amide I, II, and III bands play a vital role in determining the degree of molecular organization present in proteins and contribute to the formation of protein structures, which is facilitated by C=O stretching, N-H bending, and C-H stretching. The changes amide I region (1600-1700 cm^{-1}) indicate alternation in the C=O stretching. While amide II (1500-1600 cm^{-1}) represents N-H bending, and C-H stretching and amide I and II are sensitive to the changes in the secondary structures of proteins [248]. As shown in **Figure 33**, new peaks appeared in amide I and II regions following nsPEF treatment of BSA/EGCG mixtures. This could be attributed to the changes in the BSA's secondary structures [249]. These changes confirm the Raman results, which indicated that nsPEF induced changes in the secondary structure of BSA, facilitating the BSA/EGCG binding.

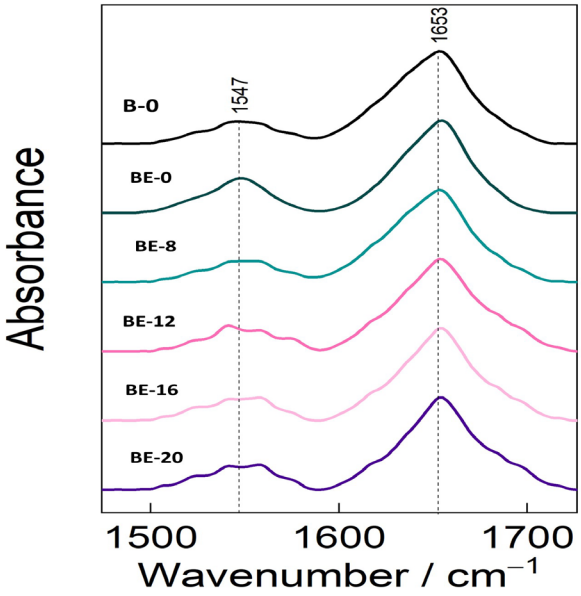

Figure 33 FTIR spectra in the Amide I and Amide II vibrational range.

Molecular Docking

The discipline of theoretical chemistry plays a crucial role as a supporting element to experimental investigations. The identification of precise interaction locations and the underlying dynamics that drive the interaction between BSA and EGCG is of crucial significance [250]. Thus, a docking theoretical approach was applied to predict EGCG and EGCG binding sites. As shown in **Figure 34,** the X-ray crystal structure of BSA was obtained from the RCSB Protein Data Bank (PDB: 3v03, Resolution: 2.7 Å) (http://www.rcsb.org/pdb) and the 2D structure of EGCG was made available from PubChem (PubChem CID: 65064, https://pubchem.ncbi.nlm.nih.gov/compound/65064).

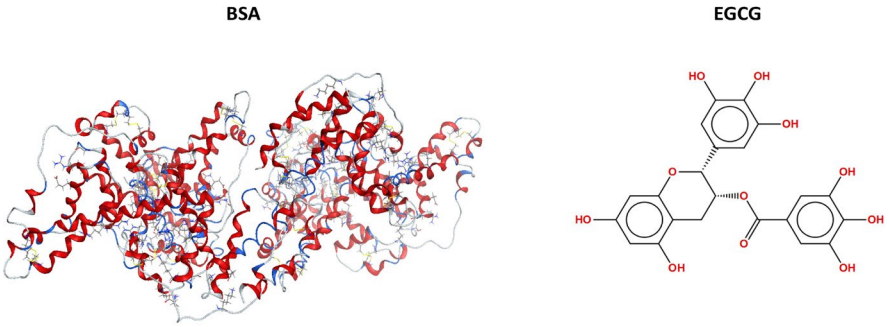

Figure 34 3D crystal structure of BSA (PDB: 3v03) and 2D chemical structure of EGCG (PubChem CID: 65064).

Figure 35A shows the penetration of EGCG to BSA molecules. As illustrated in **Figure 35B**, docking results showed that 9 amino acid residues participated in the binding of BSA/EGCG. EGCG interacted with BSA residues in three locations: Glu 186, Glu 399, and Gln 403 via 3 H-bonding. Moreover, the hydrophobicity of 6 amino acids (Thr 183, Glu 182, Leu 189, Lys 114, Thr 518, and Arg 427) was affected after adding EGCG to BSA [251,252]. These findings confirm the experimental results, which showed that the BSA structure and surface hydrophobicity were changed due to BSA/EGCG binding.

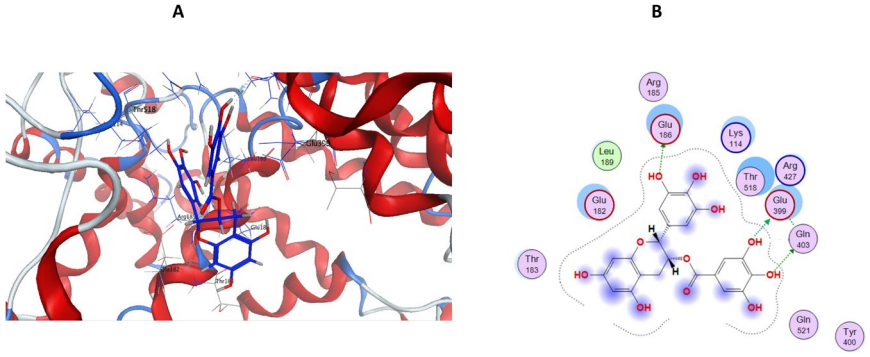

Figure 35 Penetration of EGCG to BSA molecules (A), binding sites between BSA and EGCG (B).

7.4 Conclusion

nsPEF treatment was applied to alter the structure of BSA and facilitate the BSA/EGCG binding. nsPEF increased the α-helix content, particle sizes, absolute ζ-potential, and surface hydrophobicity values of BSA. Moreover, the addition of EGCG to nsPEF-induced BSA resulted in a significant increase in particle sizes of BSA and a decrease in fluorescence intensity and surface hydrophobicity. nsPEF treatment of BSA/EGCG mixtures induced changes in BSA structures as confirmed by Raman FTIR spectroscopy. Raman's results showed that nsPEF induced changes in protein structure, mainly in S-S and S-C bonds. Changes in amide I and II were observed in FTIR spectra of nsPEF-induced BSA/EGCG mixtures. Moreover, nsPEF improved the particle sizes, absolute ζ-potential values, and UV-vis absorbance intensity while reducing the surface hydrophobicity values. Molecular docking confirmed that BSA can bind with EGCG at specific active sites on both molecules. It is recommended to study the stability of nsPEF-induced BSA/EGCG mixtures under different conditions (i.e., light, temperature, digestion system conditions, etc.) as a primary step to prepare EGCG-encapsulated functional food products.

CHAPTER 8: MAIN RESULTS REVIEW&CONCLUSIONS

Review of main results

Our literature review showed that PEF is a developing green processing technology with numerous potential applications in the food sector. As the importance of sustainability rises, it is anticipated that PEF utilization will expand in the coming years. Based on existing studies on the effects of PEF on the structure and technological qualities of plant and dairy proteins, the following conclusions can be drawn:

a. The exact PEF parameters, including EFS, treatment chambers, pulse duration, and pulse shape, have a substantial effect on the impacts of PEF on proteins' techno-functional and structure properties.

b. Depending on the type of protein being investigated, the PEF effects on protein structure and technological properties differ.

Due to the limited number of studies undertaken on the PEF effects on dietary proteins, several factors require additional research. It is essential to examine the influence of varying EFS on protein structure and techno-functional properties in order to determine the ideal PEF conditions for enhancing these capabilities. In addition, future research is advised to investigate the effect of nanoseconds PEF treatment on the structural and functional aspects of dietary proteins.

In addition, PEF could potentially produce extremely efficient emulsifiers or demulsify emulsion systems. The utilization of PEF as emulsification or demulsification technology needs to be investigated. However, it is necessary to address the difficulties associated with PEF applications, such as the impact of PEF parameters on treatment outcomes. To clarify clear mechanisms, research should focus on comprehending the thermal, chemical, and biophysical effects of PEF on protein structures. To facilitate comparisons between studies, it is imperative that authors disclose exhaustive details about treatment conditions. Referencing standards and recommendations, such as those provided by Cemazar et al. [80], help improve PEF application reporting. In addition, collaboration between the food industry and academic

institutions is essential for designing and developing PEF devices with more energy-efficient and controlled treatment conditions.

PEF treatment was utilized at an electric field strength ranging from 3.5 to 5.7 kV/cm, with a pulse duration of 50 μs, to examine the impact of PEF on BSA/soluble starch glycation. The Maillard reaction between soluble starch and BSA has been successfully facilitated using PEF treatment. The physicochemical characteristics of BSA/ soluble starch conjugates are significantly influenced by applying various EFSs during PEF treatment. Regarding the BSA/starch conjugates, PEF treatment enhanced the degree of grafting, protein solubility, and browning at EFSs between 3.5 and 5.7 kV/cm. Additionally, the conjugate particle sizes, surface hydrophobicity and fluorescence intensity were decreased. However, the protein solubility, DG, and particle sizes of BSA/starch conjugates decreased when the EFS exceeded 5.7 kV/cm. These results demonstrate the potential of PEF treatment to alter and improve the properties of food ingredients by highlighting the impact of various EFSs on the physicochemical properties of BSA/soluble starch conjugates. Emulsions stabilized by PEF-induced conjugates in the 3.5–5.7 kV/cm EFS range showed reduced droplet sizes and exhibited superior stability across various environmental conditions, such as freezing, fluctuating ionic strengths, and pH variations. On the other hand, emulsions stabilized by PEF-induced conjugates at EFS> 5.7 kV/cm exhibited bigger droplet sizes and less stability when exposed to these environmental factors.

Applying PEF treatment (0-30 kV/cm for 480 ns) proved effective in modifying the physicochemical and structural properties of CSMs. The treatment increased β-sheet contents, absolute ζ-potential values, and protein solubility. Additionally, PEF treatment reduced surface hydrophobicity, α-helix content, and particle sizes of the CSMs. Notably, no significant differences were observed in the physicochemical properties of CSMs treated at higher voltages (20-30 kV/cm) compared to those treated at 10 kV/cm. These findings suggest that using a moderate electric field (MEF) treatment could be a more energy-efficient approach when aiming to modify the structure of casein.

nsPEF treatment (0-20 kV/cm, 90ns) was applied to alter the structure of BSA and facilitate the BSA/EGCG binding. nsPEF increased the α-helix content, particle sizes, absolute ζ-potential, and surface hydrophobicity values of BSA. Moreover, the addition of EGCG to nsPEF-induced BSA resulted in a significant increase in particle sizes of BSA and a decrease in fluorescence intensity and surface hydrophobicity. nsPEF treatment of BSA/EGCG mixtures induced changes in BSA structures as confirmed by Raman FTIR

spectroscopy. Raman's results showed that nsPEF induced changes in protein structure, mainly in S-S and S-C bonds. Changes in amide I and II were observed in FTIR spectra of nsPEF-induced BSA/EGCG mixtures. Moreover, nsPEF improved the particle sizes, absolute ζ-potential values and UV-vis absorbance intensity while reducing the surface hydrophobicity values. Molecular docking confirmed that BSA can bind with EGCG at specific active sites on both molecules.

Conclusions

1. PEF treatment can enhance the properties of BSA/starch conjugates and their emulsions. Lower EFS (3.5–5.7 kV/cm) improved the stability and various characteristics, while higher strengths (> 5.7 kV/cm) had minimal effects. Future research should focus on mechanism exploration and parameter optimization.

2. PEF treatment effectively altered CSMs by increasing ζ-potential values, reducing particle sizes, and changing protein structures. These modifications were primarily due to PEF-induced polarization, free radical formation, and bond changes. Future plans involve developing a semi-automated continuous processing system with a Marx-based PEF generator.

3. nsPEF modified BSA and enhanced its binding with EGCG. This altered BSA's structure, and changed particle sizes, and surface hydrophobicity. Further investigation should focus on the stability of nsPEF-treated BSA/EGCG mixtures for potential functional food applications.

SANTRAUKA

ĮVADAS

Klimato kaita tampa itin svarbia mūsų planetai, nes ji daro didžiulį poveikį maisto saugumui, žmonių sveikatai ir biologinei įvairovei. Taigi ekologiškos perdirbimo technologijos tampa būtinos siekiant darnaus vystymosi tikslų. Impulsinis elektrinis laukas (PEF), kaip ekologiška perdirbimo technologija, pastaraisiais metais tapo potencialiu maisto produktų naudojimo būdu. PEF naudoja trumpus, galingus elektros impulsus, taikomus maisto produktams, sukeliančius įvairius struktūrinius ir fizikinius cheminius pokyčius [1]. Šis metodas tapo reikšmingesnis, nes gali padidinti fitocheminių medžiagų ekstrahavimo išeigą, pagerinti maisto saugą, išlaikyti maistinę vertę ir pailginti galiojimo laiką [2–4]. Be to, PEF suteikia galimybę modifikuoti baltymus, kurie yra labai svarbūs maisto sistemų stabilumui ir funkcinėms savybėms [5].

Pieno baltymai ypač svarbūs maisto pramonėje dėl savo funkcinės ir maistinės vertės. Kazeinai ir išrūgų baltymai, sudarantys pieno baltymus, turi skirtingą struktūrą ir funkcijas [6].

Šių baltymų struktūrinės savybės turi įtakos jų sąveikai su kitais maisto komponentais. PEF sukeltų baltymų struktūrinių pokyčių supratimas gali padėti pagerinti jų techno-funkcines savybes. Buvo atlikti keletas tyrimų PEF poveikio kai kuriems augaliniams ir gyvūniniams baltymams [7–10]. Tačiau didelės galios PEF poveikis micelinių kazeinų struktūrai dar nėra pakankamai ištirtas. Dėl savo amfifilinės struktūros baltymai naudojami daugelio maisto produktų emulsijų sistemoms stabilizuoti [11]. Tačiau baltymai yra jautrūs temperatūros, pH ir jonų stiprumo pokyčiams. Baltymų sąveika su polisacharidais yra vienas iš būdų, kaip įveikti baltymų jautrumą supančiai aplinkai. Tačiau vis dar trūksta žinių, susijusių su PEF sukelto galvijų serumo albumino (BSA) ir tirpaus krakmolo sąveikos analize.

Be to, daug dėmesio sulaukia baltymų ir polifenolių – iš augalų gaunamų bioaktyvių medžiagų – sąveika [12]. Priešuždegiminė ir antioksidacinė veikla yra pagrindinės pripažintos polifenolių sveikatą stiprinančios savybės [13]. Kai šios medžiagos sąveikauja su baltymais, gali pakisti maisto produktų stabilumas, biologinis prieinamumas ir jutiminės savybės [14–16]. Mažai žinoma apie baltymų ir polifenolių sąveiką, kai jie veikiami PEF. Todėl pagrindinis šio doktorantūros darbo tikslas – ištirti, kaip PEF veikia micelinio kazeino struktūrą, sąveiką tarp BSA ir tirpaus krakmolo bei tarp BSA ir arbatos polifenolių (Epigallocatechin Gallate, EGCG).

Šiems tikslams pasiekti buvo suformuluotos šios užduotys:

1. Ištirti, kaip apdorojimas PEF (3,5–8,1 kV/cm) gali paveikti BSA ir tirpaus krakmolo sąveiką (Maillardo reakcija) (3 skyrius).

2. Įvertinti PEF (3,5–8,1 kV/cm) apdorotais ir neapdorotais BSA/krakmolo konjugatais stabilizuotų emulsijų fizikinį-cheminį ir stabilumą (4 skyrius).

3. Ištirti, kaip PEF (0-30 kV/cm) gali paveikti kazeino micelių struktūrines savybes (5 skyrius).

4. Ištirti, kaip PEF gali turėti įtakos BSA ir EGCG sąveikai (6 skyrius).

METODIKA

A. Ištirti, kaip apdorojimas PEF (3,5–8,1 kV/cm) gali paveikti BSA ir tirpaus krakmolo sąveiką (Maillardo reakcija)

Tekste aprašytas tyrimo metodas apima BSA/krakmolo mišinių apdorojimą ir apibūdinimą naudojant impulsinį elektrinį lauką (PEF). Čia yra tyrimo metodo santrauka:

1. BSA/krakmolo mišinių paruošimas:

Tirpusis krakmolas ištirpinamas distiliuotame vandenyje, kurio koncentracija yra 2 mg/mL, ir kaitinamas iki maždaug 50 °C, kol visiškai ištirps.

Krakmolo tirpalas atšaldomas iki kambario temperatūros ir sumaišomas su BSA (taip pat 2 mg/mL koncentracija).

- Mišinys maišomas 1 valandą kambario temperatūroje.

2. Elektros laidumo matavimas:

BSA ir BSA/krakmolo mišinių elektrinis laidumas matuojamas Mettler Toledo konduktometru su InLab 738-ISM jutikliu.

Nurodytos laidumo vertės prieš apdorojimą PEF kaip 1,43±0,22 mS/cm BSA ir 1,24±0,09 mS/cm BSA/krakmolo mišiniams.

3. PEF gydymas:

Dalis (0,9 ml) BSA/krakmolo mišinio perpilama į elektroporacijos kiuvetę su 4 mm tarpu.

Kiuvetės, kuriose yra mišinių, apdorojamos PEF naudojant impulsų generatorių, sukurtą Valstybiniame tyrimų institute, Fizinių mokslų ir technologijos centre (FTMC) Vilniuje, Lietuvoje.

PEF poveikis apima 10 impulsų, kurių impulso trukmė (τ) yra 50 μs.

4. pH ir temperatūros matavimas:

- Užfiksuojamos mėginių pH vertės prieš ir po apdorojimo PEF, rodo nedidelį sumažėjimą, bet vis dar yra neutralioje ribose (6,98-7,34).
- Temperatūros pokyčiai PEF gydymo metu stebimi naudojant infraraudonųjų spindulių kamerą (FLIR one pro), prijungtą prie Android išmaniojo telefono.

5. BSA/krakmolo konjugatų apibūdinimas:

- Rudinimo intensyvumas ir UV-Vis spektrai: Maillard reakcijos produktų rudumo intensyvumas matuojamas pagal absorbciją esant 420 nm, naudojant UV-matomo spektrofotometrą. UV-Vis spektrai taip pat registruojami tarp 260 ir 340 nm.
- Skiepijimo laipsnis: Glikuoto BSA skiepijimo laipsnis nustatomas naudojant OPA (1,2-ftalio dikarboksilato) metodą.
- Paviršiaus hidrofobiškumo (H_0) matavimas: BSA ir BSA/krakmolo konjugatų hidrofobiškumo vertės matuojamos naudojant fluorescencinį zondą 1-anilino-8-naphthalenesulfonatą (ANS).
- Savosios fluorescencinės emisijos spektroskopija: BSA ir BSA/krakmolo konjugatų vidinės fluorescencijos spektrai matuojami naudojant spektrofotometrą.
- Dalelių dydis: mėginių dalelių dydis (zeta vidurkis) vertinamas naudojant dinaminę lazerio šviesos sklaidą (DLS).
- Baltymų tirpumas: baltymų tirpumas matuojamas naudojant Bradfordo baltymų tyrimą.

6. Statistinė analizė:

- Visi eksperimentai atliekami trimis pakartojimais, o duomenys pateikiami kaip vidurkis±standartinis nuokrypis.
- Statistinė analizė atliekama naudojant SPSS programą, taikant vienpusę ANOVA, o po to Dunkano testą, siekiant nustatyti skirtumų tarp vidurkių reikšmingumą ($p<0,05$).

B. Įvertinti PEF (3,5–8,1 kV/cm) apdorotais ir neapdorotais BSA/krakmolo konjugatais stabilizuotų emulsijų fizikinį-cheminį ir stabilumą

Šis tyrimo metodas orientuotas į emulsijų paruošimą ir apibūdinimą naudojant BSA ir BSA/krakmolo konjugatus. Emulsijai paruošti buvo sumaišomi BSA arba BSA/krakmolo konjugatai su saulėgrąžų aliejumi, naudojant sūkurį, o po to mišinys buvo apdorojamas ultragarsu, kad būtų galima emulsinti. Ultragarsinio apdorojimo proceso energijos tankis buvo apskaičiuotas naudojant mėginių galią, laiką ir tūrį. Emulsijos buvo apibūdintos nustatant lašelių dydį naudojant Zetasizer analizatorių ir įvertinant adsorbuotą baltymą (AP %) aplink aliejaus lašelius, naudojant centrifugavimą ir baltymų koncentracijos matavimus.

Konfokalinė mikroskopija buvo naudojama emulsijų mikrostruktūrinėms savybėms ištirti, dažant aliejaus ir baltymų komponentus. Emulsijų šiluminės savybės užšalimo sąlygomis buvo analizuojamos naudojant diferencinę nuskaitymo kalorimetriją (DSC), kuri apėmė mėginių aušinimą ir šildymą stebint šilumos srautą. Emulsijų stabilumas buvo įvertintas skirtingomis sąlygomis, įskaitant BSA izoelektrinį tašką (pI) ir esant įvairioms jonų stiprumams. Buvo įvertinti lašelių dydžiai, AP % ir emulsijų mikrostruktūra, siekiant nustatyti jų stabilumą tokiomis sąlygomis.

Tyrimo metodas apima įvairių instrumentų ir metodų, tokių kaip ultragarsinis apdorojimas, Zetasizer analizatorius, centrifugavimas, Bradfordo tyrimas, konfokalinė mikroskopija ir DSC, naudojimą. Statistinė analizė buvo atlikta naudojant SPSS programą, o skirtumų tarp vidurkių statistiniam reikšmingumui nustatyti buvo naudojama vienpusė ANOVA, po kurios buvo atliktas Duncan testas.

C. Ištirti, kaip PEF (0-30 kV/cm) gali paveikti kazeino micelių struktūrines savybes

Šis metodas apima keletą matavimų ir analizių, skirtų įvertinti įvairias baltymų mėginių savybes prieš ir po apdorojimo PEF. Čia pateikiamas metodo suskirstymas:

1. Apdorojimas PEF: Baltymų suspensijos ruošiamos kalio fosfato buferyje ir maišomos per naktį. Dalis suspensijos perkeliama į elektroporacijos kiuvetę, o PEF apdorojimas atliekamas naudojant naminį elektroporatorių. Nurodoma taikoma įtampa, srovė, impulso trukmė ir impulso forma.

2. Dalelių dydis ir ζ-potencialas: Baltymų mėginių ζ-potencialas ir dalelių dydis nustatomi naudojant Malvern Zetasizer analizatorių. Atliekant matavimus atsižvelgiama į praskiestų mėginių lūžio rodiklius.

3. Baltymų tirpumas. Baltymų mėginių tirpumas įvertinamas centrifuguojant mėginius ir išmatuojant baltymų koncentraciją supernatante, naudojant Bradfordo baltymų tyrimą.

4. Paviršiaus hidrofobiškumas (Ho): baltymų mėginių paviršiaus hidrofobiškumas nustatomas naudojant ANS, kaip fluorescencinį zondą. Paruoštos skirtingos baltymų koncentracijos, o fluorescencijos intensyvumas matuojamas naudojant spektrometrą.

5. Fluorescencijos spektroskopija: baltymų mėginių vidinės fluorescencijos spektrai registruojami naudojant spektrometrą su nurodytais sužadinimo ir emisijos bangų ilgiais. Fluorescencijos spektrai fiksuojami, kad būtų galima suprasti antrinius baltymo struktūrinius pokyčius.

6. Furjė transformacijos infraraudonųjų spindulių spektroskopija (FTIR): Baltymų mėginių IR spektrai gaunami naudojant infraraudonųjų spindulių spektrometrą. Spektrai apima platų diapazoną, o programinė įranga naudojama paslėptoms smailėms amido I srityje nustatyti, kad būtų galima analizuoti antrinius struktūrinius pokyčius.

7. Ramano spektroskopija: Ramano spektrai renkami naudojant Ramano spektrometrą su specifiniu sužadinimo šaltiniu. Dvigubų smailių santykis apskaičiuojamas siekiant ištirti vandenilio jungimosi mikroaplinką fenolio hidroksilo grupėse.

8. Skenuojanti elektroninė mikroskopija (SEM): SEM mikrografijos fiksuojamos naudojant SEM įrenginį, siekiant ištirti baltymų mėginių morfologiją. Mėginiai paruošiami dulkinant auksu ir stebimi skirtingais padidinimais.

9. Statistinė analizė: Eksperimentai atliekami trimis egzemplioriais, o duomenys analizuojami naudojant statistinę programinę įrangą. Vidurkių statistiniam reikšmingumui nustatyti naudojama vienpusė ANOVA ir Duncan testas.

D. NANOSEKUNDŽIŲ TRUKMĖS IMPULSINIS ELEKTRINIS LAUKAS (nsPEF) SKATINA BSA IR EPIGALLOCATECHIN GALATO (EGCG) SUSIRIŠIMĄ

nsPEF poveikis (900 ns, 0-20 kv/cm) buvo pritaikytas tiriant BSA struktūros pokyčius ir BSA/EGCG surišimą.

Buvo naudojami anksčiau minėti tyrimo metodai, tokie kaip dalelių dydžiai, paviršiaus hidrofobiškumas, FTIR, Ramano ir CD spektroskopija. Be to, siekiant patvirtinti BSA / EGCG surišimą, buvo pritaikytas molekulinis prijungimas.

REZULTATAI

A. Ištirti, kaip apdorojimas PEF (3,5–8,1 kV/cm) gali paveikti BSA ir tirpaus krakmolo sąveiką (Maillardo reakcija)

Pagrindinius skyriaus „Rezultatai ir diskusijos“ rezultatus ir išvadas galima apibendrinti taip:

1. Baltymų ir polisacharidų sąveika:

- PEF padidino BSA ir krakmolo konjugatų rudinimo intensyvumą (A_{420} vertės), o tai rodo, kad Maillardo reakcijos intensyvumas padidėjo.
- BSA ir krakmolo konjugatų absorbcijos intensyvumas (UV-Vis spektras) taip pat padidėjo po apdorojimo PEF, o tai rodo Schiff bazės ir pagrindinės būsenos kompleksų susidarymą.
- PEF žymiai padidino skiepijimo laipsnį, o tai rodo sustiprintą baltymų ir polisacharidų sąveiką. Tačiau esant stipresniam PEF, skiepijimo laipsnis sumažėjo.
- BSA ir krakmolo konjugatų dalelių dydis sumažėjo po PEF apdorojimo, o mažiausias dalelių dydis pastebėtas esant tam tikram eletrinio lauko stipriui (EFS). Didesnis EFS padidino dalelių dydį.
- Baltymų tirpumas padidėjo po apdorojimo PEF ir pasiekė maksimumą esant tam tikram EFS, bet tirpumas sumažėjo esant didesniam EFS.

2. Fluorescencinė ir H_0 analizės:

- BSA ir krakmolo konjugatų fluorescencijos intensyvumas sumažėjo po PEF apdorojimo, o tai rodo krakmolo apsauginį poveikį Maillardo reakcijos metu.
- BSA H_0 reikšmės palaipsniui mažėjo didėjant EFS, o tai rodo baltymo tretinės struktūros pokyčius.

Apskritai PEF paveikė baltymų ir polisacharidų sąveiką, todėl padidėjo rudos spalvos intensyvumas, skiepijimo laipsnis, sumažėjo dalelių dydis ir padidėjo baltymų tirpumas. Fluorescencijos intensyvumas ir H_0 vertės rodo, kad BSA tretinė struktūra pasikeitė po konjugacijos su krakmolu ir PEF.

B. Įvertinti PEF (3,5–8,1 kV/cm) apdorotais ir neapdorotais BSA/krakmolo konjugatais stabilizuotų emulsijų fizikinį-cheminį ir stabilumą

Pagrindinius skyriaus „Rezultatai ir diskusijos“ rezultatus ir išvadas galima apibendrinti taip:

1. Lašelių dydis ir emulsijų morfologija:

- Emulsijos, stabilizuotos BSA/krakmolo konjugatais, kurios buvo apdorotos PEF, buvo mažesnio lašelių dydžio, palyginti su stabilizuotomis natūraliu BSA.
- PEF apdoroti konjugatai su mažesniu elektrinio lauko stipriu parodė patobulintą konjugaciją, todėl lašelių dydžiai buvo mažesni ir emulsijos stabilumas pagerėjo.

2. Diferencinės nuskaitymo kalorimetrijos (DSC) analizė:

- BSA/krakmolo mišinių apdorojimas PEF sumažino emulsijų užšalimo temperatūrą, o tai rodo ledo kristalų susidarymo slopinimą.
- Užšalimo elgesio pokyčiai buvo siejami su sudėtingesnės BSA / krakmolo sudėties atsiradimu po apdorojimo PEF.

3. Emulsijos stabilumas:

- Emulsijos lašelių dydžiai kinta priklausomai nuo skirtingos NaCl koncentracijos.
- BS-PEF 1 ir BS-PEF 3 emulsijos turėjo mažiausius lašelių dydžius, kai NaCl koncentracija buvo 150 mM.
- NaCl, kartu su BSA ir krakmolu, sustiprino baltymų plėvelę aplink aliejaus lašelius, pagerindamas emulsijos stabilumą.

4. pH poveikis emulsijai:

- Emulsijos, stabilizuotos BSA/krakmolo konjugatais, turėjo mažesnius lašelių dydžius, palyginti su stabilizuotomis natūraliu BSA.
- PEF apdorotos emulsijos, kurių pH 4,6, parodė didžiausią adsorbuotą baltymą (AP%) ir mažiausią lašelių skersmenį.

- BSA ir krakmolas kartu užkirto kelią BSA agregacijai esant pH 4,6, padidindami emulsijos sistemos stabilumą.

5. Siūlomas BSA/krakmolo konjugatų glikacijos su PEF mechanizmas ir jų emulsinimo savybės:

- PEF paskatino BSA molekulių išsilankstymą, sumažino dalelių dydį, padidino tirpumą ir sukūrė daugiau laisvųjų aminorūgščių.
- BSA ir krakmolo konjugatai po PEF pasižymėjo pagerintomis emulsinimo savybėmis dėl bendros BSA ir krakmolo adsorbcijos, sudarydami dvigubą sluoksnį ir sumažindami sąveikos įtampą.

C. Ištirti, kaip PEF (0-30 kV/cm) gali paveikti kazeino micelių struktūrines savybes

Pagrindiniai skilties „Rezultatai ir diskusija“ rezultatai yra tokie:

1. PEF poveikis dalelių dydžiui ir ζ potencialui:

- PEF apdorojimas 10 kV/cm padidino baltymų molekulių dalelių dydį, o didesnis PEF stiprumas (20-30 kV/cm) sumažino dalelių dydį.
- Po PEF apdorojimo padidėjo baltymų ζ-potencialas (elektros krūvis), o tai rodo neigiamų krūvių padidėjimą baltymo paviršiuje.

2. Baltymų tirpumas ir drumstumas:

- Apdorojimas PEF pagerino baltymų tirpumą, todėl tirpumo procentas didesnis esant 10, 20 ir 30 kV/cm.
- Drumstumas (nurodantis šviesos sklaidos kiekį) žymiai padidėjo CSM, apdorotiems 10 kV/cm, o tai rodo didesnių agregatų susidarymą ir dalelių dydžio padidėjimą.

3. Tretinė struktūra ir paviršiaus hidrofobiškumas:

- Fluorescencijos intensyvumas padidėjo po PEF apdorojimo esant 10 kV/cm, o tai rodo, kad aromatinės aminorūgštys pateko į hidrofobinę aplinką.
- Hidrofobiškumas aplink fluoroforą padidėjo, o tai rodo dalinį baltymų molekulių išsiskleidimą.
- Apdorojant PEF, atsirado daugiau paslėptų hidrofobinių zonų, todėl padidėja paviršiaus hidrofobiškumas.

4. Mikrostruktūra:

- SEM vaizdai parodė, kad gydymas PEF sukėlė kazeino paviršiaus struktūros sutrikimus, o esant didesniam PEF stiprumui – sunkesni.

5. Antrinė baltymo struktūra:

- PEF sumažino α spiralės kiekį ir padidino β posūkio ir β lakšto kiekį CSM.
- Hidrofobinių sričių poveikis ir baltymų sąveikos sutrikimas gali prisidėti prie pastebėtų struktūrinių pokyčių.

6. Ramano spektroskopijos analizė:

- Ramano juostos, susijusios su disulfidinėmis jungtimis, intensyvumas padidėjo po poveikio PEF.
- Stebėti įvairių cheminių jungčių vibracijos intensyvumo pokyčiai, rodantys konformacinius CSM pokyčius.

D. NANOSEKUNDŽIŲ TRUKMĖS IMPULSINIO ELEKTRINIO LAUKO SKATINA BSA IR EPIGALLOCATECHIN GALATO (EGCG) SĄVEIKĄ

nsPEF apdoroto BSA ir (nsPEF BSA)+EGCG fizikinės ir cheminės savybės.

Ištyrėme BSA dalelių dydžių, ζ potencialo (paviršiaus krūvio) ir paviršiaus hidrofobiškumo pokyčius po apdorojimo nsPEF. Rezultatai parodė, kad nsPEF padidino dalelių dydį, galbūt dėl dalinės BSA molekulių agregacijos. Panašūs pastebėjimai buvo atlikti kitame tyrime, kuriame naudojome CSM. BSA ζ potencialas padidėjo po poveikio nsPEF, greičiausiai dėl neigiamo krūvio grupių poveikio ir dėl dalinio BSA molekulių išsiskleidimo.

Nustatyta, kad BSA paviršiaus hidrofobiškumas palaipsniui gerėja po poveikio nsPEF ir pasiekia aukščiausią tašką esant tam tikram nsPEF intensyvumui. Šis pagerėjimas gali būti siejamas su hidrofobinių grupių mažėjimu BSA molekulėse. Tyrėjai įvedė EGCG arbatos polifenolį į nsPEF apdorotą BSA, kad ištirtų jų sąveiką. Pridėjus EGCG, padidėjo dalelių dydis, o tai rodo BSA ir EGCG jungimąsi. Ši sąveika taip pat sumažino paviršiaus hidrofobiškumą, o tai rodo, kad EGCG prisijungia prie hidrofobinių aminorūgščių BSA paviršiuje.

Fluorescencijos intensyvumo matavimai parodė, kad esant mažesniam nsPEF intensyvumui, tiek nsPEF apdoroto BSA, tiek su EGCG surišto BSA intensyvumas padidėjo, tačiau jis sumažėjo esant didesniam intensyvumui. EGCG pridėjimas prie nsPEF apdoroto BSA sukėlė mažesnį fluorescencijos intensyvumą ir bangos ilgio poslinkį, o tai rodo triptofano ir EGCG sąveiką.

Žiedinio dichroizmo (CD) analizė atskleidė antrinės BSA struktūros pokyčius po poveikio nsPEF. α-spiralės kiekis padidėjo, o β lakštų, β posūkių ir netvarkingų struktūrų sumažėjo. Šie struktūriniai pokyčiai buvo panašūs į tyrimo, apimančio ultragarsinį BSA gydymą, rezultatus.

Šioje tyrimo dalyje gilinamasi į sudėtingas fizikines ir chemines BSA-EGCG kompleksų savybes po nanosekundžių impulsinių elektrinių laukų (nsPEF) poveikio.

Norėdami atskleisti poveikį, sumaišėme BSA ir EGCG santykiu 1: 1, pasiekdami galutinę 1% BSA ir 0,5 mmol/l EGCG koncentraciją. Gautas mišinys buvo apdorotas nsPEF, apimantis 3 impulsus. Rezultatai, atskleidė reikšmingus BSA molekulių dalelių dydžių pokyčius, o didžiausias padidėjimas pastebėtas, kai BSA-EGCG mišinys buvo apdorotas 8 kV/cm nsPEF. Šis padidėjimas buvo siejamas su kovalentinio EGCG prisijungimo prie BSA, dalinio baltymo struktūros išsiskleidimo ir naujo BSA-EGCG biopolimero atsiradimo sąveika. Tai rodo, kad nsPEF gali paskatinti EGCG susiejimą su BSA, skatindamas dalinį baltymų atsiskleidimą ir padarydamas poliarines grupes labiau prieinamas baltymo paviršiuje.

Be to, absoliučios ζ-potencialo vertės pastebimai padidėjo – nuo 8,7 mV neapdorotam BSA-EGCG mišiniui (BE-0) iki 33,7 mV po gydymo nsPEF esant 8 kV/cm. Šis poslinkis buvo suprantamas kaip nsPEF gebėjimo padidinti baltymų molekulių poliarizaciją pasekmė, taip atskleidžiant didesnį neigiamo krūvio grupių kiekį baltymo išorėje. Ši tendencija atkartojo kito Tan ir kt. tyrimo išvadas, kuriose buvo panašus absoliučios ζ-potencialo vertės padidėjimas po apdorojimo aukštu hidrostatiniu slėgiu panašiuose mišiniuose.

Be to, į BSA mišinį įvedus EGCG, paviršiaus hidrofobiškumas, įtakingas faktorius, lemiantis baltymų sąveiką, smarkiai sumažėjo. Šis sumažėjimas galėjo būti siejamas su fluorescencijos gesimu, atsirandančiu dėl EGCG ir BSA prisijungimo. Šis reiškinys sustiprėjo po nsPEF poveikio, tikriausiai dėl BSA išsilankstimo, kuris gali atskleisti papildomas surišimo vietas baltymo paviršiuje, sustiprindamas BSA ir EGCG sąveiką ir, atitinkamai,

sustiprindamas fluorescencijos gesinimą, o tai baigtųsi sumažėjusiu paviršiaus hidrofobiškumu.

Norint toliau išnagrinėti struktūrinius poslinkius, kuriuos sukelia nsPEF, buvo naudojama UV-vis spektroskopija. Padidėjęs UV spindulių spektro absorbcijos smailių intensyvumas po nsPEF apdorojimo ir vėlesnio EGCG pridėjimo prie natūralios BSA reiškė sudėtingų kompleksų, atsirandančių dėl molekulinės sąveikos, susidarymą, galinčių sukelti naujus perėjimus, susijusius su aromatinėmis aminorūgštimis.

Be to, Ramano spektroskopija buvo panaudota siekiant pagrįsti struktūrinius BSA-EGCG kompleksų pokyčius, kuriuos sukelia nsPEF. Pažymėtina, kad Ramano signalo, susijusio su disulfidiniais ryšiais, intensyvumas padidėjo po nsPEF poveikio, o tai rodo izomerizacijos reakcijas, susijusias su SS jungtimis. Ramano tyrimai dar labiau atskleidė cisteino disulfido sąveikos pokyčius, kurie gali būti priskirti S-S jungties izomerizacijos reakcijoms, o tai rodo reikšmingą nsPEF poveikį baltymų disulfido jungtims.

Ramano spektro tirozino (Tyr) dubletas, jautrus vandenilio jungčių konfigūracijoms ir vietinei hidrofobinei ar hidrofilinei aplinkai, parodė mažėjantį I850/I830 santykį, padidinus nsPEF intensyvumą. Ši tendencija patvirtina, kad Tyr liekanos atsiduria labiau hidrofobinėje aplinkoje, galbūt dėl to, kad susidaro naujas vandenilio jungtis, panašiai kaip stebėjimai, atlikti baltymų ir antocianino sąveikos kontekste.

Galiausiai tiriant BSA-EGCG kompleksus Furjė transformacijos infraraudonųjų spindulių (FTIR) spektroskopija pastebėta, kad naujų smailių atsiradimas amido regionuose siejamas su BSA antrinių struktūrų pokyčiais. Šios išvados pakartojo Ramano rezultatus, o tai rodo, kad nsPEF iš tikrųjų paveikė BSA antrinę struktūrą, galbūt tarnaujantis kaip BSA ir EGCG sąveikos katalizatorius.

Apibendrinant, šio skyriaus tyrimus atskleistas daugialypis nsPEF poveikis sudėtingoms BSA-EGCG kompleksų fizikinėms ir cheminėms savybėms. Išvados pabrėžė sudėtingą sąveiką tarp nsPEF sukeltų struktūrinių pokyčių, BSA-EGCG sąveikos ir vėlesnių dalelių dydžių, paviršiaus krūvio, paviršiaus hidrofobiškumo ir baltymų struktūrų pokyčių.

IŠVADOS

PEF paveikė baltymų ir polisacharidų sąveiką, todėl padidėjo rudos spalvos intensyvumas, skiepijimo laipsnis, sumažėjo dalelių dydis ir padidėjo baltymų tirpumas. Fluorescencijos intensyvumas ir H_0 vertės rodo, kad BSA tretinė struktūra pasikeitė po konjugacijos su krakmolu PEF poveikyje.

BSA / krakmolo konjugatų apdorojimas PEF sumažino lašelių dydžius, padidino emulsijos stabilumą esant įvairiems aplinkos įtempiams ir pagerino užšalimo elgesį, todėl jie buvo perspektyvūs įvairiems maisto produktams.

Apdorojimas PEF paveikė baltymų molekulių dalelių dydį, tirpumą, drumstumą, tretinę ir antrinę struktūras, paviršiaus hidrofobiškumą ir mikrostruktūrą. Šie rezultatai rodo, kad PEF gali sukelti struktūrinius kazeino micelių pokyčius, galinčius turėti įtakos jų funkcinėms savybėms.

nsPEF buvo taikomas siekiant pakeisti BSA struktūrą ir palengvinti BSA / EGCG surišimą. nsPEF padidino BSA α-spiralės kiekį, dalelių dydžius, absoliutų ζ potencialą ir paviršiaus hidrofobiškumo reikšmes. Be to, pridėjus EGCG į nsPEF sukeltą BSA, žymiai padidėjo BSA dalelių dydis ir sumažėjo fluorescencijos intensyvumas bei paviršiaus hidrofobiškumas. BSA / EGCG mišinių nsPEF apdorojimas sukėlė BSA struktūrų pokyčius, kaip patvirtino Ramano FTIR spektroskopija. Ramano rezultatai parodė, kad nsPEF sukėlė baltymų struktūros pokyčius, daugiausia S-S ir S-C ryšiuose. Amido I ir II pokyčiai buvo pastebėti nsPEF sukeltų BSA/EGCG mišinių FTIR spektruose. Be to, nsPEF pagerino dalelių dydžius, absoliučiąsias ζ-potencialų vertes ir UV-vis absorbcijos intensyvumą, tuo pačiu sumažindamas paviršiaus hidrofobiškumo vertes. Molekulinis modeliavimas patvirtino, kad BSA gali prisijungti prie EGCG tam tikrose aktyviose abiejų molekulių vietose. Rekomenduojama tirti nsPEF sukeltų BSA/EGCG mišinių stabilumą esant skirtingoms sąlygoms (t.y. šviesai, temperatūrai, virškinimo sistemos sąlygoms ir kt.), kaip pirminį etapą ruošiant funkcinius maisto produktus su EGCG kapsulėmis.

REFERENCES

[1] Taha, A.; Casanova, F.; Šimonis, P.; Stankevič, V.; Gomaa, M. A. E.; Stirkė, A. Pulsed Electric Field: Fundamentals and Effects on the Structural and Techno-Functional Properties of Dairy and Plant Proteins. *Foods* **2022**, *11* (11), 1556.

[2] Vega-Mercado, H.; Martín-Belloso, O.; Qin, B.-L.; Chang, F.-J.; Góngora-Nieto, M. M.; Barbosa-Cánovas, G. V; Swanson, B. G. Non-Thermal Food Preservation: Pulsed Electric Fields. *Trends Food Sci Technol* **1997**.

[3] Kumari, B.; Tiwari, B. K.; Hossain, M. B.; Brunton, N. P.; Rai, D. K. Recent Advances on Application of Ultrasound and Pulsed Electric Field Technologies in the Extraction of Bioactives from Agro-Industrial By-Products. *Food Bioproc Tech* **2018**, *11* (2), 223–241.

[4] Wiktor, A.; Dadan, M.; Nowacka, M.; Rybak, K.; Witrowa-Rajchert, D. The Impact of Combination of Pulsed Electric Field and Ultrasound Treatment on Air Drying Kinetics and Quality of Carrot Tissue. *Lwt* **2019**, *110*, 71–79.

[5] Middendorf, D.; Bindrich, U.; Siemer, C.; Töpfl, S.; Heinz, V. Affecting Casein Micelles by Pulsed Electrical Field (PEF) for Inclusion of Lipophilic Organic Compounds. *Applied Sciences 2021, Vol. 11, Page 4611* **2021**, *11* (10), 4611.

[6] Goulding, D. A.; Fox, P. F.; O'Mahony, J. A. Milk Proteins: An Overview. In *Milk Proteins: From Expression to Food*; Academic Press, 2020; pp 21–98.

[7] Li, Y.; Chen, Z.; Mo, H. Effects of Pulsed Electric Fields on Physicochemical Properties of Soybean Protein Isolates. *LWT - Food Science and Technology* **2007**, *40* (7), 1167–1175.

[8] Perez, O. E.; Pilosof, A. M. R. Pulsed Electric Fields Effects on the Molecular Structure and Gelation of β-Lactoglobulin Concentrate and Egg White. *Food Research International* **2004**, *37* (1), 102–110.

[9] Xiang, B. Y.; Ngadi, M. O.; Ochoa-Martinez, L. A.; Simpson, M. V. Pulsed Electric Field-Induced Structural Modification of Whey Protein Isolate. *Food Bioproc Tech* **2011**, *4* (8), 1341–1348.

[10] Giteru, S. G.; Oey, I.; Ali, M. A. Feasibility of Using Pulsed Electric Fields to Modify Biomacromolecules: A Review. *Trends Food Sci Technol* **2018**, *72* (January 2017), 91–113.

[11] McClements, D. J. Protein-Stabilized Emulsions. *Curr Opin Colloid Interface Sci* **2004**, *9* (5), 305–313.

[12] Sajilata, M. G.; Bajaj, P. R.; Singhal, R. S. Tea Polyphenols as Nutraceuticals. *Comprehensive Reviews in Food Science and Food Safety*. 2008, pp 229–254.

[13] Cutrim, C. S.; Cortez, M. A. S. A Review on Polyphenols: Classification, Beneficial Effects and Their Application in Dairy Products. *Int J Dairy Technol* **2018**, *71* (3), 564–578.

[14] Tong, X.; Cao, J.; Tian, T.; Lyu, B.; Miao, L.; Lian, Z.; Cui, W.; Liu, S.; Wang, H.; Jiang, L. Changes in Structure, Rheological Property and Antioxidant Activity of Soy Protein Isolate Fibrils by Ultrasound Pretreatment and EGCG. *Food Hydrocoll* **2022**, *122*, 107084.

[15] Wei, Z.; Gao, Y. Physicochemical Properties of β-Carotene Bilayer Emulsions Coated by Milk Proteins and Chitosan-EGCG Conjugates. *Food Hydrocoll* **2016**, *52*, 590–599.

[16] Shpigelman, A.; Israeli, G.; Livney, Y. D. Thermally-Induced Protein–Polyphenol Co-Assemblies: Beta Lactoglobulin-Based Nanocomplexes as Protective Nanovehicles for EGCG. *Food Hydrocoll* **2010**, *24* (8), 735–743.

[17] Jambrak, A. R.; Mason, T. J.; Lelas, V.; Herceg, Z.; Herceg, I. L. Effect of Ultrasound Treatment on Solubility and Foaming Properties of Whey Protein Suspensions. *J Food Eng* **2008**, *86* (2), 281–287.

[18] Wagoner, T.; Vardhanabhuti, B.; Foegeding, E. A. Designing Whey Protein-Polysaccharide Particles for Colloidal Stability. *Annu Rev Food Sci Technol* **2016**, *7*, 93–116.

[19] European Comission. *Milk Market Observatory*. https://ec.europa.eu/info/food-farming-fisheries/farming/facts-and-figures/markets/trade/trade-sector/animal-products/milk-and-dairy-products_en (accessed 2020-12-21).

[20] Nunes, L.; Tavares, G. M. Thermal Treatments and Emerging Technologies: Impacts on the Structure and Techno-Functional Properties of Milk Proteins. *Trends Food Sci Technol* **2019**, *90* (December 2018), 88–99.

[21] Han, Z.; Cai, M. jie; Cheng, J. H.; Sun, D. W. Effects of Electric Fields and Electromagnetic Wave on Food Protein Structure and Functionality: A Review. *Trends Food Sci Technol* **2018**, *75* (March), 1–9.

[22] Sá, A. G. A.; Moreno, Y. M. F.; Carciofi, B. A. M. Plant Proteins as High-Quality Nutritional Source for Human Diet. *Trends Food Sci Technol* **2020**, *97*, 170–184.

[23] Geng, M.; Wang, Z.; Qin, L.; Taha, A.; Du, L.; Xu, X.; Pan, S.; Hu, H. Effect of Ultrasound and Coagulant Types on Properties of β-Carotene

Bulk Emulsion Gels Stabilized by Soy Protein. *Food Hydrocoll* **2022**, *123*, 107146.

[24] Akharume, F. U.; Aluko, R. E.; Adedeji, A. A. Modification of Plant Proteins for Improved Functionality: A Review. *Compr Rev Food Sci Food Saf* **2021**, *20* (1), 198–224.

[25] Geng, M.; Hu, T.; Zhou, Q.; Taha, A.; Qin, L.; Lv, W.; Xu, X.; Pan, S.; Hu, H. Effects of Different Nut Oils on the Structures and Properties of Gel-like Emulsions Induced by Ultrasound Using Soy Protein as an Emulsifier. *Int J Food Sci Technol* **2021**, *56* (4), 1649–1660.

[26] Nishinari, K.; Fang, Y.; Guo, S.; Phillips, G. O. Soy Proteins: A Review on Composition, Aggregation and Emulsification. *Food Hydrocoll* **2014**, *39*, 301–318.

[27] Jaeger, H.; Meneses, N.; Knorr, D. Impact of PEF Treatment Inhomogeneity Such as Electric Field Distribution, Flow Characteristics and Temperature Effects on the Inactivation of E. Coli and Milk Alkaline Phosphatase. *Innovative Food Science and Emerging Technologies* **2009**, *10* (4), 470–480.

[28] Alirezalu, K.; Munekata, P. E. S.; Parniakov, O.; Barba, F. J.; Witt, J.; Toepfl, S.; Wiktor, A.; Lorenzo, J. M. Pulsed Electric Field and Mild Heating for Milk Processing: A Review on Recent Advances. *J Sci Food Agric* **2020**, *100* (1), 16–24.

[29] Soltanzadeh, M.; Peighambardoust, S. H.; Gullon, P.; Hesari, J.; Gullón, B.; Alirezalu, K.; Lorenzo, J. Quality Aspects and Safety of Pulsed Electric Field (PEF) Processing on Dairy Products: A Comprehensive Review. *Food Reviews International* **2020**, *00* (00), 1–22.

[30] Simonis, P.; Kersulis, S.; Stankevich, V.; Sinkevic, K.; Striguniene, K.; Ragoza, G.; Stirke, A. Pulsed Electric Field Effects on Inactivation of Microorganisms in Acid Whey. *Int J Food Microbiol* **2019**, *291* (November 2018), 128–134.

[31] Knorr, D.; Froehling, A.; Jaeger, H.; Reineke, K.; Schlueter, O.; Schoessler, K. Emerging Technologies in Food Processing. *Annu Rev Food Sci Technol* **2011**, *2* (1), 203–235.

[32] Jin, W.; Wang, Z.; Peng, D.; Shen, W.; Zhu, Z.; Cheng, S.; Li, B.; Huang, Q. Effect of Pulsed Electric Field on Assembly Structure of α-Amylase and Pectin Electrostatic Complexes. *Food Hydrocoll* **2020**, *101* (September 2019), 105547.

[33] Toepfl, S.; Heinz, V.; Knorr, D. High Intensity Pulsed Electric Fields Applied for Food Preservation. *Chemical Engineering and Processing: Process Intensification* **2007**, *46* (6), 537–546.

[34] Arshad, R. N.; Abdul-Malek, Z.; Munir, A.; Buntat, Z.; Ahmad, M. H.; Jusoh, Y. M. M.; Bekhit, A. E. D.; Roobab, U.; Manzoor, M. F.; Aadil, R. M. Electrical Systems for Pulsed Electric Field Applications in the Food Industry: An Engineering Perspective. *Trends Food Sci Technol* **2020**, *104* (January), 1–13.

[35] Jaeger, H.; Balasa, A.; Knorr, D. Food Industry Applications for Pulsed Electric Fields. In *Food Engineering Series*; Springer, 2008; pp 181–216.

[36] Zhang, S.; Sun, L.; Ju, H.; Bao, Z.; Zeng, X.; Lin, S. Research Advances and Application of Pulsed Electric Field on Proteins and Peptides in Food. *Food Research International* **2020**, 109914.

[37] Sui, Q.; Roginski, H.; Williams, R. P. W.; Versteeg, C.; Wan, J. Effect of Pulsed Electric Field and Thermal Treatment on the Physicochemical Properties of Lactoferrin with Different Iron Saturation Levels. *Int Dairy J* **2010**, *20* (10), 707–714.

[38] Fernandez-Diaz, M. D.; Barsotti, L.; Dumay, E.; Cheftel, J. C. Effects of Pulsed Electric Fields on Ovalbumin Solutions and Dialyzed Egg White. *J Agric Food Chem* **2000**, *48* (6), 2332–2339.

[39] Sharma, P.; Oey, I.; Everett, D. W. Effect of Pulsed Electric Field Processing on the Functional Properties of Bovine Milk. *Trends Food Sci Technol* **2014**, *35* (2), 87–101.

[40] Zhao, W.; Yang, R. Pulsed Electric Field Induced Aggregation of Food Proteins: Ovalbumin and Bovine Serum Albumin. *Food Bioproc Tech* **2012**, *5* (5), 1706–1714.

[41] Franco, I.; Pérez, M. D.; Conesa, C.; Calvo, M.; Sánchez, L. Effect of Technological Treatments on Bovine Lactoferrin: An Overview. *Food Research International* **2018**, *106* (December 2017), 173–182.

[42] Li, Y.-Q. Structure Changes of Soybean Protein Isolates by Pulsed Electric Fields. *Phys Procedia* **2012**, *33*, 132–137.

[43] Wei, J. N.; Zeng, X. A.; Tang, T.; Jiang, Z.; Liu, Y. Y. Unfolding and Nanotube Formation of Ovalbumin Induced by Pulsed Electric Field. *Innovative Food Science and Emerging Technologies* **2018**, *45* (May 2017), 249–254.

[44] Subaşı, B. G.; Jahromi, M.; Casanova, F.; Capanoglu, E.; Ajalloueian, F.; Mohammadifar, M. A. Effect of Moderate Electric Field on Structural and Thermo-Physical Properties of Sunflower Protein and

Sodium Caseinate. *Innovative Food Science & Emerging Technologies* **2021**, *67*, 102593.

[45] Tobajas, A. P.; Agulló-García, A.; Cubero, J. L.; Colás, C.; Segura-Gil, I.; Sánchez, L.; Calvo, M.; Pérez, M. D. Effect of High Pressure and Pulsed Electric Field on Denaturation and Allergenicity of Pru p 3 Protein from Peach. *Food Chem* **2020**, *321* (December 2019), 126745.

[46] Jaeger, H.; Meneses, N.; Knorr, D. Food Technologies: Pulsed Electric Field Technology. In *Encyclopedia of Food Safety*; Motarjemi, Y. B. T.-E. of F. S., Ed.; Academic Press: Waltham, 2014; pp 239–244.

[47] Knorr, D.; Geulen, M.; Grahl, T.; Sitzmann, W. Food Application of High Electric Field Pulses. *Trends in Food Science and Technology*. Elsevier March 1, 1994, pp 71–75.

[48] Soliva-Fortuny, R.; Balasa, A.; Knorr, D.; Martín-Belloso, O. Effects of Pulsed Electric Fields on Bioactive Compounds in Foods: A Review. *Trends Food Sci Technol* **2009**, *20* (11–12), 544–556.

[49] Liu, Y.-F.; Oey, I.; Bremer, P.; Carne, A.; Silcock, P. Modifying the Functional Properties of Egg Proteins Using Novel Processing Techniques: A Review. *Compr Rev Food Sci Food Saf* **2019**, *18* (4), 986–1002.

[50] Gerlach, D.; Alleborn, N.; Baars, A.; Delgado, A.; Moritz, J.; Knorr, D. Numerical Simulations of Pulsed Electric Fields for Food Preservation: A Review. *Innovative Food Science and Emerging Technologies* **2008**, *9* (4), 408–417.

[51] Mosqueda-Melgar, J.; Elez-Martínez, P.; Raybaudi-Massilia, R. M.; Martín-Belloso, O. Effects of Pulsed Electric Fields on Pathogenic Microorganisms of Major Concern in Fluid Foods: A Review. *Crit Rev Food Sci Nutr* **2008**, *48* (8), 747–759.

[52] Huang, K.; Wang, J. Designs of Pulsed Electric Fields Treatment Chambers for Liquid Foods Pasteurization Process: A Review. *J Food Eng* **2009**, *95* (2), 227–239.

[53] Gabrić, D.; Barba, F.; Roohinejad, S.; Gharibzahedi, S. M. T.; Radojčin, M.; Putnik, P.; Bursać Kovačević, D. Pulsed Electric Fields as an Alternative to Thermal Processing for Preservation of Nutritive and Physicochemical Properties of Beverages: A Review. *J Food Process Eng* **2018**, *41* (1), 1–14.

[54] Huang, K.; Tian, H.; Gai, L.; Wang, J. A Review of Kinetic Models for Inactivating Microorganisms and Enzymes by Pulsed Electric Field Processing. *J Food Eng* **2012**, *111* (2), 191–207.

[55] Buckow, R.; Ng, S.; Toepfl, S. Pulsed Electric Field Processing of Orange Juice: A Review on Microbial, Enzymatic, Nutritional, and

Sensory Quality and Stability. *Compr Rev Food Sci Food Saf* **2013**, *12* (5), 455–467.

[56] Niu, D.; Zeng, X. A.; Ren, E. F.; Xu, F. Y.; Li, J.; Wang, M. S.; Wang, R. Review of the Application of Pulsed Electric Fields (PEF) Technology for Food Processing in China. *Food Research International* **2020**, *137* (August), 109715.

[57] Yogesh, K. Pulsed Electric Field Processing of Egg Products: A Review. *J Food Sci Technol* **2016**, *53* (2), 934–945.

[58] Gómez, B.; Munekata, P. E. S.; Gavahian, M.; Barba, F. J.; Martí-Quijal, F. J.; Bolumar, T.; Campagnol, P. C. B.; Tomasevic, I.; Lorenzo, J. M. Application of Pulsed Electric Fields in Meat and Fish Processing Industries: An Overview. *Food Research International* **2019**, *123* (March), 95–105.

[59] Moosavi, M. H.; Khani, M. R.; Shokri, B.; Hosseini, S. M.; Shojaee-Aliabadi, S.; Mirmoghtadaie, L. Modifications of Protein-Based Films Using Cold Plasma. *Int J Biol Macromol* **2020**, *142*, 769–777.

[60] Sharma, S.; Singh, R. k. Cold Plasma Treatment of Dairy Proteins in Relation to Functionality Enhancement. *Trends Food Sci Technol* **2020**, *102*, 30–36.

[61] Pérez-Andrés, J. M.; Álvarez, C.; Cullen, P. J.; Tiwari, B. K. Effect of Cold Plasma on the Techno-Functional Properties of Animal Protein Food Ingredients. *Innovative Food Science and Emerging Technologies* **2019**, *58* (January), 102205.

[62] Zheng, Y.; Li, Z.; Zhang, C.; Zheng, B.; Tian, Y. Effects of Microwave-Vacuum Pre-Treatment with Different Power Levels on the Structural and Emulsifying Properties of Lotus Seed Protein Isolates. *Food Chem* **2020**, *311*, 125932.

[63] Wei, S.; Yang, Y.; Feng, X.; Li, S.; Zhou, L.; Wang, J.; Tang, X. Structures and Properties of Chicken Myofibrillar Protein Gel Induced by Microwave Heating. *Int J Food Sci Technol* **2020**, *55* (7), 2691–2699.

[64] Xiang, S.; Zou, H.; Liu, Y.; Ruan, R. Effects of Microwave Heating on the Protein Structure, Digestion Properties and Maillard Products of Gluten. *J Food Sci Technol* **2020**, *57* (6), 2139–2149.

[65] Sun, X.; Ohanenye, I. C.; Ahmed, T.; Udenigwe, C. C. Microwave Treatment Increased Protein Digestibility of Pigeon Pea (Cajanus Cajan) Flour: Elucidation of Underlying Mechanisms. *Food Chem* **2020**, *329* (February), 127196.

[66] Xue, S.; Xu, X.; Shan, H.; Wang, H.; Yang, J.; Zhou, G. Effects of High-Intensity Ultrasound, High-Pressure Processing, and High-

Pressure Homogenization on the Physicochemical and Functional Properties of Myofibrillar Proteins. *Innovative Food Science and Emerging Technologies* **2018**, *45* (December 2017), 354–360.

[67] Zhu, S. M.; Lin, S. L.; Ramaswamy, H. S.; Yu, Y.; Zhang, Q. T. Enhancement of Functional Properties of Rice Bran Proteins by High Pressure Treatment and Their Correlation with Surface Hydrophobicity. *Food Bioproc Tech* **2017**, *10* (2), 317–327.

[68] Tang, C. H.; Ma, C. Y. Effect of High Pressure Treatment on Aggregation and Structural Properties of Soy Protein Isolate. *LWT - Food Science and Technology* **2009**, *42* (2), 606–611.

[69] He, X. H.; Liu, H. Z.; Liu, L.; Zhao, G. L.; Wang, Q.; Chen, Q. L. Effects of High Pressure on the Physicochemical and Functional Properties of Peanut Protein Isolates. *Food Hydrocoll* **2014**, *36*, 123–129.

[70] Flores-Jiménez, N. T.; Ulloa, J. A.; Silvas, J. E. U.; Ramírez, J. C. R.; Ulloa, P. R.; Rosales, P. U. B.; Carrillo, Y. S.; Leyva, R. G. Effect of High-Intensity Ultrasound on the Compositional, Physicochemical, Biochemical, Functional and Structural Properties of Canola (Brassica Napus L.) Protein Isolate. *Food Research International* **2019**, *121*, 947–956.

[71] Geng, M.; Liu, J.; Hu, H.; Qin, L.; Taha, A.; Zhang, Z. A Comprehensive Study on Structures and Characterizations of 7S Protein Treated by High Intensity Ultrasound at Different PH and Ionic Strengths. *Food Chem* **2021**, 131378.

[72] Zheng, T.; Li, X.; Taha, A.; Wei, Y.; Hu, T.; Fatamorgana, P. B.; Zhang, Z.; Liu, F.; Xu, X.; Pan, S.; Hu, H. Effect of High Intensity Ultrasound on the Structure and Physicochemical Properties of Soy Protein Isolates Produced by Different Denaturation Methods. *Food Hydrocoll* **2019**, *97*, 105216.

[73] Hu, H.; Wu, J.; Li-Chan, E. C. Y.; Zhu, L.; Zhang, F.; Xu, X.; Fan, G.; Wang, L.; Huang, X.; Pan, S. Effects of Ultrasound on Structural and Physical Properties of Soy Protein Isolate (SPI) Dispersions. *Food Hydrocoll* **2013**, *30* (2), 647–655.

[74] Parniakov, O.; Wiktor, A.; Toepfl, S. Application Concepts for PEF in Food and Biotechnology. *Innovative Food Processing Technologies: A Comprehensive Review* **2021**, 160–172.

[75] Shorstkii, I.; Sosnin, M.; Smetana, S.; Toepfl, S.; Parniakov, O.; Wiktor, A. Correlation of the Cell Disintegration Index with Luikov's Heat and Mass Transfer Parameters for Drying of Pulsed Electric Field (PEF) Pretreated Plant Materials. *J Food Eng* **2022**, *316*, 110822.

[76] Hill, K.; Ostermeier, R.; Töpfl, S.; Heinz, V. Pulsed Electric Fields in the Potato Industry. *Food Engineering Series* **2022**, 325–335.

[77] Ammelt, D.; Lammerskitten, A.; Wiktor, A.; Barba, F. J.; Toepfl, S.; Parniakov, O. The Impact of Pulsed Electric Fields on Quality Parameters of Freeze-Dried Red Beets and Pineapples. *Int J Food Sci Technol* **2021**, *56* (4), 1777–1787.

[78] Wan, J.; Coventry, J.; Swiergon, P.; Sanguansri, P.; Versteeg, C. Advances in Innovative Processing Technologies for Microbial Inactivation and Enhancement of Food Safety – Pulsed Electric Field and Low-Temperature Plasma. *Trends Food Sci Technol* **2009**, *20* (9), 414–424.

[79] Gómez, B.; Munekata, P. E. S.; Gavahian, M.; Barba, F. J.; Martí-Quijal, F. J.; Bolumar, T.; Campagnol, P. C. B.; Tomasevic, I.; Lorenzo, J. M. Application of Pulsed Electric Fields in Meat and Fish Processing Industries: An Overview. *Food Research International* **2019**, *123*, 95–105.

[80] Cemazar, M.; Sersa, G.; Frey, W.; Miklavcic, D.; Teissié, J. Recommendations and Requirements for Reporting on Applications of Electric Pulse Delivery for Electroporation of Biological Samples. *Bioelectrochemistry* **2018**, *122*, 69–76.

[81] Zhang, L.; Wang, L. J.; Jiang, W.; Qian, J. Y. Effect of Pulsed Electric Field on Functional and Structural Properties of Canola Protein by Pretreating Seeds to Elevate Oil Yield. *LWT - Food Science and Technology* **2017**, *84*, 73–81.

[82] Taha, A.; Ahmed, E.; Ismaiel, A.; Ashokkumar, M.; Xu, X.; Pan, S.; Hu, H. Ultrasonic Emulsification: An Overview on the Preparation of Different Emulsifiers-Stabilized Emulsions. *Trends Food Sci Technol* **2020**, *105*, 363–377.

[83] Hu, H.; Taha, A.; Khalifa, I. Effects of Novel Processing Methods on Structure, Functional Properties, and Health Benefits of Soy Protein. *Phytochemicals in Soybeans* **2022**, 301–318.

[84] Rahman, M. M.; Lamsal, B. P. Ultrasound-Assisted Extraction and Modification of Plant-Based Proteins: Impact on Physicochemical, Functional, and Nutritional Properties. *Compr Rev Food Sci Food Saf* **2021**, *20* (2), 1457–1480.

[85] Liu, H. H.; Kuo, M. I. Ultra High Pressure Homogenization Effect on the Proteins in Soy Flour. *Food Hydrocoll* **2016**, *52*, 741–748.

[86] Wang, C.; Wang, J.; Zhu, D.; Hu, S.; Kang, Z.; Ma, H. Effect of Dynamic Ultra-High Pressure Homogenization on the Structure and

Functional Properties of Whey Protein. *J Food Sci Technol* **2020**, *57* (4), 1301–1309.

[87] Cao, H.; Jiao, X.; Fan, D.; Huang, J.; Zhao, J.; Yan, B.; Zhou, W.; Zhang, H.; Wang, M. Microwave Irradiation Promotes Aggregation Behavior of Myosin through Conformation Changes. *Food Hydrocoll* **2019**, *96*, 11–19.

[88] Solaesa, Á. G.; Villanueva, M.; Muñoz, J. M.; Ronda, F. Dry-Heat Treatment vs. Heat-Moisture Treatment Assisted by Microwave Radiation: Techno-Functional and Rheological Modifications of Rice Flour. *LWT* **2021**, *141*, 110851.

[89] Thirumdas, R.; Sarangapani, C.; Annapure, U. S. Cold Plasma: A Novel Non-Thermal Technology for Food Processing. *Food Biophys* **2014**, *10* (1), 1–11.

[90] Ji, H.; Dong, S.; Han, F.; Li, Y.; Chen, G.; Li, L.; Chen, Y. Effects of Dielectric Barrier Discharge (DBD) Cold Plasma Treatment on Physicochemical and Functional Properties of Peanut Protein. *Food Bioproc Tech* **2018**, *11* (2), 344–354.

[91] Sharma, S.; Singh, R. k. Cold Plasma Treatment of Dairy Proteins in Relation to Functionality Enhancement. *Trends Food Sci Technol* **2020**, *102*, 30–36.

[92] Akiyama, H.; Katsuki, S.; Redondo, L.; Akiyama, M.; Pemen, A. J. M.; Huiskamp, T.; Beckers, F. J. C. M.; van Heesch, E. J. M.; Winands, G. J. J.; Voeten, S. J.; Zhen, L.; van Bree, J. W. M.; Xiao, S.; Petrella, R. Pulsed Power Technology. In *Bioelectrics*; Springer Japan, 2017; pp 41–107.

[93] Barbosa-Cánovas, G. V.; Altunakar, B. Pulsed Electric Fields Processing of Foods: An Overview. In *Food Engineering Series*; Springer, 2006; pp 3–26.

[94] Buchmann, L. Emerging Pulsed Electric Field Process Development for Bio-Based Applications, ETH Zurich, 2020.

[95] Schoenbach, K. H.; Neumann, E.; Heller, R.; Vernier, P. T.; Teissie, J.; Beebe, S. J. Introduction. In *Bioelectrics*; Springer Japan, 2017; pp 1–40.

[96] Charles Platt. *Encyclopedia of Electronic Components*; O'Reilly Media, Inc., 2012; Vol. 2012.

[97] Sharma, P.; Bhatti, T. S. A Review on Electrochemical Double-Layer Capacitors. *Energy Convers Manag* **2010**, *51* (12), 2901–2912.

[98] Toepfl, S.; Heinz, V.; Knorr, D. Overview of Pulsed Electric Field Processing for Food. In *Emerging Technologies for Food Processing*; Elsevier Ltd, 2005; pp 69–97.

[99] Nishino, A. Capacitors: Operating Principles, Current Market and Technical Trends. *Journal of Power Sources*. Elsevier June 1, 1996, pp 137–147.

[100] Maged Mohamed; Amer Eissa, A. H. Pulsed Electric Fields for Food Processing Technology. In *Structure and Function of Food Engineering*; InTech, 2012.

[101] Charles K. Alexander; Matthew Sadiku. *FUNDAMENTALS OF ELECTRIC CIRCUITS*, SIXTH EDIT.; McGraw-Hill Education, 2017.

[102] Aoude, C.; Lammerskitten, A.; Parniakov, O.; Zhang, R.; Grimi, N.; El Zakhem, H.; Vorobiev, E. Equipment and Recent Advances in Pulsed Electric Fields. *Innovative and Emerging Technologies in the Bio-marine Food Sector* **2022**, 149–172.

[103] Heinz, V.; Toepfl, S. Pulsed Electric Fields Industrial Equipment Design. *Food Engineering Series* **2022**, 489–504.

[104] Huppertz, T.; Vasiljevic, T.; Zisu, B.; Deeth, H. *Novel Processing Technologies*; Elsevier Inc., 2018.

[105] Abd El-Salam, M. H.; El-Shibiny, S.; Salem, A. Factors Affecting the Functional Properties of Whey Protein Products: A Review. *Food Reviews International* **2009**, *25* (3), 251–270.

[106] Onwulata, C. I.; Tunick, M. H.; Qi, P. X. *Extrusion Texturized Dairy Proteins. Processing and Application*, 1st ed.; Elsevier Inc., 2011; Vol. 62.

[107] Mazurkiewicz, J.; Kołoczek, H.; Tomasik, P. Effect of the External Electric Field on Selected Tripeptides. *Amino Acids* **2015**, *47* (7), 1399–1408.

[108] Sui, Q.; Roginski, H.; Williams, R. P. W.; Versteeg, C.; Wan, J. Effect of Pulsed Electric Field and Thermal Treatment on the Physicochemical and Functional Properties of Whey Protein Isolate. *Int Dairy J* **2011**, *21* (4), 206–213.

[109] Bekard, I.; Dunstan, D. E. Electric Field Induced Changes in Protein Conformation. *Soft Matter* **2014**, *10* (3), 431–437.

[110] Sharma, P.; Oey, I.; Everett, D. W. Thermal Properties of Milk Fat, Xanthine Oxidase, Caseins and Whey Proteins in Pulsed Electric Field-Treated Bovine Whole Milk. *Food Chem* **2016**, *207*, 34–42.

[111] Iametti, S.; Gregori, B.; Vecchio, G.; Bonomi, F. Modifications Occur at Different Structural Levels During the Heat Denaturation of Beta-Lactoglobulin. *Eur J Biochem* **1996**, *237* (1), 106–112.

[112] Rodrigues, R. M.; Vicente, A. A.; Petersen, S. B.; Pereira, R. N. Electric Field Effects on β-Lactoglobulin Thermal Unfolding as a

Function of PH – Impact on Protein Functionality. *Innovative Food Science and Emerging Technologies* **2019**, *52* (July 2018), 1–7.

[113] Odriozola-Serrano, I.; Bendicho-Porta, S.; Martín-Belloso, O. Comparative Study on Shelf Life of Whole Milk Processed by High-Intensity Pulsed Electric Field or Heat Treatment. *J Dairy Sci* **2006**, *89* (3), 905–911.

[114] Sui, Q.; Roginski, H.; Williams, R. P. W.; Versteeg, C.; Wan, J. Effect of Pulsed Electric Field and Thermal Treatment on the Physicochemical and Functional Properties of Whey Protein Isolate. *Int Dairy J* **2011**, *21* (4), 206–213.

[115] Liu, Y. Y.; Zeng, X. A.; Deng, Z.; Yu, S. J.; Yamasaki, S. Effect of Pulsed Electric Field on the Secondary Structure and Thermal Properties of Soy Protein Isolate. *European Food Research and Technology* **2011**, *233* (5), 841–850.

[116] Zhang, L.; Wang, L. J.; Jiang, W.; Qian, J. Y. Effect of Pulsed Electric Field on Functional and Structural Properties of Canola Protein by Pretreating Seeds to Elevate Oil Yield. *LWT - Food Science and Technology* **2017**, *84*, 73–81.

[117] Chen, Y.; Wang, T.; Zhang, Y.; Yang, X.; Du, J.; Yu, D.; Xie, F. Effect of Moderate Electric Fields on the Structural and Gelation Properties of Pea Protein Isolate. *Innovative Food Science & Emerging Technologies* **2022**, *77*, 102959.

[118] Liu, Y. Y.; Zeng, X. A.; Deng, Z.; Yu, S. J.; Yamasaki, S. Effect of Pulsed Electric Field on the Secondary Structure and Thermal Properties of Soy Protein Isolate. *European Food Research and Technology* **2011**, *233* (5), 841–850.

[119] Kinsella, J. E.; Whitehead, D. M. Proteins in Whey: Chemical, Physical, and Functional Properties. *Adv Food Nutr Res* **1989**, *33* (C), 343–438.

[120] Kostić, A. T.; Barać, M. B.; Stanojević, S. P.; Milojković-Opsenica, D. M.; Tešić, Ž. L.; Šikoparija, B.; Radišić, P.; Prentović, M.; Pešić, M. B. Physicochemical Composition and Techno-Functional Properties of Bee Pollen Collected in Serbia. *LWT - Food Science and Technology* **2015**, *62* (1), 301–309.

[121] Yu, L. J.; Ngadi, M.; Raghavan, G. S. V. Effect of Temperature and Pulsed Electric Field Treatment on Rennet Coagulation Properties of Milk. *J Food Eng* **2009**, *95* (1), 115–118.

[122] Rodrigues, R. M.; Martins, A. J.; Ramos, O. L.; Malcata, F. X.; Teixeira, J. A.; Vicente, A. A.; Pereira, R. N. Influence of Moderate

Electric Fields on Gelation of Whey Protein Isolate. *Food Hydrocoll* **2015**, *43*, 329–339.

[123] Jin, S.; Yin, Y.; Wang, Y. Effects of Combined Pulsed Electric Field and Heat Treatment on Texture Characteristics of Whey Protein Gels. *Nongye Jixie Xuebao/Transactions of the Chinese Society for Agricultural Machinery* **2013**.

[124] Tian, Y.; Zhang, Z.; Zhang, P.; Taha, A.; Hu, H.; Pan, S. The Role of Conformational State of PH-Shifted β-Conglycinin on the Oil/Water Interfacial Properties and Emulsifying Capacities. *Food Hydrocoll* **2020**, *108*, 105990.

[125] Golovanov, A. P.; Hautbergue, G. M.; Wilson, S. A.; Lian, L. Y. A Simple Method for Improving Protein Solubility and Long-Term Stability. *J Am Chem Soc* **2004**, *126* (29), 8933–8939.

[126] Kramer, R. M.; Shende, V. R.; Motl, N.; Pace, C. N.; Scholtz, J. M. Toward a Molecular Understanding of Protein Solubility: Increased Negative Surface Charge Correlates with Increased Solubility. *Biophys J* **2012**, *102* (8), 1907–1915.

[127] Zayas, J. F. Solubility of Proteins. In *Functionality of Proteins in Food*; Springer Berlin Heidelberg, 1997; pp 6–75.

[128] Wu, L.; Zhao, W.; Yang, R.; Chen, X. Effects of Pulsed Electric Fields Processing on Stability of Egg White Proteins. *J Food Eng* **2014**, *139*, 13–18.

[129] Melchior, S.; Calligaris, S.; Bisson, G.; Manzocco, L. Understanding the Impact of Moderate-Intensity Pulsed Electric Fields (MIPEF) on Structural and Functional Characteristics of Pea, Rice and Gluten Concentrates. *Food Bioproc Tech* **2020**, *13* (12), 2145–2155.

[130] Lucey, J. A. Formation and Physical Properties of Milk Protein Gels. *J Dairy Sci* **2002**, *85* (2), 281–294.

[131] Schmitt, C.; Bovay, C.; Rouvet, M.; Shojaei-Rami, S.; Kolodziejczyk, E. Whey Protein Soluble Aggregates from Heating with NaCl: Physicochemical, Interfacial, and Foaming Properties. *Langmuir* **2007**, *23* (8), 4155–4166.

[132] Taha, A.; Ahmed, E.; Hu, T.; Xu, X.; Pan, S.; Hu, H. Effects of Different Ionic Strengths on the Physicochemical Properties of Plant and Animal Proteins-Stabilized Emulsions Fabricated Using Ultrasound Emulsification. *Ultrason Sonochem* **2019**, *58* (May), 104627.

[133] O'Sullivan, J.; Murray, B.; Flynn, C.; Norton, I. The Effect of Ultrasound Treatment on the Structural, Physical and Emulsifying

Properties of Animal and Vegetable Proteins. *Food Hydrocoll* **2016**, *53*, 141–154.

[134] Sun, W. W.; Yu, S. J.; Zeng, X. A.; Yang, X. Q.; Jia, X. Properties of Whey Protein Isolate-Dextran Conjugate Prepared Using Pulsed Electric Field. *Food Research International* **2011**, *44* (4), 1052–1058.

[135] Rodrigues, R. M.; Avelar, Z.; Machado, L.; Pereira, R. N.; Vicente, A. A. Electric Field Effects on Proteins – Novel Perspectives on Food and Potential Health Implications. *Food Research International* **2020**, *137*, 109709.

[136] Knorr, D.; Froehling, A.; Jaeger, H.; Reineke, K.; Schlueter, O.; Schoessler, K. Emerging Technologies in Food Processing. *Annu Rev Food Sci Technol* **2011**, *2* (1), 203–235.

[137] Subaşı, B. G.; Jahromi, M.; Casanova, F.; Capanoglu, E.; Ajalloueian, F.; Mohammadifar, M. A. Effect of Moderate Electric Field on Structural and Thermo-Physical Properties of Sunflower Protein and Sodium Caseinate. *Innovative Food Science & Emerging Technologies* **2021**, *67* (December 2020), 102593.

[138] Rodrigues, R. M.; Avelar, Z.; Machado, L.; Pereira, R. N.; Vicente, A. A. Electric Field Effects on Proteins – Novel Perspectives on Food and Potential Health Implications. *Food Research International* **2020**, *137* (September).

[139] Guan, Y. G.; Lin, H.; Han, Z.; Wang, J.; Yu, S. J.; Zeng, X. A.; Liu, Y. Y.; Xu, C. H.; Sun, W. W. Effects of Pulsed Electric Field Treatment on a Bovine Serum Albumin-Dextran Model System, a Means of Promoting the Maillard Reaction. *Food Chem* **2010**, *123* (2), 275–280.

[140] Jian, W.; Wang, L.; Wu, L.; Sun, Y. M. Physicochemical Properties of Bovine Serum Albumin-Glucose and Bovine Serum Albumin-Mannose Conjugates Prepared by Pulsed Electric Fields Treatment. *Molecules* **2018**, *23* (3).

[141] Li, J.; Shin, G. H.; Lee, I. W.; Chen, X.; Park, H. J. Soluble Starch Formulated Nanocomposite Increases Water Solubility and Stability of Curcumin. *Food Hydrocoll* **2016**, *56*, 41–49.

[142] Stankevic, V.; Simonis, P.; Zurauskiene, N.; Stirke, A.; Dervinis, A.; Bleizgys, V.; Kersulis, S.; Balevicius, S. Compact Square-Wave Pulse Electroporator with Controlled Electroporation Efficiency and Cell Viability. *Symmetry (Basel)* **2020**, *12* (3), 412.

[143] Taha, A.; Casanova, F.; Šimonis, P.; Jonikaitė-Švėgždienė, J.; Jurkūnas, M.; Gomaa, M. A. E.; Stirkė, A. Pulsed Electric Field-Assisted Glycation of Bovine Serum Albumin/Starch Conjugates

Improved Their Emulsifying Properties. *Innovative Food Science & Emerging Technologies* **2022**, *82*, 103190.

[144] Ji, N.; Qiu, C.; Li, X.; Xiong, L.; Sun, Q. Study on the Interaction between Bovine Serum Albumin and Starch Nanoparticles Prepared by Isoamylolysis and Recrystallization. *Colloids Surf B Biointerfaces* **2015**, *128*, 594–599.

[145] Ma, C.; Jiang, W.; Chen, G.; Wang, Q.; McClements, D. J.; Liu, X.; Liu, F.; Ngai, T. Sonochemical Effects on Formation and Emulsifying Properties of Zein-Gum Arabic Complexes. *Food Hydrocoll* **2021**, *114* (December 2020), 106557.

[146] Wan, Y.; Li, Y.; Guo, S. Characteristics of Soy Protein Isolate Gel Induced by Glucono-δ-Lactone: Effects of the Protein Concentration during Preheating. *Food Hydrocoll* **2021**, *113*, 106525.

[147] Xia, W.; Zhu, L.; Delahaije, R. J. B. M.; Cheng, Z.; Zhou, X.; Sagis, L. M. C. Acid-Induced Gels from Soy and Whey Protein Thermally-Induced Mixed Aggregates: Rheology and Microstructure. *Food Hydrocoll* **2022**, *125*, 107376.

[148] Fan, Y.; Yi, J.; Zhang, Y.; Yokoyama, W. Fabrication of Curcumin-Loaded Bovine Serum Albumin (BSA)-Dextran Nanoparticles and the Cellular Antioxidant Activity. *Food Chem* **2018**, *239*, 1210–1218.

[149] Sun, J.; Mu, Y.; Obadi, M.; Dong, S.; Xu, B. Effects of Single-Mode Microwave Heating and Dextran Conjugation on the Structure and Functionality of Ovalbumin–Dextran Conjugates. *Food Research International* **2020**, *137* (June), 109468.

[150] Jiang, W.; Chen, Y.; He, X.; Hu, S.; Li, S.; Liu, Y. A Study of the Tyramine/Glucose Maillard Reaction: Variables, Characterization, Cytotoxicity and Preliminary Application. *Food Chem* **2018**, *239*, 377–384.

[151] Yu, J. jiao; Ji, H.; Chen, Y.; Zhang, Y. fu; Zheng, X. chao; Li, S. hong; Chen, Y. Analysis of the Glycosylation Products of Peanut Protein and Lactose by Cold Plasma Treatment: Solubility and Structural Characteristics. *Int J Biol Macromol* **2020**, *158*, 1194–1203.

[152] Ravindran, A.; Singh, A.; Raichur, A. M.; Chandrasekaran, N.; Mukherjee, A. Studies on Interaction of Colloidal Ag Nanoparticles with Bovine Serum Albumin (BSA). *Colloids Surf B Biointerfaces* **2010**, *76* (1), 32–37.

[153] Fan, H.; Ji, N.; Zhao, M.; Xiong, L.; Sun, Q. Interaction of Bovine Serum Albumin with Starch Nanoparticles Prepared by TEMPO-Mediated Oxidation. *Int J Biol Macromol* **2015**, *78*, 333–338.

[154] Chen, W.; Ma, X.; Wang, W.; Lv, R.; Guo, M.; Ding, T.; Ye, X.; Miao, S.; Liu, D. Preparation of Modified Whey Protein Isolate with Gum Acacia by Ultrasound Maillard Reaction. *Food Hydrocoll* **2019**, *95*, 298–307.

[155] Li, R.; Cui, Q.; Wang, G.; Liu, J.; Chen, S.; Wang, X.; Wang, X.; Jiang, L. Relationship between Surface Functional Properties and Flexibility of Soy Protein Isolate-Glucose Conjugates. *Food Hydrocoll* **2019**, *95*, 349–357.

[156] Wang, W. D.; Li, C.; Bin, Z.; Huang, Q.; You, L. J.; Chen, C.; Fu, X.; Liu, R. H. Physicochemical Properties and Bioactivity of Whey Protein Isolate-Inulin Conjugates Obtained by Maillard Reaction. *Int J Biol Macromol* **2020**, *150*, 326–335.

[157] Wang, Y.; Zhang, A.; Wang, Y.; Wang, X.; Xu, N.; Jiang, L. Effects of Irradiation on the Structure and Properties of Glycosylated Soybean Proteins. *Food Funct* **2020**, *11* (2), 1635–1646.

[158] Qu, W.; Zhang, X.; Chen, W.; Wang, Z.; He, R.; Ma, H. Effects of Ultrasonic and Graft Treatments on Grafting Degree, Structure, Functionality, and Digestibility of Rapeseed Protein Isolate-Dextran Conjugates. *Ultrason Sonochem* **2018**, *42* (August 2017), 250–259.

[159] Saatchi, A.; Kiani, H.; Labbafi, M. A New Functional Protein-polysaccharide Conjugate Based on Protein Concentrate from Sesame Processing By-Products: Functional and Physico-Chemical Properties. *Int J Biol Macromol* **2019**, *122*, 659–666.

[160] Wang, N.; Zhou, X.; Wang, W.; Wang, L.; Jiang, L.; Liu, T.; Yu, D. Effect of High Intensity Ultrasound on the Structure and Solubility of Soy Protein Isolate-Pectin Complex. *Ultrason Sonochem* **2021**, *80*, 105808.

[161] Zhao, W.; Tang, Y.; Lu, L.; Chen, X.; Li, C. Review: Pulsed Electric Fields Processing of Protein-Based Foods. *Food Bioproc Tech* **2014**, *7* (1), 114–125.

[162] Dong, M.; Xu, Y.; Zhang, Y.; Han, M.; Wang, P.; Xu, X.; Zhou, G. Physicochemical and Structural Properties of Myofibrillar Proteins Isolated from Pale, Soft, Exudative (PSE)-like Chicken Breast Meat: Effects of Pulsed Electric Field (PEF). *Innovative Food Science & Emerging Technologies* **2020**, *59*, 102277.

[163] Rodrigues, R. M.; Vicente, A. A.; Petersen, S. B.; Pereira, R. N. Electric Field Effects on β-Lactoglobulin Thermal Unfolding as a Function of PH – Impact on Protein Functionality. *Innovative Food Science & Emerging Technologies* **2019**, *52*, 1–7.

[164] Hu, H.; Cheung, I. W. Y.; Pan, S.; Li-Chan, E. C. Y. Effect of High Intensity Ultrasound on Physicochemical and Functional Properties of Aggregated Soybean β-Conglycinin and Glycinin. *Food Hydrocoll* **2015**, *45*, 102–110.

[165] Ma, X.; Hou, F.; Zhao, H.; Wang, D.; Chen, W.; Miao, S.; Liu, D. Conjugation of Soy Protein Isolate (SPI) with Pectin by Ultrasound Treatment. *Food Hydrocoll* **2020**, *108* (January), 106056.

[166] Wen, H.; Ning, Z.; Li, J.; Guan, Y.; Zhang, B.; Shang, X.; Liu, X.; Du, Z.; Liu, J.; Zhang, T. Stability of Oil-in-Water Emulsions Improved by Ovalbumin-Procyanidins Mixture: A Promising Substrate with Emulsifying and Antioxidant Activity. *Colloids Surf B Biointerfaces* **2022**, *215*, 112473.

[167] Zhao, C.; Yin, H.; Yan, J.; Niu, X.; Qi, B.; Liu, J. Structure and Acid-Induced Gelation Properties of Soy Protein Isolate–Maltodextrin Glycation Conjugates with Ultrasonic Pretreatment. *Food Hydrocoll* **2021**, *112*, 106278.

[168] McClements, D. J.; Rao, J. Food-Grade Nanoemulsions: Formulation, Fabrication, Properties, Performance, Biological Fate, and Potential Toxicity. *Crit Rev Food Sci Nutr* **2011**, *51* (4), 285–330.

[169] Dickinson, E. Hydrocolloids as Emulsifiers and Emulsion Stabilizers. *Food Hydrocoll* **2009**.

[170] Taha, A.; Hu, T.; Zhang, Z.; Bakry, A. M.; Khalifa, I.; Pan, S.; Hu, H. Effect of Different Oils and Ultrasound Emulsification Conditions on the Physicochemical Properties of Emulsions Stabilized by Soy Protein Isolate. *Ultrason Sonochem* **2018**, *49* (August), 283–293.

[171] Pei, Y.; Wan, J.; You, M.; McClements, D. J.; Li, Y.; Li, B. Impact of Whey Protein Complexation with Phytic Acid on Its Emulsification and Stabilization Properties. *Food Hydrocoll* **2019**, *87* (June 2018), 90–96.

[172] Guo, B.; Hu, X.; Wu, J.; Chen, R.; Dai, T.; Liu, Y.; Luo, S.; Liu, C. Soluble Starch/Whey Protein Isolate Complex-Stabilized High Internal Phase Emulsion: Interaction and Stability. *Food Hydrocoll* **2021**, *111* (September 2020), 106377.

[173] Tian, Y.; Zhang, Z.; Taha, A.; Chen, Y.; Hu, H.; Pan, S. Interfacial and Emulsifying Properties of β-Conglycinin/Pectin Mixtures at the Oil/Water Interface: Effect of PH. *Food Hydrocoll* **2020**, 106145.

[174] Gentile, L. Protein–Polysaccharide Interactions and Aggregates in Food Formulations. *Curr Opin Colloid Interface Sci* **2020**, *48*, 18–27.

[175] Setiowati, A. D.; Wijaya, W.; Van der Meeren, P. Whey Protein-Polysaccharide Conjugates Obtained via Dry Heat Treatment to

Improve the Heat Stability of Whey Protein Stabilized Emulsions. *Trends Food Sci Technol* **2020**, *98*, 150–161.

[176] Rodriguez Patino, J. M.; Pilosof, A. M. R. Protein-Polysaccharide Interactions at Fluid Interfaces. *Food Hydrocoll* **2011**, *25* (8), 1925–1937.

[177] Albano, K. M.; Nicoletti, V. R. Ultrasound Impact on Whey Protein Concentrate-Pectin Complexes and in the O/W Emulsions with Low Oil Soybean Content Stabilization. *Ultrason Sonochem* **2018**, *41*, 562–571.

[178] Ma, X.; Yan, T.; Hou, F.; Chen, W.; Miao, S.; Liu, D. Formation of Soy Protein Isolate (SPI)-Citrus Pectin (CP) Electrostatic Complexes under a High-Intensity Ultrasonic Field: Linking the Enhanced Emulsifying Properties to Physicochemical and Structural Properties. *Ultrason Sonochem* **2019**, *59* (August), 104748.

[179] Dickinson, E. Interfacial Structure and Stability of Food Emulsions as Affected by Protein-Polysaccharide Interactions. *Soft Matter* **2008**, *4* (5), 932–942.

[180] Consoli, L.; Dias, R. A. O.; Rabelo, R. S.; Furtado, G. F.; Sussulini, A.; Cunha, R. L.; Hubinger, M. D. Sodium Caseinate-Corn Starch Hydrolysates Conjugates Obtained through the Maillard Reaction as Stabilizing Agents in Resveratrol-Loaded Emulsions. *Food Hydrocoll* **2018**, *84* (March), 458–472.

[181] Koh, L. L. A.; Chandrapala, J.; Zisu, B.; Martin, G. J. O.; Kentish, S. E.; Ashokkumar, M. A Comparison of the Effectiveness of Sonication, High Shear Mixing and Homogenisation on Improving the Heat Stability of Whey Protein Solutions. *Food Bioproc Tech* **2014**, *7* (2), 556–566.

[182] He, F. Bradford Protein Assay. *Bio Protoc* **2011**, *1* (6).

[183] Zhu, X. F.; Zhang, N.; Lin, W. F.; Tang, C. H. Freeze-Thaw Stability of Pickering Emulsions Stabilized by Soy and Whey Protein Particles. *Food Hydrocoll* **2017**, *69*, 173–184.

[184] Phan, H. T. M.; Bartelt-Hunt, S.; Rodenhausen, K. B.; Schubert, M.; Bartz, J. C. Investigation of Bovine Serum Albumin (BSA) Attachment onto Self-Assembled Monolayers (SAMs) Using Combinatorial Quartz Crystal Microbalance with Dissipation (QCM-D) and Spectroscopic Ellipsometry (SE). *PLoS One* **2015**, *10* (10).

[185] Raghuwanshi, V. S.; Yu, B.; Browne, C.; Garnier, G. Reversible PH Responsive Bovine Serum Albumin Hydrogel Sponge Nanolayer. *Front Bioeng Biotechnol* **2020**, *8*, 573.

[186] Zha, F.; Dong, S.; Rao, J.; Chen, B. Pea Protein Isolate-Gum Arabic Maillard Conjugates Improves Physical and Oxidative Stability of Oil-in-Water Emulsions. *Food Chem* **2019**, *285*, 130–138.

[187] Wen, C.; Zhang, J.; Qin, W.; Gu, J.; Zhang, H.; Duan, Y.; Ma, H. Structure and Functional Properties of Soy Protein Isolate-Lentinan Conjugates Obtained in Maillard Reaction by Slit Divergent Ultrasonic Assisted Wet Heating and the Stability of Oil-in-Water Emulsions. *Food Chem* **2020**, *331*, 127374.

[188] Schuch, A.; Köhler, K.; Schuchmann, H. P. Differential Scanning Calorimetry (DSC) in Multiple W/O/W Emulsions: A Method to Characterize the Stability of Inner Droplets. *J Therm Anal Calorim* **2013**, *111* (3), 1881–1890.

[189] Clausse, D.; Gomez, F.; Pezron, I.; Komunjer, L.; Dalmazzone, C. Morphology Characterization of Emulsions by Differential Scanning Calorimetry. *Adv Colloid Interface Sci* **2005**, *117* (1–3), 59–74.

[190] Zhu, X. F.; Zheng, J.; Liu, F.; Qiu, C. Y.; Lin, W. F.; Tang, C. H. The Influence of Ionic Strength on the Characteristics of Heat-Induced Soy Protein Aggregate Nanoparticles and the Freeze-Thaw Stability of the Resultant Pickering Emulsions. *Food Funct* **2017**, *8* (8), 2974–2981.

[191] Gmach, O.; Golda, J.; Kulozik, U. Freeze-Thaw Stability of Emulsions Made with Native and Enzymatically Modified Egg Yolk Fractions. *Food Hydrocoll* **2022**, *123* (January 2021), 107109.

[192] Zeng, F.; Gao, Q. Y.; Han, Z.; Zeng, X. A.; Yu, S. J. Structural Properties and Digestibility of Pulsed Electric Field Treated Waxy Rice Starch. *Food Chem* **2016**, *194*, 1313–1319.

[193] Rodrigues, R. M.; Avelar, Z.; Vicente, A. A.; Petersen, S. B.; Pereira, R. N. Influence of Moderate Electric Fields in β-Lactoglobulin Thermal Unfolding and Interactions. *Food Chem* **2020**, *304*, 125442.

[194] Rodrigues, R. M.; Fasolin, L. H.; Avelar, Z.; Petersen, S. B.; Vicente, A. A.; Pereira, R. N. Effects of Moderate Electric Fields on Cold-Set Gelation of Whey Proteins – From Molecular Interactions to Functional Properties. *Food Hydrocoll* **2020**, *101*, 105505.

[195] Wu, S.; Li, G.; Xue, Y.; Ashokkumar, M.; Zhao, H.; Liu, D.; Zhou, P.; Sun, Y.; Hemar, Y. Solubilisation of Micellar Casein Powders by High-Power Ultrasound. *Ultrason Sonochem* **2020**, *67*, 105131.

[196] Yang, M.; Zeng, Q.; Wang, Y.; Qin, J.; Zheng, J.; Wa, W. Effect of Ultrasound Pretreatment on the Physicochemical Properties and Simulated Gastrointestinal Digestibility of Micellar Casein Concentrates. *LWT* **2021**, *136*, 110319.

[197] Ravash, N.; Peighambardoust, S. H.; Soltanzadeh, M.; Pateiro, M.; Lorenzo, J. M. Impact of High-Pressure Treatment on Casein Micelles, Whey Proteins, Fat Globules and Enzymes Activity in Dairy Products: A Review. *https://doi.org/10.1080/10408398.2020.1860899* **2020**, *62* (11), 2888–2908.

[198] Taha, A.; Casanova, F.; Talaikis, M.; Stankevič, V.; Žurauskienė, N.; Šimonis, P.; Pakštas, V.; Jurkūnas, M.; Gomaa, M. A. E.; Stirkė, A. Effects of Pulsed Electric Field on the Physicochemical and Structural Properties of Micellar Casein. *Polymers* **2023**, *15* (15).

[199] Garcia, A.; Alting, A.; Huppertz, T. Effect of Sodium Hexametaphosphate on Heat-Induced Changes in Micellar Casein Isolate Solutions. *Int Dairy J* **2023**, *140*, 105583.

[200] Li, M.; Fokkink, R.; Ni, Y.; Kleijn, J. M. Bovine Beta-Casein Micelles as Delivery Systems for Hydrophobic Flavonoids. *Food Hydrocoll* **2019**, *96*, 653–662.

[201] Wang, H.; Wang, N.; Chen, X.; Wu, Z.; Zhong, W.; Yu, D.; Zhang, H. Effects of Moderate Electric Field on the Structural Properties and Aggregation Characteristics of Soybean Protein Isolate. *Food Hydrocoll* **2022**, *133*, 107911.

[202] Jiang, S.; Ding, J.; Andrade, J.; Rababah, T. M.; Almajwal, A.; Abulmeaty, M. M.; Feng, H. Modifying the Physicochemical Properties of Pea Protein by PH-Shifting and Ultrasound Combined Treatments. *Ultrason Sonochem* **2017**, *38*, 835–842.

[203] Shevkani, K.; Singh, N.; Chen, Y.; Kaur, A.; Yu, L. Pulse Proteins: Secondary Structure, Functionality and Applications. *J Food Sci Technol* **2019**, *56* (6), 2787–2798.

[204] Wan, Y.; Liu, J.; Guo, S. Effects of Succinylation on the Structure and Thermal Aggregation of Soy Protein Isolate. *Food Chem* **2018**, *245*, 542–550.

[205] Wang, Y. R.; Yang, Q.; Fan, J. L.; Zhang, B.; Chen, H. Q. The Effects of Phosphorylation Modification on the Structure, Interactions and Rheological Properties of Rice Glutelin during Heat Treatment. *Food Chem* **2019**, *297*, 124978.

[206] Wang, Q.; Wei, R.; Hu, J.; Luan, Y.; Liu, R.; Ge, Q.; Yu, H.; Wu, M. Moderate Pulsed Electric Field-Induced Structural Unfolding Ameliorated the Gelling Properties of Porcine Muscle Myofibrillar Protein. *Innovative Food Science and Emerging Technologies* **2022**, *81*.

[207] Li, M.; Kong, J.; Chen, Y.; Li, Y.; Xuan, H.; Liu, M.; Zhang, Q.; Liu, J. Comparative Interaction Study of Soy Protein Isolate and Three

Flavonoids (Chrysin, Apigenin and Luteolin) and Their Potential as Natural Preservatives. *Food Chem* **2023**, *414*, 135738.

[208] Guo, Z.; Huang, Z.; Guo, Y.; Li, B.; Yu, W.; Zhou, L.; Jiang, L.; Teng, F.; Wang, Z. Effects of High-Pressure Homogenization on Structural and Emulsifying Properties of Thermally Soluble Aggregated Kidney Bean (Phaseolus Vulgaris L.) Proteins. *Food Hydrocoll* **2021**, *119*, 106835.

[209] Rao, W.; Syamaladevi, R. M.; Pan, D.; Du, L. Enhanced Gel Properties of Duck Myofibrillar Protein by Plasma-Activated Water: Through Mild Structure Modifications. *Foods 2023, Vol. 12, Page 877* **2023**, *12* (4), 877.

[210] Zheng, Y.; Li, Z.; Zhang, C.; Zheng, B.; Tian, Y. Effects of Microwave-Vacuum Pre-Treatment with Different Power Levels on the Structural and Emulsifying Properties of Lotus Seed Protein Isolates. *Food Chem* **2020**, *311*, 125932.

[211] Kong, F.; Kang, S.; An, Y.; Li, W.; Han, H.; Guan, B.; Yang, M.; Zheng, Y.; Yue, X. The Effect of Non-Covalent Interactions of Xylitol with Whey Protein and Casein on Structure and Functionality of Protein. *Int Dairy J* **2020**, *111*, 104841.

[212] Wang, M. P.; Chen, X. W.; Guo, J.; Yang, J.; Wang, J. M.; Yang, X. Q. Stabilization of Foam and Emulsion by Subcritical Water-Treated Soy Protein: Effect of Aggregation State. *Food Hydrocoll* **2019**, *87*, 619–628.

[213] Liu, H.; Zhang, H.; Liu, Q.; Chen, Q.; Kong, B. Solubilization and Stable Dispersion of Myofibrillar Proteins in Water through the Destruction and Inhibition of the Assembly of Filaments Using High-Intensity Ultrasound. *Ultrason Sonochem* **2020**, *67*, 105160.

[214] Tian, R.; Feng, J.; Huang, G.; Tian, B.; Zhang, Y.; Jiang, L.; Sui, X. Ultrasound Driven Conformational and Physicochemical Changes of Soy Protein Hydrolysates. *Ultrason Sonochem* **2020**, *68*, 105202.

[215] Movasaghi, Z.; Rehman, S.; Rehman, I. U. Raman Spectroscopy of Biological Tissues. *Applied Spectroscopy Reviews* **2007**, *42* (5), 493–541.

[216] Sadiq, U.; Gill, H.; Chandrapala, J.; Shahid, F. Influence of Spray Drying on Encapsulation Efficiencies and Structure of Casein Micelles Loaded with Anthraquinones Extracted from Aloe Vera Plant. *Applied Sciences* **2022**, *13* (1).

[217] Cobb, J. S.; Zai-Rose, V.; Correia, J. J.; Janorkar, A. V. FT-IR Spectroscopic Analysis of the Secondary Structures Present during the

Desiccation Induced Aggregation of Elastin-Like Polypeptide on Silica. *ACS Omega* **2020**, *5* (14), 8403–8413.

[218] Xu, B.; Yuan, J.; Wang, L.; Lu, F.; Wei, B.; Azam, R. S. M.; Ren, X.; Zhou, C.; Ma, H.; Bhandari, B. Effect of Multi-Frequency Power Ultrasound (MFPU) Treatment on Enzyme Hydrolysis of Casein. *Ultrason Sonochem* **2020**, *63*, 104930.

[219] Zhang, R.; Pang, X.; Lu, J.; Liu, L.; Zhang, S.; Lv, J. Effect of High Intensity Ultrasound Pretreatment on Functional and Structural Properties of Micellar Casein Concentrates. *Ultrason Sonochem* **2018**, *47*, 10–16.

[220] Nickless, E.; Holroyd, S. E. Raman Imaging of Protein in a Model Cheese System. *Journal of Spectral Imaging* **2020**, *9*, 1–11.

[221] Wen, Z.-Q. Raman Spectroscopy of Protein Pharmaceuticals. *J Pharm Sci* **2007**, *96* (11), 2861–2878.

[222] Kocherbitov, V.; Latynis, J.; Misiuì, A.; Barauskas, J.; Niaura, G. Hydration of Lysozyme Studied by Raman Spectroscopy. *Journal of Physical Chemistry B* **2013**, *117* (17), 4981–4992.

[223] Xia, W.; Pan, S.; Cheng, Z.; Tian, Y.; Huang, X. High-Intensity Ultrasound Treatment on Soy Protein after Selectively Proteolyzing Glycinin Component: Physical, Structural, and Aggregation Properties. *Foods* **2020**, *9* (6).

[224] Lam, R. S. H.; Nickerson, M. T. Food Proteins: A Review on Their Emulsifying Properties Using a Structure-Function Approach. *Food Chem* **2013**, *141* (2), 975–984.

[225] Sharangi, A. B. Medicinal and Therapeutic Potentialities of Tea (Camellia Sinensis L.) – A Review. *Food Research International* **2009**, *42* (5–6), 529–535.

[226] Zaveri, N. T. Green Tea and Its Polyphenolic Catechins: Medicinal Uses in Cancer and Noncancer Applications. *Life Sci* **2006**, *78* (18), 2073–2080.

[227] Sobhy, R.; Khalifa, I.; Liang, H.; Li, B. Phytosterols Disaggregate Bovine Serum Albumin under the Glycation Conditions through Interacting with Its Glycation Sites and Altering Its Secondary Structure Elements. *Bioorg Chem* **2020**, *101*, 104047.

[228] Khalifa, I.; Sobhy, R.; Nawaz, A.; Xiaoou, W.; Li, Z.; Zou, X. Cyanidin 3-Rutinoside Defibrillated Bovine Serum Albumin under the Glycation-Promoting Conditions: A Study with Multispectral, Microstructural, and Computational Analysis. *Int J Biol Macromol* **2020**, *162*, 1195–1203.

[229] Wang, R.; Wen, Q. H.; Zeng, X. A.; Lin, J. W.; Li, J.; Xu, F. Y. Binding Affinity of Curcumin to Bovine Serum Albumin Enhanced by Pulsed Electric Field Pretreatment. *Food Chem* **2022**, *377*, 131945.

[230] Chen, Z. L.; Li, Y.; Wang, J. H.; Wang, R.; Teng, Y. X.; Lin, J. W.; Zeng, X. A.; Woo, M. W.; Wang, L.; Han, Z. Pulsed Electric Field Improves the EGCG Binding Ability of Pea Protein Isolate Unraveled by Multi-Spectroscopy and Computer Simulation. *Int J Biol Macromol* **2023**, *244*, 125082.

[231] Balevicius, S.; Stankevic, V.; Zurauskiene, N.; Shatkovskis, E.; Stirke, A.; Bitinaite, A.; Saule, R.; Maciuleviciene, R.; Saulis, G. System for the Nanoporation of Biological Cells Based on an Optically-Triggered High-Voltage Spark-Gap Switch. *IEEE Transactions on Plasma Science* **2013**, *41* (10), 2706–2711.

[232] Whitmore, L.; Wallace, B. A. Protein Secondary Structure Analyses from Circular Dichroism Spectroscopy: Methods and Reference Databases. *Biopolymers* **2008**, *89* (5), 392–400.

[233] Negrea, E.; Oancea, P.; Leonties, A.; Ana Maria, U.; Avram, S.; Raducan, A. Spectroscopic Studies on Binding of Ibuprofen and Drotaverine with Bovine Serum Albumin. *J Photochem Photobiol A Chem* **2023**, *438*, 114512.

[234] Khalifa, I.; Nie, R.; Ge, Z.; Li, K.; Li, C. Understanding the Shielding Effects of Whey Protein on Mulberry Anthocyanins: Insights from Multispectral and Molecular Modelling Investigations. *Int J Biol Macromol* **2018**, *119*, 116–124.

[235] Geng, M.; Li, L.; Feng, X.; Xu, J.; Huang, Y.; Teng, F.; Li, Y. Encapsulation of β-Carotene in High Internal Phase Pickering Emulsions Stabilized by Soy Protein Isolate – Epigallocatechin-3-Gallate Covalent Composite Microgel Particles. *J Mol Liq* **2022**, *360*.

[236] Han, X.; Liang, Z.; Tian, S.; Liu, L.; Wang, S. Epigallocatechin Gallate (EGCG) Modification of Structural and Functional Properties of Whey Protein Isolate. *Food Research International* **2022**, *158*.

[237] Parolia, S.; Maley, J.; Sammynaiken, R.; Green, R.; Nickerson, M.; Ghosh, S. Structure – Functionality of Lentil Protein-Polyphenol Conjugates. *Food Chem* **2022**, *367*.

[238] Liu, X.; Song, Q.; Li, X.; Chen, Y.; Liu, C.; Zhu, X.; Liu, J.; Granato, D.; Wang, Y.; Huang, J. Effects of Different Dietary Polyphenols on Conformational Changes and Functional Properties of Protein–Polyphenol Covalent Complexes. *Food Chem* **2021**, *361*.

[239] Jia, Y.; Yan, X.; Huang, Y.; Zhu, H.; Qi, B.; Li, Y. Different Interactions Driving the Binding of Soy Proteins (7S/11S) and

Flavonoids (Quercetin/Rutin): Alterations in the Conformational and Functional Properties of Soy Proteins. *Food Chem* **2022**, *396*.

[240] Zhang, Q. A.; Fu, X. Z.; García Martín, J. F. Effect of Ultrasound on the Interaction between (−)-Epicatechin Gallate and Bovine Serum Albumin in a Model Wine. *Ultrason Sonochem* **2017**, *37*, 405–413.

[241] Tan, C.; Li, D.; Wang, H.; Tong, Y.; Zhao, Y.; Deng, H.; Kong, Y.; Shu, C.; Yan, T.; Meng, X. Effects of High Hydrostatic Pressure on the Binding Capacity, Interaction, and Antioxidant Activity of the Binding Products of Cyanidin-3-Glucoside and Blueberry Pectin. *Food Chem* **2021**, *344*.

[242] Zhao, J.; Lin, W.; Gao, J.; Gong, H.; Mao, X. Limited Hydrolysis as a Strategy to Improve the Non-Covalent Interaction of Epigallocatechin-3-Gallate (EGCG) with Whey Protein Isolate near the Isoelectric Point. *Food Research International* **2022**, *161*.

[243] Yu, X.; Cai, X.; Li, S.; Luo, L.; Wang, J.; Wang, M.; Zeng, L. Studies on the Interactions of Theaflavin-3,3′-Digallate with Bovine Serum Albumin: Multi-Spectroscopic Analysis and Molecular Docking. *Food Chem* **2022**, *366*, 130422.

[244] Ma, C. M.; Zhao, X. H. Depicting the Non-Covalent Interaction of Whey Proteins with Galangin or Genistein Using the Multi-Spectroscopic Techniques and Molecular Docking. *Foods 2019, Vol. 8, Page 360* **2019**, *8* (9), 360.

[245] Taddei, P.; Zanna, N.; Tozzi, S. Raman Characterization of the Interactions between Gliadins and Anthocyanins. *Journal of Raman Spectroscopy* **2013**, *44* (10), 1435–1439.

[246] Krekora, M.; Szymańska-Chargot, M.; Niewiadomski, Z.; Miś, A.; Nawrocka, A. Effect of Cinnamic Acid and Its Derivatives on Structure of Gluten Proteins – A Study on Model Dough with Application of FT-Raman Spectroscopy. *Food Hydrocoll* **2020**, *107*, 105935.

[247] Cebi, N.; Durak, M. Z.; Toker, O. S.; Sagdic, O.; Arici, M. An Evaluation of Fourier Transforms Infrared Spectroscopy Method for the Classification and Discrimination of Bovine, Porcine and Fish Gelatins. *Food Chem* **2016**, *190*, 1109–1115.

[248] Casanova, F.; Mohammadifar, M. A.; Jahromi, M.; Petersen, H. O.; Sloth, J. J.; Eybye, K. L.; Kobbelgaard, S.; Jakobsen, G.; Jessen, F. Physico-Chemical, Structural and Techno-Functional Properties of Gelatin from Saithe (Pollachius Virens) Skin. *Int J Biol Macromol* **2020**, *156*, 918–927.

[249] Sadat, A.; Joye, I. J. Peak Fitting Applied to Fourier Transform Infrared and Raman Spectroscopic Analysis of Proteins. *Applied Sciences 2020, Vol. 10, Page 5918* **2020**, *10* (17), 5918.

[250] Sobhy, R.; Zhan, F.; Mekawi, E.; Khalifa, I.; Liang, H.; Li, B. The Noncovalent Conjugations of Bovine Serum Albumin with Three Structurally Different Phytosterols Exerted Antiglycation Effects: A Study with AGEs-Inhibition, Multispectral, and Docking Investigations. *Bioorg Chem* **2020**, *94*.

[251] Mishra, P. M.; Chethana Rao; Ankita Sarkar; Yadav, A.; Kaushik, K.; Jaiswal, A.; Nandi, C. K. Super-Resolution Microscopy Revealed the Lysosomal Expansion during Epigallocatechin Gallate-Mediated Apoptosis. *Langmuir* **2021**, *37* (36), 10818–10826.

[252] Khalifa, I.; Lorenzo, J. M.; Bangar, S. P.; Morsy, O. M.; Nawaz, A.; Walayat, N.; Sobhy, R. Effect of the Non-Covalent and Covalent Interactions between Proteins and Mono- or Di-Glucoside Anthocyanins on β-Lactoglobulin-Digestibility. *Food Hydrocoll* **2022**, *133*.

CURRICULUM VITAE

Full Name: Ahmed Mohamed Taha Abdelhamid Alfa

Nationality: Egyptian

Date of Birth: 1992-09-10

Email: ahmed.taha@ftmc.lt; ahmed-taha@alexu.edu.eg

Education

2006- 2009 Elshahid Issac Zakaria **High school**, Al Birijat - Kom Hamada, Egypt

2009- 2013 **B.Sc. of Agricultural Sciences**; Faculty of Agriculture (Saba Basha), Alexandria University, Egypt

2015 - 2016 **Master courses** completed at the Department of Food Sciences (**Dairy technology program**), Faculty of Agriculture (Saba Basha), Alexandria University, Egypt (**Completed courses**; Dairy chemistry, Dairy Microbiology, Cheese production, Fermented Dairy products, Dairy Technology).

2016-2019 **M.Sc. of Engineering degree** (Major: **Food biotechnology**); College of Food Sciences and Technology, Huazhong Agricultural university, Wuhan, People's Republic of China.
Thesis title: ″Effects of Ultrasound Emulsification on the Physicochemical Properties of Soy Protein Isolate Stabilized Emulsions‟

2020-now **PhD student**; Center for Physical sciences and Technology (FTMC) & Vilnius University

Work Experience

2015- now Teaching assistant- Department of Food Sciences, Faculty of Agriculture (Saba Basha), Alexandria University, Egypt (**Study leave**)

Training

June 2020	Focus on Peer Review, A Nature Masterclasses online course
April 2021	American Chemical Society (ACS) Reviewer Lab – online course
March 2023	Evidence Synthesis for Agri-food Systems Transformation Spring School (**7.1 ECTS credits**). A workshop focusing on evidence synthesis methodology training in the context of transformational food, farming and agricultural research. University of Almeria, Spain.

Awards

2014	Alexandria University award for outstanding bachelor students- Alexandria University, Alexandria, Egypt
2019	Research contribution Award – Huazhong Agricultural university, Wuhan, China
2020	Best Research Paper Award in Food sciences in Egypt, Awarded by the Egyptian society of food industries, Egypt

Volunteer work

2012-2013	Scientific committee coordinator – Alexandria University Student Union, Egypt
2017- 2019	Member and coordinator at the department of scientific research & development, Volunteer Center of International College, Huazhong Agricultural University, Wuhan, China
2020-2021	English/Arabic translator at Caritas Lithuania
2022-now	Academic peer reviewer (Elsevier, Springer, Wiley, Taylor &Francis and MDPI)

PUBLICATIONS INCLUDED IN THE THESIS

1. **Ahmed Taha**, Federico Casanova, Povilas Šimonis, Voitech Stankevič, Mohamed AE Gomaa, and Arūnas Stirkė. "Pulsed Electric Field: Fundamentals and Effects on the Structural and Techno-Functional Properties of Dairy and Plant Proteins." ***Foods*** 11 (2022): 1556. https://doi.org/10.3390/foods11111556

2. **Ahmed Taha,** Federico Casanova, Povilas Šimonis, Jūratė Jonikaitė-Švėgždienė, Marijus Jurkūnas, Mohamed AE Gomaa, and Arūnas Stirkė. "Pulsed electric field-assisted glycation of bovine serum albumin/starch conjugates improved their emulsifying properties." ***Innovative Food Science & Emerging Technologies*** 82 (2022): 103190, https://doi.org/10.1016/j.ifset.2022.103190

3. **Ahmed Taha**, Federico Casanova, Martynas Talaikis, Voitech Stankevič, Nerija Žurauskienė, Povilas Šimonis, Vidas Pakštas, Marijus Jurkūnas, Mohamed AE Gomaa, and Arūnas Stirkė. "Effects of Pulsed Electric Field on the Physicochemical and Structural Properties of Micellar Casein." Polymers 15, 15 (2023): 3311. https://doi.org/10.3390/polym15153311

4. **Ahmed Taha**, Federico Casanova, Martynas Talaikis, Voitech Stankevič, Nerija Žurauskienė, Povilas Šimonis, skirmantas keršulis, and Arūnas Stirkė**. Nanosecond pulsed electric field promoted the binding between BSA and epigallocatechin gallate (EGCG)**, under publication. This part is still under preparation, and it will be published soon.

Publications Not included in the thesis:

Research articles

1. **Ahmed Taha**, Tan Hu, Zhuo Zhang, Amr M. Bakry, Ibrahim Khalifa, Siyi Pan, and Hao Hu. "Effect of different oils and ultrasound emulsification conditions on the physicochemical properties of emulsions stabilized by soy protein isolate." ***Ultrasonics Sonochemistry*** 49 (2018): 283-293.
2. **Ahmed Taha**, Eman Ahmed, Tan Hu, Xiaoyun Xu, Siyi Pan, and Hao Hu. "Effects of different ionic strengths on the physicochemical properties of plant and animal proteins-stabilized emulsions fabricated using ultrasound emulsification." ***Ultrasonics Sonochemistry*** 58 (2019): 104627.

3. Lv, Siyi, **Ahmed Taha**, Hao Hu, Qi Lu, and Siyi Pan. "Effects of ultrasonic-assisted extraction on the physicochemical properties of different walnut proteins." ***Molecules*** 24, no. 23 (2019): 4260.
4. Zheng, Ting, Xiaohui Li, **Ahmed Taha**, Yue Wei, Tan Hu, Pijiar Beyna Fatamorgana, Zhuo Zhang et al. "Effect of high intensity ultrasound on the structure and physicochemical properties of soy protein isolates produced by different denaturation methods." ***Food Hydrocolloids*** 97 (2019): 105216.
5. Lv, Wenhui, Tan Hu, **Ahmed Taha**, Zhongkun Wang, Xiaoyun Xu, Siyi Pan, and Hao Hu. "Lipo-dipeptide as an emulsifier: performance and possible mechanism." ***Journal of agricultural and food chemistry*** 67, no. 22 (2019): 6377-6386.
6. Tian Yan, Zhen Zhang, Peipei Zhang, **Ahmed Taha**, Hao Hu, and Siyi Pan. "The role of conformational state of pH-shifted β-conglycinin on the oil/water interfacial properties and emulsifying capacities." ***Food Hydrocolloids*** 108 (2020): 105990.
7. Tian Yan, **Ahmed Taha**, Peipei Zhang, Zhen Zhang, Hao Hu, and Siyi Pan. "Effects of protein concentration, pH, and NaCl concentration on the physicochemical, interfacial, and emulsifying properties of β-conglycinin." ***Food Hydrocolloids*** 118 (2021): 106784.
8. Li Letian, **Ahmed Taha**, Mengjie Geng, Zhongli Zhang, Hongchen Su, Xiaoyun Xu, Siyi Pan, and Hao Hu. "Ultrasound-assisted gelation of β-carotene enriched oleogels based on candelilla wax-nut oils: Physical properties and in-vitro digestion analysis." ***Ultrasonics sonochemistry*** 79 (2021): 105762.
9. Geng, Mengjie, Tan Hu, Qi Zhou, **Ahmed Taha**, Lang Qin, Wenhui Lv, Xiaoyun Xu, Siyi Pan, and Hao Hu. "Effects of different nut oils on the structures and properties of gel-like emulsions induced by ultrasound using soy protein as an emulsifier." *International* ***Journal of Food Science & Technology*** 56, no. 4 (2021): 1649-1660.
10. Tian, Yan, Gang Xu, Weiwei Cao, Jiaxing Li, **Ahmed Taha**, Hao Hu, and Siyi Pan. "Interaction between pH-shifted β-conglycinin and flavonoids hesperetin/hesperidin: Characterization of nanocomplexes and binding mechanism." ***Lwt*** 140 (2021): 110698.
11. Geng, Mengjie, Zhongkun Wang, Lang Qin, **Ahmed Taha**, Linxiao Du, Xiaoyun Xu, Siyi Pan, and Hao Hu. "Effect of ultrasound and coagulant types on properties of β-carotene bulk emulsion gels stabilized by soy protein." ***Food Hydrocolloids*** 123 (2022): 107146.
12. Geng, Mengjie, Jian Liu, Hao Hu, Lang Qin, **Ahmed Taha**, and Zhuo Zhang. "A comprehensive study on structures and characterizations of 7S

protein treated by high intensity ultrasound at different pH and ionic strengths." ***Food Chemistry*** 373 (2022): 131378.

Review articles

1. **Ahmed Taha**, Eman Ahmed, Amr Ismaiel, Muthupandian Ashokkumar, Xiaoyun Xu, Siyi Pan, and Hao Hu. "Ultrasonic emulsification: An overview on the preparation of different emulsifiers-stabilized emulsions." ***Trends in Food Science & Technology*** 105 (2020): 363-377.

2. **Ahmed Taha**, Taha Mehany, Ravi Pandiselvam, Shahida Anusha Siddiqui, Nisar A. Mir, Mudasir Ahmad Malik, O. J. Sujayasree et al. "Sonoprocessing: Mechanisms and recent applications of power ultrasound in food." ***Critical Reviews in Food Science and Nutrition*** (2023): 1-39.

3. Shahida Anusha Siddiqui, Nur Alim Bahmid, **Ahmed Taha**, Ibrahim Khalifa, Sipper Khan, Hadis Rostamabadi, and Seid Mahdi Jafari. "Recent advances in food applications of phenolic-loaded micro/nanodelivery systems." **Critical Reviews in Food Science and Nutrition** (2022): 1-21.

4. Shahida Anusha Siddiqui, Nur Alim Bahmid, **Ahmed Taha**, Abdel-Moneim Eid Abdel-Moneim, Abdelrazeq M. Shehata, Chen Tan, Mohammad Saeed Kharazmi et al. "Bioactive-loaded nanodelivery systems for the feed and drugs of livestock; purposes, techniques and applications." **Advances in Colloid and Interface Science** (2022): 102772.

Book chapters

1. Hu, Hao, **Ahmed Taha**, and Ibrahim Khalifa. "Effects of Novel Processing Methods on Structure, Functional Properties, and Health Benefits of Soy Protein." In *Phytochemicals in Soybeans*, pp. 301-318. **CRC Press, 2022.**

2. Taha Mehany, **Ahmed Taha**, Babatunde Olawoye, Sameh A. Korma, Oyekemi Olabisi Popoola, Okon Johnson Esua, and Muhammad Faisal Manzoor. "Pigmented Pseudocereals: Chemistry, Functionality, and Technological Aspects in Food Systems." In *Pigmented Cereals and*

Millets: Bioactive Profile and Food Applications, pp. 144-180. **The Royal Society of Chemistry (RSC)**, 2023.

3. Siddiqui, Shahida Anusha, Maximilian Julius Pahmeyer, Mohammad Mehdizadeh, Andrey Ashotovich Nagdalian, Natalya Pavlovna Oboturova, and **Ahmed Taha**. "Consumer Behavior and Industry Implications." In *The Age of Clean Label Foods*, pp. 209-247. **Springer, 2022.**

Attended Conferences

1. **Ahmed Taha**, Federico Casanova, Arūnas Stirkė, Applications of green technologies in food processing. FizTech conference 2021, Vilnius, **Lithuania** (Oral presentation).
2. **Ahmed Taha**, Applications of Ultrasound and Electroporation Techniques in Food Processing, International Conference on Frontier Technology of Food Science, 2021, Huazhong Agricultural University, Wuhan, **China** (Oral Presentation-Online-Invited speaker).
3. Nerija Zurauskiene, **Ahmed Taha**, Kamile Jonaityte, Arunas Stirke, Aldas Dervinis, Voitech Stankevic, Protein treatment and extraction by using solid-state Marx generator, 9th Euro-Asian Pulsed Power Conference (EAPPC), Seoul, **South Korea** (Poster Presentation).
4. **Ahmed Taha**, Federico Casanova, Povilas Šimonis, Arūnas Stirkė, Emulsifying Properties of PEF-treated BSA/Soluble Starch Conjugates, 3rd Baltic Biophysics Conference (2022), Vilnius, **Lithuania** (Poster Presentation).
5. **Ahmed Taha**, Federico Casanova, Povilas Šimonis, Arūnas Stirkė, Emulsifying Properties of PEF-treated BSA/Soluble Conjugates, FizTech conference 2022, Vilnius, **Lithuania** (Oral presentation).
6. **Ahmed Taha**, Federico Casanova, Arunas Stirke, Effects of pulsed electric field on the structural and emulsifying properties of dairy proteins, 16th Baltic Conference on Food Science and Technology FOODBALT 2023, Jelgava, **Latvia**.

ACKNOWLEDGEMENTS

I am deeply thankful to Allah for granting me the strength, patience, and perseverance to overcome challenges and obstacles along the journey.

I extend my sincere appreciation to my supervisor Dr. Arūnas Stirkė, whose guidance, understanding, expertise, and mentorship have been invaluable throughout this research endeavor. His dedication to achieving excellence and your unwavering faith in my skills have been my motivation for moving forward. His unforgettable support in hard times significantly pushed me to keep working to finish this project.

I am also grateful to my co-supervisor and academic consultant, Dr. Federico Casanova from the Technical University of Denmark (DTU). His essential advice, knowledge, and experience have greatly improved the depth and quality of this research. His deliberative contributions and collaboration approach contributed significantly to this project's direction.

I want to thank the Center for Physical Science and Technology (FTMC) and Vilnius University for providing this opportunity and scholarship to complete my PhD study in Vilnius.

Moreover, I would like to express my gratitude to the Functional Materials and Electronics Department - Laboratory of nanostructured materials and Sensors. I would especially like to thank Prof. Dr. N. Žurauskienė, Prof. Voitech Stankevič, and Dr. Skirmantas Keršulis for their contribution and for sharing their scientific knowledge. I am deeply grateful to my colleagues and lab mates in the Bioelectrics Laboratory, namely Dr. Povilas Šimonis, Dr. Monika Marija Kirsnytė, Dr. Wanessa Melo, Dr. Antanas Strakšys, as well as Kamilė Jonynaitė, Neringa Bakutė, Greta Gančytė, and Ernesta Pocevičiūtė. Their exceptional warmth, support, and valuable contributions have created an environment of growth that has been invaluable to my research journey.

I appreciate the significant contribution from my colleagues, Dr. Martynas Talaikis for his support in Raman and IR spectroscopy analysis, Dr. Jūratė Jonikaitė-Švėgždienė for DSC analysis, and Dr. Vidas Pakštas for SEM imaging. I am also grateful to my colleague Marijus Jurkūnas for facilitating the use of the DLS instrument in my research and for valuable discussions and recommendations. I also thank Justina Jurgelevičiūtė for providing an ultrasound probe for emulsion preparation.

I extend my gratitude to my family, especially my father, Mohamed Taha, and mother, Sohier Gomaa; without their sacrifices, prayers and ultimate love for more than 30 years, I wouldn't be able to complete my BSc, MSc and PhD. My heartfelt thanks go to my beloved wife, Eman Ahmed, son Ibrahim and our soon-to-arrive twins for their unconditional love, sacrifices, prayers and encouragement. I would like to thank my brother Mahmoud and sisters Walaa and Fatima for their support, prayers, and ultimate love. This work is dedicated to my family. I want to thank my dear friend and countrymate Fathy Mahfouz for his company and support during my study period in Vilnius.

NOTES

NOTES

Vilniaus universiteto leidykla
Saulėtekio al. 9, III rūmai, LT-10222 Vilnius
El. p. info@leidykla.vu.lt, www.leidykla.vu.lt
bookshop.vu.lt, journals.vu.lt
Tiražas 20 egz.